Ubiquitination and Degradation of Neuronal Nitric Oxide Synthase

by

Gary J. Jenkins

A dissertation submitted in partial fulfillment
of the requirements for the degree of
Doctor of Philosophy
(Pharmacology)
in The University of Michigan
2008

Doctoral Committee:

Professor Yoichi Osawa, Chair
Professor Paul F. Hollenberg
Professor William B. Pratt
Professor Rudy J. Richardson

Table of Contents

List of Figures

Chapter IV

Chapter I

Introduction

Nitric Oxide

Nitric Oxide (NO) is a known atmospheric pollutant formed upon the combustion of nitrogen containing compounds, such as in automobile exhaust and industrial processes. Beginning in 1980 with the observations of Furchgott and Zawadzki (1), scientists have discovered that NO is also an important regulator in a wide variety of physiological responses, such as homeostatic regulation of blood pressure, blood clotting, neurotransmission and host defense. Pure NO is a gas under standard temperature and pressure, but it behaves as a dissolved nonelectrolyte under most biological conditions. NO is a free radical that is much more soluble in apolar solvents than in water, so it is able to diffuse across cell membranes. As a result of these characteristics, NO is able to function both as an intracellular and an intercellular signaling molecule. The NO free radical has a high chemical reactivity and is unstable in biological systems, with a half life of less than 10 seconds (2).

NO is an uncharged radical molecule that has 11 valence electrons, one unpaired electron and is paramagnetic. The most common chemical interactions of NO in biological systems involve the stabilization of the unpaired electron (3). This stabilization can occur through the reaction of NO with other paramagnetic species, such

as oxygen, superoxide, and peroxy radicals, or by forming an NO-metal complex. Two molecules of NO can react with oxygen to form 2 molecules of the paramagnetic radical nitrogen dioxide. Nitrogen dioxide can then react further to form the highly reactive molecules dinitrogen tetroxide and dinitrogen trioxide. One molecule of NO will react extremely rapidly with superoxide to produce the reactive species peroxynitrite. Peroxynitrite is a potent oxidant capable of oxidizing thiols (4) and DNA bases (5), and it can initiate metal-independent lipid peroxidation (6). NO is able to interact with the partially filled d orbitals of many biologically important metals. NO is also a dioxygen analogue, allowing it to react with proteins that bind dioxygen, such as cytochromes P450, myoglobin, peroxidases, hemoglobin, cytochrome oxidase, and dioxygenases (3). NO is also able to inhibit many heme- and nonheme-iron-containing enzymes. These enzymes include cytochrome P450, nitric oxide synthase (NOS), several nitrite reductases, and cytochrome oxidase (7).

Formation of Nitric Oxide

NO is biosynthesized from the amino acid L-arginine, which is present in high concentrations in the blood, extracellular fluid, and within cells (8). The enzyme NO-synthase (NOS) catalyzes the five-electron oxidation of the guanidine nitrogen of L-arginine in the presence of molecular oxygen to form NO and citrulline (Figure 1.1). The reaction also depends on the availability of the NOS cofactors (6R)-5,6,7,8-tetrahydrobiopterin (BH_4), flavin adenine dinucleotide (FAD), flavin mononucleotide (FMN), calmodulin (CaM), and iron protoporphorin IX (heme), as well as nicotinamide adenine dinucleotide phosphate (NADPH) as an electron source. The electrons from

NADPH are transferred through the flavins FAD and FMN before they arrive at the heme active site where O_2 is activated and L-arginine oxidized. Bound calmodulin is required to trigger this flow of electrons from the flavins to the active site (9). It is widely accepted that *N*-hydroxy-arginine is an intermediate in the formation of NO (10). This intermediate is formed from a two electron oxidation of L-arginine supported by one molecule of NADPH. *N*-hydroxy-arginine is then converted to NO and citrulline by the insertion of a second oxygen involving an additional three-electron oxidation supported by 0.5 NADPH molecules (11).

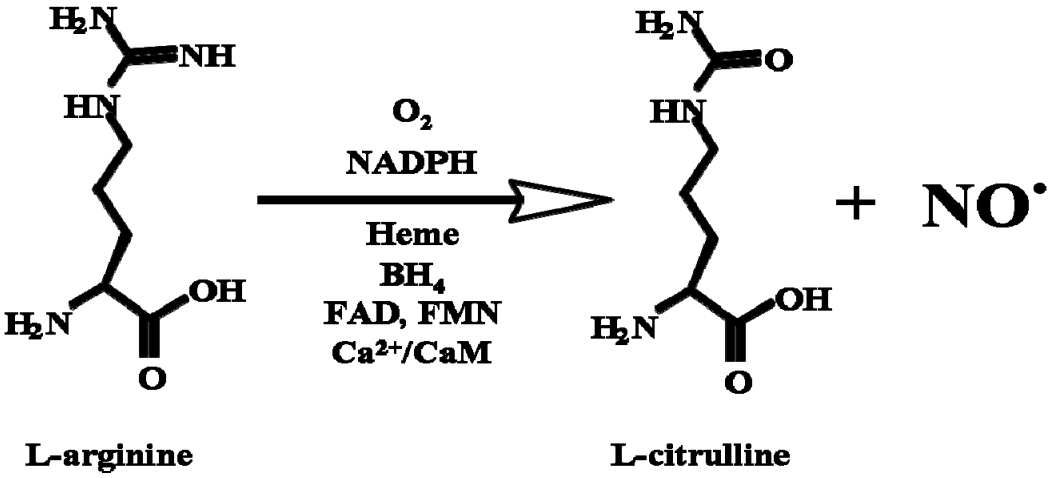

Figure 1.1 Reaction Catalyzed by NOS

Structure of Nitric Oxide Synthase

NOS is a large multi-domain polypeptide that is catalytically active only as a homodimer. It consists of two domains, an N-terminal oxygenase domain and a C-terminal reductase domain. The domains are joined by a calmodulin binding region consisting of 30 amino acids (12-14). Each subunit of the dimer binds heme, FAD, FMN

and BH_4 as prosthetic groups (figure 1.2). The two flavins are part of the reductase domain, which shares strong sequence similarity to cytochrome P450 reductase, and is able to function independently in the monomeric state (15). Unlike the reductase domain, the oxygenase domain requires bound substrate, BH_4, and heme for the formation of a fully functional homodimer (16). The heme is incorporated into the oxygenase domain in which a cysteine residue coordinates with the iron atom (17-19). This coordination is the same as in cytochrome P450 enzymes, providing NOS with the characteristic reduced CO difference spectrum containing a Soret maximum near 450 nm (17).

It has been shown, through the crystal structures of two of the isoforms of NOS, inducible (iNOS) and endothelial (eNOS), that NOS is able to dimerize through interactions of its oxygenase domain (20-22), although some reports suggest that the reductase domain or CaM binding site may help regulate the interaction in eNOS (23-25). The dimerization of iNOS is promoted by heme incorporation, BH_4 and L-arginine (14), whereas eNOS and neuronal NOS (nNOS) dimer assembly requires heme incorporation (25-28), but may not require BH_4, although BH_4 is able to stabilize the nNOS dimer once it is formed (29). Investigation of the ability of protoporphyrin IX to incorporate into heme-deficient monomeric nNOS (apo-nNOS) led to the discovery that the formation of a metal-thiolate bond is a critical step that alters nNOS conformation and enables monomers to dimerize (27). Comparison between the iNOS monomer and dimer structures shows that dimerization may recruit part of both the N- and C-termini of the oxygenase domain into a core region that forms the hydrophobic dimer interface, BH_4 binding site and substrate binding pocket (30). The flow of electrons during the catalytic cycle of NOS occurs from the reductase domain of one monomer subunit to the

oxygenase domain of the other monomer (31), highlighting the critical importance of dimerization in NOS function.

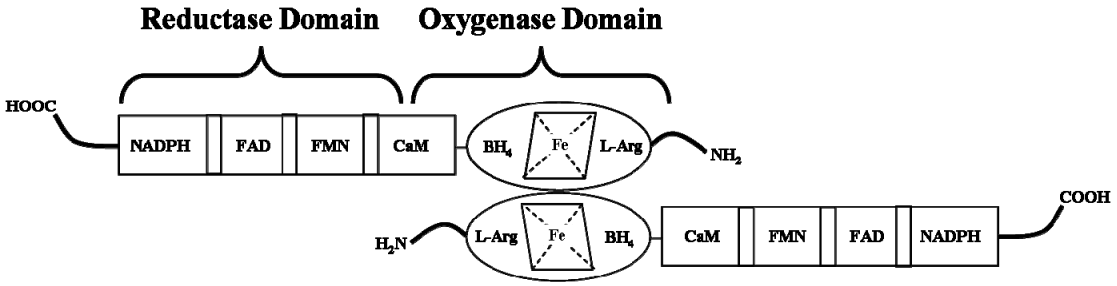

Figure 1.2 NOS Domains and Structure

Isoforms of Nitric Oxide Synthase

Three main isoforms of NOS have been identified: isoform I (nNOS), which is constitutively expressed in a variety of neuronal cells; isoform II (iNOS), which is usually not constitutively expressed, but can be induced by bacterial lipopolysaccharide and/or cytokines in macrophages and other cells; and isoform III (eNOS), which is expressed in endothelial cells (32-33). The cDNAs for these enzymes have been isolated and are encoded for by three different genes in humans, located on chromosomes 12, 17 and 7, respectively (34-35). The deduced amino acid sequences of the human isozymes show less than 59% identity (32, 36-41), although they do have highly similar structures. Across species, amino acid sequences for each isoform are well conserved with >90% sequence identity for nNOS (15, 32, 36) and eNOS (32, 40-44), and >80% identity for iNOS (32, 37-39, 45-50).

The three isoforms are characterized by regions of high homology, namely the oxygenase and reductase domains, but at the same time the isoforms have some

significant differences. The constitutively expressed isoforms, nNOS and eNOS, are regulated by levels of intercellular Ca^{2+} due to the Ca^{2+} dependent binding of CaM to these isoforms. It has been shown that both isoforms are inactive at 100 nmol/L Ca^{2+} and fully active at 500 nmol/L (50-53). These levels represent typical changes in intracellular Ca^{2+} concentrations upon receptor stimulation of excitatory cells such as neurons. Conversly, the inducible isoform, iNOS, is transcriptionally regulated by various cytokines (54-55). Bound CaM is required for iNOS activity, but due to its high binding affinity and ability to bind at very low levels of Ca^{2+}, CaM can actually be considered a subunit of iNOS (56). The isoforms also differ significantly in size, with nNOS having the largest molecular mass of 160 kDa due to the addition of a 300 amino acid sequence at the N-terminus containing a PDZ domain (57-58). The other two isoforms are similar in size with molecular masses of 130 kDa and 135 kDa for iNOS and eNOS, respectively. The N-terminus of eNOS is also unique since it is the only isoform to contain myristoylation and palmitoylation sites that regulate the localization of the enzyme to the plasmalemmal caveolae (59).

Physiological Roles of Nitric Oxide Synthase

NO has very diverse physiological roles that can be attributed to the existence of the three NOS isoforms and the varied locations of the isoforms within the body. NO formed by nNOS in neurons is a neurotransmitter in the central and peripheral nervous systems. NO produced in the central nervous system is involved in a myriad of processes, including pain perception (57, 60) and neuronal plasticity, which is important in behavioral activity (57, 60), memory formation (32, 57, 60), weight and appetite

control (61-62), as well as brain development (3, 57, 60, 63). There is also evidence that NO produced in the central nervous system contributes to the regulation of blood pressure by reducing vascular sympatheic tone (32). In the peripheral nervous system, NO acts as an inhibitor of non-adrenergic, non-cholinergic nerves that relaxes smooth muscle in the gastrointestinal, respiratory, vascular and urogenital systems (60). Skeletal muscle contains high levels of the nNOS splice variant nNOSμ, which is specifically localized beneath the sarcolemma of fast twitch fibres, highlighting NO's role in muscle contraction (36, 64).

The vascular endothelium behaves as an endocrine gland, and NO derived from eNOS is one of the most potent substances that it releases (3). Endothelial NO acts as an autocrine homeostatic modulator for the vascular system, mediating basal dilatory vascular tone, platelet aggregation and cardiac load (3, 65). The eNOS isoform is also found in cardiac myocytes and in the brain, where it produces NO that acts as a negative inotrope (65-66) and a retrograde messenger in the development of long-term potentiation (67), respectively. iNOS is expressed primarily in the cells of the immune system (68), but is also found in astrocytes, chondrocytes, hepatocytes and myocytes (65). NO is produced by iNOS during infection and chronic inflammation, and is involved in host-defense mechanisms, such as the destruction of tumor cells and invading pathogens (69-71). iNOS-derived NO also promotes collagen synthesis and angiogenesis, two processes critical for wound healing (65, 68, 72).

Pathophysiology of Nitric Oxide Synthase

Since NO plays an important role in a wide variety of physiological processes, any changes in the amount of NO produced by NOS can result in pathology. Overproduction of NO as a result of nNOS dysfunction is associated with many neurodegenerative disorders such as Alzheimer's disease, migraine, schizophrenia, Parkinson's disease, ischemia, stroke, Huntington's disease, and multiple sclerosis (57, 73-77). Induction of iNOS has been shown to enhance cellular damage in the later stages of cerebral ischemia and stroke (78-79), whereas eNOS-derived NO seems to have a protective effect in ischemic brain tissue (65). Severe hypotension and vasodilation during both septic and endotoxic shock occurs because of bacterial lipopolysaccharide-induced overproduction of NO by iNOS (80-81). Chronic inflammation results in the over expression of iNOS, which then produces levels of NO that are cytotoxic to the host cell, a phenomenon seen in many autoimmune disorders (82). Specifically, iNOS protein has been detected in chondrocytes from osteoarthritic cartilage but is not present in non-arthritic cartilage (65, 70). There is also evidence that iNOS plays a role in mediating tissue damage in rheumatoid arthritis, psoriasis, inflammatory bowel disease, diabetes, and myocardial dysfunction (65, 83-89).

The loss of NOS activity resulting in the depletion of NO levels has been implicated in the etiology of a number of diseases and in the generation of side effects of certain drugs and xenobiotics. NO deficiency plays an important role in many of the current models for hypertension, and consistent with these models, dietary supplementation with calcium, which increases NOS activity, has been shown to reduce blood pressure in animals and humans (69, 90-91). A reduction in the release of NO

from the vascular endothelium has been demonstrated in vascular tissue from rabbit atherosclerotic models (92-96) and in atherosclerotic coronary arteries from humans (97). Aging and diabetes are both associated with an increased incidence of impotence in patients that is paralleled with a loss of penile NOS activity (60, 98-99). Drug-induced impotence is a problem facing many people today, and the antihypertensive agents, in particular, have a high probability of inducing impotence (100, 23). It was discovered that treatment of rats with the antihypertensive agent guanabenz, known to cause impotence (100, 102-104), results in the loss of penile nNOS activity and nNOS protein levels (105). Impotence occurs frequently in smokers (106-108), and it was recently determined that components of cigarettes and cigarette smoke are able to inactivate nNOS (109). Even passive exposure of rats to cigarette smoke results in loss of penile nNOS activity and nNOS protein (110).

Pharmacology of Nitric Oxide Synthase

Because perturbations in the production of NO from NOS are involved in the pathophysiology of many diseases, many researchers have focused on NOS as a therapeutic target. Administration of the NOS substrate, L-arginine, has been used to treat conditions where there is a loss of NOS function, such as pulmonary hypertension (111), tobacco use (112), hypercholesterolemia (113-115), and ischemia-reperfusion (116). Supplementation of the cofactor BH_4 has also been used to reverse impaired NOS function in smokers (118) and patients with Type II diabetes (119), as well as in rats with ischemic acute renal failure (117).

There has been considerable interest in developing safe and selective inactivators of nNOS and iNOS, while eNOS has not been targeted for inhibition due to its important cardiovascular functions. One approach is to inhibit the dimerization of NOS (120-122). Since iNOS monomers are induced rapidly and then form active dimers, whereas eNOS and nNOS are constitutively present as active dimers, these compounds will most likely be more successful in targeting iNOS. However, since any newly synthesized enzyme must still dimerize to become functional, such compounds may be effective in inhibiting eNOS and nNOS when given chronically (120). N-substituted amino pteridines are able to interact with the pterin-binding site of NOS and have recently been patented as allosteric inhibitors of NOS (120).

Most inhibitors are analogues of the substrate L-arginine that are able to bind to the catalytic site of NOS. Two different types of compounds are being developed for this purpose, reversible inhibitors and suicide inactivators. Reversible inhibitors simply compete with L-arginine for the substrate binding site on NOS, and include compounds such as 7-nitroindazole (7-NI), N^G-nitro-L-arginine (NNA) and thio-L-citrulline. Suicide inactivators, otherwise known as metabolism-based inactivators, not only require binding specificity, but also must be metabolized to reactive intermediates by the enzyme, so they have the potential to be highly selective drugs (123). Suicide inactivators have been, and continue to be used as tools to study complex, highly regulated, biological systems. In the case of the P450 cytochromes, inactivation and covalent modification by suicide inactivators results in decreased drug metabolism, as well as enhanced proteolysis and turnover of the enzymes (124-130). NOS is a P450-like enzyme that shares many similarities with the P450 cytochromes, and suicide inactivators are just beginning to be

utilized in the study of NOS. The compounds N^G-methyl-L-arginine, guanabenz and aminoguanidine, among others, have been identified as suicide inactivators of NOS (65, 131).

Post-translational Regulation of Nitric Oxide Synthase

The complex, tightly controlled regulation of NO production by NOS is very important, not only because of its potent chemical reactivity and high diffusibility but also because NO cannot be stored, released or inactivated after release by conventional regulatory mechanisms. NOS activity is subject to a wide variety of transcriptional, translational, and post-translational controls that dictate the specificity of NO signaling and limit NO toxicity. The post-translational controls include lipid modifications, phosphorylation events, and interactions with protein partners, and they are responsible for the timing, magnitude and distribution of NO release (132). BH_4 is a critical cofactor because it couples heme iron reduction to NO synthesis and is required for iNOS dimerization (14), and there is now evidence that insufficient BH_4 levels can limit NO synthesis (133, 134). eNOS and nNOS are both phosphorylated in their oxygenase domains (13, 135-137), and serine or tyrosine phosphorylation of nNOS lowers its activity by over 50% (137). eNOS has been reported to be myristoylated, palmitoylated, farnesylated, and acetylated within its oxygenase domain, all of which are involved in the cellular trafficking of the enzyme (13, 135, 136).

A large number of protein partners for NOS have been identified. CAPON (carboxy-terminal PDZ ligand of nNOS) and PIN (protein inhibitor of nNOS) interact with nNOS through its PDZ and PIN binding domains, respectively (138-140). These

binding regions are only found in nNOS, and are located in its unique leader sequence. CAPON binding can restrict NO generation (141), whereas the function of PIN binding is a topic of ongoing debate, but was originally reported to destabilize the nNOS dimer (140). The Rho family GTPase, Rac2, interacts with iNOS and serves as an allosteric activator of the enzyme in macrophages (141, 142). Calmodulin was discovered to be an allosteric activator of all three isoforms of NOS (143). It is interesting to note that a 40-50 amino acid insert is present in nNOS and eNOS (144) that functions as an autoinhibitory loop that can destabilize calmodulin binding at low Ca^{2+} levels (145, 146). eNOS and nNOS are localized in the caveolae of endothelial cells and cardiac myocytes through their interactions with caveolin-1 and caveolin-3 (147). Binding to caveolin-3 has also been shown to inhibit NO production from nNOS and eNOS (25, 148-150), and caveolin-1 binding has been shown to inhibit NO production from all three NOS isoforms (25, 148-152) and to enhance the degradation of iNOS in cells (152). The inhibition of eNOS by caveolin-1 and -3 is reversed by calmodulin binding (153, 154). The highly abundant cytosolic protein chaperone hsp90 (heat-shock protein 90) can form heterocomplexes with nNOS (155) and eNOS (156), resulting in enhanced NO production in both cases (132, 155-157). Hsp90 is also involved in the insertion of the heme prosthetic group into nNOS (155, 158), and in the protection of the enzyme from proteasomal degradation (155). NOS enzymes are also regulated, in part, by post-translational proteolysis. The ubiquitin-proteasome is the major proteolytic pathway in regulating the turnover of nNOS (159-161) and iNOS (162-164), and has recently been implicated in eNOS degradation (165).

Ubiquitin-Proteasome System

The ubiquitin-proteasome system is the major pathway for the degradation of short-lived, regulatory proteins. In this pathway, a protein is selectively recognized and conjugated to the conserved 76-residue polypeptide ubiquitin through the sequential action of activating (E1), conjugating (E2), and ligating (E3) enzymes (166) (fig 1.3). Substrates conjugated to ubiquitin can then be selectively targeted to the multisubunit, ATP-dependent protease known as the 26 proteasome, where they are hydrolyzed to small peptides (166-168) (fig 1.3). Ubiquitination results in the formation of a peptide bond between the ε-amino group of a substrate lysine residue and the C-terminal glycine (G76) of ubiquitin (169, 170). The E1 enzyme forms a high-energy thioester linkage with the carboxyl group of G76. The activated ubiquitin is then transiently carried by the E2 protein and transferred to the substrate lysine residue by the E3 ligase (170). There is one known E1 enzyme, a significant but limited number of E2 conjugating enzymes, and a large number of E3 ligases (169). The E3 ligases can be separated into three groups based on their mechanisms of action: a covalent mechanism (Homologous to E6AP C-Terminus (HECT)-domain E3s), a non-covalent mechanism (Really Interesting New Gene (RING) finger) and a chaperone dependent mechanism (U-box E3s). Each E3 ligase recognizes a restricted set of substrates and is served by one or a few E2 enzymes (169).

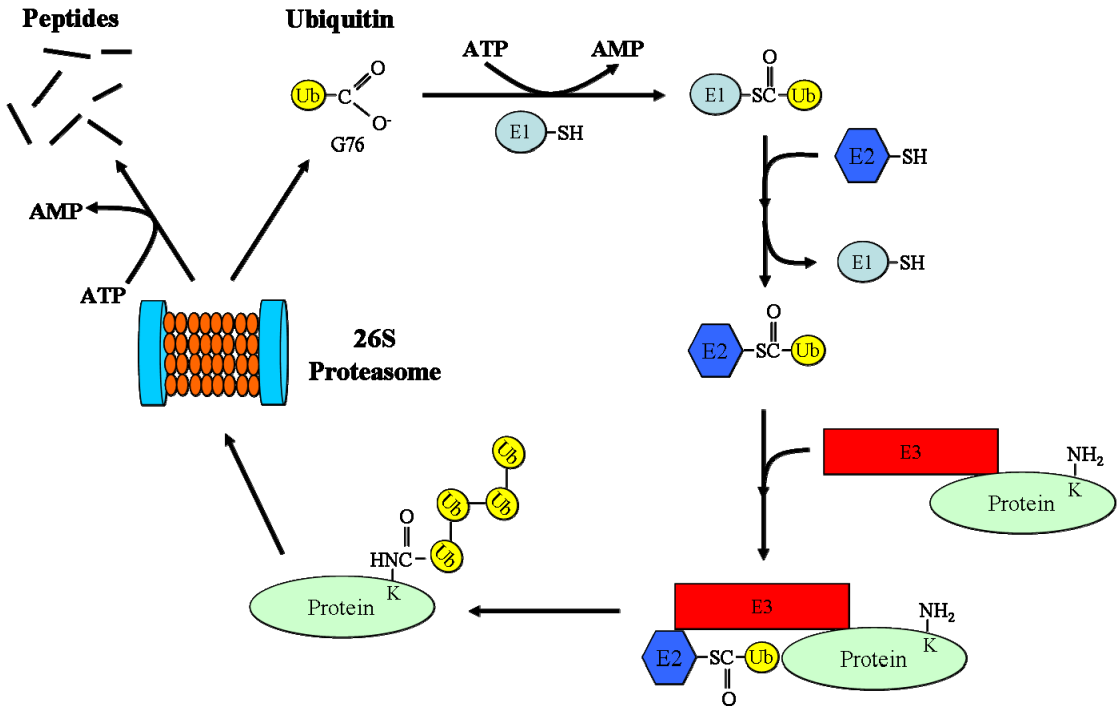

Figure 1.3 Ubiquitin-Proteasome System

It is clear that the recognition of substrates for ubiquitination is a highly selective process that is initiated by the availability of an ubiquitinatable lysine residue (171) and the presence and accessibility of ubiquitination signals in the substrate that are recognized by E3 ligases (169). Some specific ubiquitination signals have been identified. In 1986, Varshavsky and coworkers discovered the relationship between the N-terminal amino acid and substrate stability, called the N-end rule (172). For example, the yeast E3 ligase (Ubr1) recognizes this determinant, which, in combination with a lysine residue subject to ubiquitination, is both necessary and sufficient for substrate ubiquitination (173). Another ubiquitination signal is the destruction box sequence, R-x-A-L-G-x-I-x-N, found in substrates of the Anaphase Promoting Complex (APC) (174-177). Regions rich in the amino acids proline (P), glutamic acid (E), serine (S), or threonine (T), termed PEST

sequences, are known to mediate the ubiquitination of the carboxy-terminal domain of Rpb1, the large subunit of yeast RNA polymerase II, and the human epithelial sodium channel (ENaC) through interactions with the di-tryptophan domains (WW) of the ubiquitin ligases Rsp5 (171) and Nedd4 (178), respectively. A short, closely related, phosphopeptide motif was identified as the E3 ligase recognition element in the NF-κB inhibitor IκB (171, 179-182) and in the short-lived transcription factor β-catenin (183). The F box domain of the protein β-TrCP is the E3 ligase component that binds to this element (180-182). F box proteins function as the substrate receptors for SCF complexes (SkP1, Cullin, F box protein), a large family of multisubunit ubiquitin-protein ligases in yeast (171). N-linked high-mannose oligosaccharides were also discovered to be substrates of a specific cytosolic SCF E3 ligase (184), part of a process known as ERAD (ER-associated degradation) (185).

A very different type of degradation determinant, a solvent-exposed hydrophobic protein surface, is found in the yeast transcription factors MATa1 and MATα2, where heterodimerization buries the hydrophobic protein surfaces, stabilizing and protecting the factors from ubiquitination (186). In the case of nNOS, exposure of hydrophobic residues in the heme active site cleft is proposed as a possible trigger for the ubiquitination and degradation of the enzyme (187). This recognition motif may be utilized primarily for protein quality control, and could serve to identify misfolded or otherwise abnormal proteins in conjunction with molecular chaperones. Direct interaction of molecular chaperones with some E3 ligases has been reported (188). Phosphorylation (176, 189-191), deacetylation (192), aminoacylation (173, 193), oxidation (193), hydroxylation (194), glycosylation (194) and specific protein

interactions (194) are also known to regulate the recognition of cognate substrates by different E3 ligases.

Thesis Rationale

As described above, nNOS is degraded by the highly regulated ubiquitin-proteasome system. The observation that some metabolism-based inhibitors of nNOS enhance the proteasomal degradation of the enzyme suggests there must be a selective labilization of nNOS for recognition by the ubiquitin-proteasome system (105, 159). This labilization is not merely due to the loss of nNOS function per se, as some reversible inhibitors do not enhance the degradation of the protein (105, 159). To better understand this labilization process I will examine how the clinically used antihypertensive agent guanabenz labilizes nNOS for enhanced ubiquitination and proteasomal degradation. Guanabenz is a useful model compound for these studies since it is the best characterized metabolism-based inactivator of nNOS with respect to protein turnover. Using pulse-chase experiments, it was shown that guanabenz enhances the proteolytic turnover of nNOS in cells (159). Consistent with this finding, treatment of rats with guanabenz was found to inhibit NOS activity and cause the loss of immunodetectable penile nNOS protein (105). The question of how guanabenz labilizes nNOS for ubiquitination and proteasomal degradation will be examined in Chapter II.

In the course of studies on guanabenz, it was discovered that the loss of BH_4 was the mechanism of inhibition of nNOS and that the guanabenz treated nNOS was more susceptible to ubiquitination. Moreover, even in the absence of metabolism-based inactivators, nNOS is inactivated, suggesting that an "auto-inactivation" process may be

responsible for the "natural" turnover of nNOS protein. This auto-inactivation is, in part, ameliorated by the addition of exogenous BH_4. Thus, it is possible that BH_4 serves as an endogenous regulator of the ubiquitination and degradation of nNOS. It is clear that an inadequate level of BH_4 is an important factor in a variety of pathological conditions involving NOS, from impaired vascular function (195) to inhibited immune response (196). The specific effects of BH_4 depletion on nNOS have not been well characterized, although both an increased vulnerability to hypoxia and nNOS dysfunction in neurons have been observed (197). The possibility that the loss of BH_4 serves as an endogenous signal for the ubiquitination and proteasomal degradation of nNOS will be examined in Chapter III.

It is apparent that certain changes on nNOS allow for it to be selectively targeted for ubiquitination and proteasomal degradation. To further understand this labilization process, I will map the ubiquitination site on nNOS. These studies will aid in defining the site on nNOS that confers recognition of the altered protein. I will identify the site(s) of ubiquitin conjugation to nNOS in Chapter IV.

The Specific Aims of my thesis are:

I. **To determine how guanabenz labilizes nNOS for enhanced ubiquitination and proteasomal degradation.**
II. **To determine if the loss of BH_4 from nNOS can serve as an endogenous signal for nNOS ubiquitination and degradation.**
III. **To identify the site(s) of ubiquitin conjugation to nNOS.**

These studies will address how nNOS becomes a susceptible substrate for ubiquitination and proteasomal degradation. Many factors such as drug treatment, xenobiotics or cellular conditions can produce dysfunctional proteins. Determining the process by which these dysfunctional proteins become targeted for ubiquitination will aid in predicting potential drug toxicities and in the development of specific inhibitors.

References

1. Furchgott, R. F., Zawadzki, J. V. (1980) The obligatory role of endothelial cells in the relaxation of arterial smooth muscle by acetylcholine *Nature* **288,** 373-376
2. Stamler, J. S., Singel, D. J., Loscalzo, J. (1992) Biochemistry of nitric oxide and its redox-activated forms Sc*ience* **258**, 1898-1902
3. Kerwin, J. F., Lancaster, J. R., Feldman, P. L. (1995) Nitric oxide: a new paradigm for second messengers *J. Med. Chem.* **38**, 4343-4362
4. Gatti, R. M., Radi, R., Augusto, O. (1994) Peroxynitrite-mediated oxidation of albumin to the protein-thiyl free radical *FEBS Letters* **348,** 287-290
5. King, P. A., Jamison, E., Strahs, D., Anderson, V. E., Grenowitz, M. (1993) 'Footprinting' proteins on DNA with peroxonitrous acid *Nucleic Acids Res.* **21,** 2473-2478
6. Radi, R., Beckman, J. S., Bush, K. M., Freeman, B. A. (1991) Peroxynitrite-induced membrane lipid peroxidation: the cytotoxic potential of superoxide and nitric oxide *Arch. Biochem. Biophys.* **288,** 481-487
7. Griscavage, J. M., Fukuto, J. M., Komori, Y., Ignarro, L. J. (1994) Nitric oxide inhibits neuronal nitric oxide synthase by interacting with the heme prosthetic group *J. Biol. Chem.* **269,** 21644-21649
8. Palmer, R. M., Rees, D. D., Ashton, D. S., Moncada, S. (1988) L-arginine is the physiological precursor for the formation of nitric oxide in endothelium-dependent relaxation *Biochem. Biophys. Res. Commun.* **153,** 1251-1256
9. Guggenheim, E. A. (1966) Dimerization of gaseous nitric oxide *Mol. Phys.* **10,** 401-404
10. Stuehr, D. J., Kwon, N. S., Nathan, C. F., Griffith, O. W., Feldman, P. L., Wiseman, J. (1991) N^{ω}-hydroxy-L-arginine is an intermediate in the biosynthesis of nitric oxide from L-arginine *J. Biol. Chem.* **266,** 6259-6263
11. Feldman, P. L., Griffith, O. W., Stuehr, D. J. (1993) *Chem. Eng. News,* 26-38
12. Masters, B. S. S., McMillan, K., Sheta, E. A., Nishimura, J. S., Roman, L. J., and Marasek, P. (1996) Neuronal nitric oxide synthase, a modular enzyme formed by convergent evolution: structure studies of a cysteine thiolate-liganded heme protein that hydroxylates L-arginine to produce NO• as a cellular signal *FASEB J.* **10,** 552-558
13. Hemmens, B., and Mayer, B. (1998) Enzymology of nitric oxide synthases *Methods Mol. Biol.* **100,** 1-32
14. Stuehr, D. J. (1997) Structure-function aspects in the nitric oxide synthases *Annu. Rev. Pharmacol. Toxicol.* **37,** 339-359
15. Bredt, D. S., Hwang, P. M., Glatt, C. E., Lowenstein, C., Reed, R. R., Snyder, S. H. (1991) Cloned and expressed nitric oxide synthase structurally resembles cytochrome P-450 reductase *Nature* **351,** 714-718
16. Klatt, P., Pfeiffer, S., List, B. M., Lehner, D., Glatter, Ol, Bachinger, H. P., Werner, E. R., Schmidt, K., Mayer, B. (1996) Characterization of heme-deficient neuronal nitric-oxide synthase reveals a role for heme in subunit dimerization and binding of the amino acid substrate and tetrahydrobiopterin *J. Biol. Chem.* **271,** 7336-7342
17. Stuehr, D. J., Ikeda-Saito, M., (1992) Spectral characterization of brain and macrophage nitric oxide synthases *J. Biol. Chem.* **267,** 20547-20550

18. McMillan, K., Bredt, D. S., Hirsch, D. J., Snyder, S. H., Clark, J. E., Masters, B. S. S. (1992) Cloned, expressed rat cerebellar nitric oxide synthase contains stoichiometric amounts of heme, which binds carbon monoxide *Proc. Natl. Acad. Sci. USA* **89,** 11141-11145
19. White, K. A., Marletta, M. A. (1992) Nitric oxide synthase is a cytochrome P-450 type hemoprotein *Biochemistry* **31,** 6627-6631
20. Chen, P. F., Tsai, A. L., Berka, V., Wu, K. K. (1996) Endothelial nitric-oxide synthase *J. Biol. Chem.* **271,** 14631-14635
21. McMillan, K., Masters, B. S. S. (1995) Prokaryotic expression of the heme- and flavin-binding domains of rat neuronal nitric oxide synthase as distinct polypeptides: identification of the heme-binding proximal thiolate ligand as cysteine-415 *Biochem.* **34,** 3686-3693
22. Ghosh, D. K., Wu, C., Pitters, E., Molony, M., Werner, E. R., Mayer, B., Stuehr, D. J. (1997) Characterization of the inducible nitric oxide synthase oxygenase domain identifies a 49 amino acid segment required for subunit dimerization and tetrahydrobiopterin interaction *Biochem.* **36,** 10609-10619
23. Lee, C. M., Robinson, L. J., Michel, T. (1995) Oligomerization of endothelial nitric oxide synthase *J. Biol. Chem.* **270,** 27403-27406
24. Hellermann, G. R., Solomonson, L. P. (1997) Calmodulin promotes dimerization of the oxygenase domain of human endothelial nitric-oxide synthase *J. Biol. Chem.* **272,** 12030-12034
25. Venema, R. C., Ju, H., Zou, R., Ryan, J. W., Venema, V. J. (1997) Subunit interactions of endothelial nitric-oxide synthase *J. Biol. Chem.* **272,** 1276-1282
26. Rodriguez-Crespo, I., Oriz de Montellano, P. R. (1996) Human endothelial nitric oxide synthase: expression in escherichia coli, coexpression with calmodulin, and characterization *Arch. Biochem. Biophys.* **336,** 151-156
27. Hemmens, B., Gorren, A. C. F., Schmidt, K., Werner, E. R., Mayer, B. (1998) Haem insertion, dimerization and reactivation of haem-free rat neuronal nitric oxide synthase *Biochem. J.* **332,** 337-342
28. List, B. M., Klosch, B., Volker, C., Gorren, A. C. F., Sessa, W. C., Werner, E. R., Kukovetz, W. R., Schmidt, K., Mayer, B. (1997) Characterization of bovine endothelial nitric oxide synthase as a homodimer with down-regulated uncoupled NADPH oxidase activity: tetrahydrobiopterin binding kinetics and role of haem in dimerization *Biochem. J.* **323,** 159-165
29. Klatt, P., Schmidt, K., Lehner, D., Glatter, O., Bachinger, H. P., Mayer, B. (1995) Structural analysis of porcine brain nitric oxide synthase reveals a role for tetrahydrobiopterin and L-arginine in the formation of an SDS-resistant dimer *EMBO J.* **14,** 3687-3695
30. Crane, B. R., Arvai, A. S., Ghosh, D. K., Wu, C., Getzoff, E. D., Stuehr, D. J., Tainer, J. A. (1998) Structure of nitric oxide synthase oxygenase dimer with pterin and substrate *Science* **279,** 2121-2126
31. Siddhanta, U., Presta, A., Fan, B., Wolan, D., Rousseau, D. L., Stuehr, D. J. (1998) Domain swapping in inducible nitric-oxide synthase *J. Biol. Chem.* **273,** 18950-18958

32. Forstermann, U., Closs, E. I., Pollock, J. S., Nakane, M., Schwarz, P., Gath, I., Kleinert, H. (1994) Nitric oxide synthase isozymes. Characterization, purification, molecular cloning, and functions *Hypertension* **23,** 1121-1131
33. Lancaster, J. R., Jr., Hibbs, J. B., Jr. (1990) EPR demonstration of iron-nitrosyl complex formation by cytotoxic activated macrophages *Proc. Natl. Acad. Sci. U.S.A.* **87,** 1223-1227
34. Marsden, P. A., Heng, H. H. Q., Scherer, S. W., Stewart, R. J., Hall, A. V., Shi, X. M., Tsui, L. C., Schappert, K. T. (1993) Structure and chromosomal localization of the human constitutive endothelial nitric oxide synthase gene *J. Biol. Chem.* **268,** 17478-17488
35. Xu, W. M., Gorman, P., Sheer, D., Bates, G., Kishimoto, J., Lizhi, L., Emson, P. (1993) Regional localization of the gene coding for human brain nitric oxide synthase (NOS1) to 12q24.2→24.31 by fluorescent in situ hybridization *Cytogenet. Cell. Genet.* **64,** 62-63
36. Nakane, M., Schmidt, H. H., Pollock, J. S., Forstermann, U., Murad, F. (1993) Cloned human brain nitric oxide synthase is highly expressed in skeletal muscle *FEBS Lett.* **316,** 175-180
37. Geller, D. A., Lowenstein, C. J., Shapiro, R. A., Nussler, A. K., Di, S. M., Wang, S. C., Nakayama, D. K., Simmons, R. L., Snyder, S. H., Billiar, T. R. (1993) Molecular cloning and expression of inducible nitric oxide synthase from human hepatocytes *Proc. Natl. Acad. Sci. U.S.A.* **90,** 3491-3495
38. Charles, I. G., Palmer, R. M. J., Hickery, M. S., Bayliss, M. T., Chubb, A. P., Hall, V. S., Moss D. W., Moncada, S. (1993) Cloning, characterization and expression of a cDNA encoding an inducible nitric oxide synthase from the human chondrocyte *Proc. Natl. Acad. Sci. U.S.A.* **90,** 11419-11423
39. Sherman, P. A., Laubach, V. E., Reep, B. R., Wood, E. R. (1993) Purification and cDNA sequence of an inducible nitric oxide synthase from a human tumor cell line *Biochemistry* **32,** 11600-11605
40. Janssens, S. P., Shimouchi, A., Quertermous, T., Bloch, D. B., Bloch, K. D. (1992) Cloning and expression of a cDNA encoding human endothelium-derived relaxing factor/nitric oxide synthase *J. Biol. Chem.* **267,** 14519-14522 [published erratum in (1992) *J. Biol. Chem.* **267,** 22694]
41. Marsden, P. A., Schappert, K. T., Chen, H. S., Flowers, M., Sundell, C. L., Wilcox, J. N., Lamas, S., Michel, T. (1992) Molecular cloning and characterization of human endothelial nitric oxide sythase *FEBS Lett.* **307,** 287-293
42. Sessa, W. C., Harrison, J. K., Barber, C. M., Zeng, D., Durieux, M. E., D'Angelo, D. D., Lynch, K. R., Peach, M. J. (1992) Molecular cloning and expression of a cDNA encoding endothelial cell nitric oxide synthase *J. Biol. Chem.* **267,** 15274-15276
43. Lamas, S., Marsden, P. A., Li, G. K., Tempst, P., Michel, T. (1992) Endothelial nitric oxide synthase: molecular cloning and characterization of a distinct constitutive enzyme isoform *Proc. Natl. Acad. Sci. U.S.A.* **89,** 6348-6352
44. Nishida, K., Harrison, D. G., Navas, J. P., Fisher, A. A., Dockery, S. P., Uematsu, M., Nerem, R. M., Alexander, R. W., Murphy, T. J. (1992) Molecular cloning and characterization of the constitutive bovine aortic endothelial cell nitric oxide synthase *J. Clin. Invest.* **90,** 2092-2096

45. Xie, Q. W., Cho, H. J., Calaycay, J., Mumford, R. A., Swiderek, K. M., Lee, T. D., Ding, A., Troso, T., Nathan, C. (1992) Cloning and characterization of inducible nitric oxide synthase from mouse macrophages *Science* **256,** 225-228
46. Lyons, C. R., Orloff, G. J., Cunningham, J. M. (1992) Molecular cloning and functional expression of an inducible nitric oxide synthase from a murine macrophage cell line *J. Biol. Chem.* **267,** 6370-6374
47. Lowenstein, C. J., Glatt, C. S., Bredt, D. S., Snyder, S. H. (1992) Cloned and expressed macrophage nitric oxide synthase contrasts with the brain enzyme *Proc. Natl. Acad. Sci. U. S. A.* **89,** 6711-6715
48. Nunokawa, Y., Ishida, N., Tanaka, S. (1993) Cloning of inducible nitric oxide synthase in rat vascular smooth muscle cells *Biochem. Biophys. Res. Commun.* **191,** 767-774
49. Adachi, H. Iida, S., Oguchi, S., Ohshima, H., Suzuki, H., Nagasaki, K., Kawasaki, H., Sugimura, T., Esumi, H. (1993) Molecular cloning of a cDNA encoding an inducible calmodulin-dependent nitric-oxide synthase from rat liver and its expression in COS-1 cells *Eur. J. Biochem.* **217,** 37-43
50. Forstermann, U., Gorsky, L. D., Pollock, J. S., Ishii, K., Schmidt, H. H., Heller, M., Murad, F. (1990) Hormone-induced biosynthesis of endothelium-derived relaxing factor/nitric oxide-like material in N1E-115 neuroblastoma cells requires calcium and calmodulin *Mol. Pharmacol.* **38,** 7-13
51. Schmidt, H. H. H. W., Pollock, J. S., Nakane, M., Gorsky, L. D., Forstermann, U., Murad, F. (1991) Purification of a soluble isoform of guanylyl cyclase-activating-factor synthase *Proc. Natl. Acad. Sci. U. S. A.* **88,** 365-369
52. Pollock, J. S., Forstermann, U., Mitchell, J. A., Warner, T. D., Schmidt, H. H. H. W., Nakane, M., Murad, F. (1991) Purification and characterization of particulate endothelium-derived relaxing factor synthase from cultured and native bovine aortic endothelial cells *Proc. Natl. Acad. Sci. U. S. A.* **88,** 10480-10484
53. Forstermann, U., Pollock, J. S., Schmidt, H. H., Heller, M., Murad, F. (1991) Calmodulin-dependent endothelium-derived relaxing factor/nitric oxide synthase activity is present in the particulate and cytosolic fractions of bovine aortic endothelial cells *Proc. Natl. Acad. Sci. U. S. A.* **88,** 1788-1792
54. Stuehr, D. J., Cho, H. J., Kwon, N. S., Weise, M. F., Nathan, C. F. (1991) Purification and characterization of the cytokine-induced macrophage nitric oxide synthase: an FAD- and FMN-containing flavoprotein *Proc. Natl. Acad. Sci. U. S. A.* **88,** 7773-7777
55. Hevel, J. M., White, K. A., Marletta, M. A. (1991) Purification of the inducible murine macrophage nitric oxide synthase: identification as a flavoprotein *J. Biol. Chem.* **266,** 22789-22791
56. Cho, H. J., Xie, Q. W., Calaycay, J., Mumford, R. A., Swiderek, K. M., Lee, T. D., Nathan, C. (1992) Calmodulin is a subunit of nitric oxide synthase from macrophages *J. Exp. Med.* **176,** 599-604
57. Christopherson, K. S., Bredt, D. S. (1997) Nitric oxide in excitable tissues: physiological roles and disease *J. Clin. Invest.* **100,** 2424-2429
58. Andrew, P. J., Mayer, B. (1999) Enzymatic function of nitric oxide synthases *Cardiovasc. Res.* **43,** 521-531

59. Papapetropoulos, A., Rudic, R. D., Sessa, W. C. (1999) Molecular control of nitric oxide synthases in the cardiovascular system *Cardiovasc. Res.* **43,** 509-520
60. Esplugues, J. V. (2002) NO as a signaling molecule in the nervous system *Br. J. Pharmacol.* **135,** 1079-1095
61. Calapai, G., Squandrito, F., Altavilla, D., Zingarelli, B., Campo, G. M., Cilia, M., Caputi, A. P. (1992) Evidence that nitric oxide modulates drinking behaviour *Neurpharmacology* **31,** 761-764
62. Morley, J. E., Flood, J. F. (1992) Evidence that nitric oxide modulates food intake in mice *Life Sci.* **49,** 707-711
63. Bredt, D. S., Snyder, S. H. (1994) Nitric oxide: a physiological messenger molecule *Annu. Rev. Biochem.* **63,** 175-195
64. Kobzik, L., Reid, M. B., Bredt, D. S., Stamler, J. S. (1994) Nitric oxide in skeletal muscle *Nature* **372,** 546-548
65. Bryk, R., Wolff, D. J. (1999) Pharmacological modulation of nitric oxide synthesis by mechanism-based inactivators and related inhibitors *Pharmacol. Ther.* **84,** 157-178
66. Schulz, R., Triggle, C. R. (1994) Role of NO in vascular smooth muscle and cardiac muscle function *Trends Pharmacol. Sci.* **15,** 255-259
67. Wilson, R. I., Yanovsky, J., Godecke, A., Stevens, D. R., Schrader, J., Haas, H. L. (1997) Endothelial nitric oxide and LTP *Nature* **386,** 338
68. MacMicking, J., Xie, Q., Nathan, C. (1997) Nitric oxide and macrophage function *Annu. Rev. Immunol.* **15,** 323-350
69. Moncada, S., Palmer, R. M., Higgs, E. A. (1991) Nitric oxide: physiology, pathophysiology, and pharmacology *Pharmacol. Rev.* **43,** 109-141
70. Clancy, R. M., Abramson, S. B. (1995) Nitric oxide: a novel mediator of inflammation *Proc. Soc. Exp. Biol. Med.* **210,** 93-101
71. Nathan, C. (1997) Inducible nitric oxide synthase: what difference does it make? *J. Clin. Invest.* **100,** 2417-2423
72. Tzeng, E., Billiar, T. R. (1997) Nitric oxide and the surgical patient *Arch. Surg.* **132,** 977-982
73. Dawson, V. L., Dawson, T. M., London, E. D., Bredt, D. S., Snyder, S. H. (1991) Nitric oxide mediates glutamate toxicity in primary cortical cultures *Proc. Natl. Acad. Sci. U. S. A.* **88,** 6368-6371
74. Paakkari, I., Lindsberg, P. (1995) Nitric oxide in the central nervous system *Ann. Med.* **27,** 369-377
75. Mayer, B., Hemmens, B. (1997) Biosynthesis and action of nitric oxide in mammalian cells *Trends Biochem. Sci.* **22,** 477-481
76. Gonzales-Zulueta, M., Ensz, L. M., Mukhina, G., Lebovitz, R. M., Zwacka, R. M., Engelhardt, J. F., Oberley, L. W., Dawson, V. L., Dawson, T. M. (1998) Manganese superoxide dismutase protects nNOS neurons from NMDA and nitric oxide-mediated neurotoxicity *J. Neurosci.* **18,** 2040-2055
77. Moncada, S., Bolaños, J. P. (2006) Nitric oxide, cell bioenergetics and neurodegeneration *J. Neurochem.* **97,** 1676-1689
78. Huang, Z., Huang, P. L., Panahian, N., Dalkara, T., Fishman, M. C., Moskowitz, M. A. (1994) Effects of cerebral ischemia in mice deficient in neuronal nitric oxide synthase *Science* **265,** 1883-1885

79. Iadecola, C. (1997) Bright and dark sides of nitric oxide in ischemic brain injury *Trends Neurosci.* **20,** 132-139
80. Cobb, J. P., Danner, R. L. (1996) Nitric oxide and septic shock. *J. A. M. A.* **275,** 1192-1196
81. Johnson, M. J., Billiar, T. R. (1998) Roles of nitric oxide in surgical infection and sepsis *World J. Surg.* **22,** 187-196
82. Moilanen, E., Vapaatalo, H. (1995) Nitric oxide in inflammation and immune response *Ann. Med.* **27,** 359-367
83. Evans, C. H., Stefanovic-Racic, M., Lancaster, J. (1995) Nitric oxide and its role in orthopaedic disease *Clin. Orthop.* **312,** 275-294
84. Dusting, G. J., Macdonald, P. S. (1995) Endogenous nitric oxide in cardiovascular disease and transplantation *Ann. Med.* **27,** 395-405
85. Klahr, S., Morrissey, J. (1995) Renal disease: two faces of nitric oxide *Lab Invest.* **72,** 1-3
86. Tikkanen, I., Fyhrquist, F. (1995) Nitric oxide in hypertension and renal disease *Ann. Med.* **27,** 353-357
87. Loscalzo, J., Welch, G. (1995) Nitric oxide and its role in the cardiovascular system *Prog. Cardiovasc. Dis.* **38,** 87-104
88. Nava, E., Noll, G., Luscher, T. F. (1995) Nitric oxide in cardiovascular diseases *Ann. Med.* **27,** 343-351
89. Oyama, J., -I., Shimokawa, H., Momii, H., Cheng, X., -S., Fukuyama, N., Arai, Y., Egashira, K., Nakazawa, H., Takeshita, A. (1998) Role of nitric oxide and peroxynitrite in the cytokine-induced sustained myocardial dysfunction in dogs in vivo *J. Clin. Invest.* **101,** 2207-2214
90. Sowers, J. R., Zemel, M. B., Standley, P. R., Zemel, P. C. (1989) Calcium and hypertension *J. Lab. Clin. Med.* **114,** 338-348
91. Lopez-Jaramillo, P., Narvaez, M., Weigel, R. M., Yepez, R. (1989) Calcium supplementation reduces the risk of pregnancy-induced hypertension in an Andes population *Br. J. Obstet. Gynaecol.* **96,** 648-655
92. Coene, M. -C., Herman, A. G., Jordaens, F., Van Hove, C., Verbeuren, T. J., Zonnekeyn, L. (1985) Endothelium-dependent relaxations in isolated arteries of control and hypercholesterolemic rabbits *Br. J. Pharmacol.* **85,** 267
93. Verbeuren, T. J., Jordaens, F. H., Zonnekeyn, L. L., Van Hove, C. E., Coene, M. -C., Herman, A. G. (1986) Effect of hypercholesterolemia on vascular reactivity in the rabbit. I. Endothelium-dependent and endothelium-independent contractions and relaxation in isolated arteries of control and hypercholesterolemic rabbits *Circ. Res.* **58,** 552-564
94. Sreeharan, N., Jayakody, R. L., Senaratne, M. P. J., Thomson, A. B. R., Kappagoda, C. T. (1986) Endothelium-dependent relaxation and experimental atherosclerosis in the rabbit aorta *Can. J. Physiol. Pharmacol.* **64,** 1451-1453
95. Henry, P. D., Bossaller, C., Yamamoto, H. (1987) Impaired endothelium-dependent relaxation and cyclic guanosine 5'-monophosphate formation in atherosclerotic human coronary artery and rabbit aorta *Thromb. Res. Suppl.* **VII,** 6
96. Guerra, R., Jr., Brotherton, A. F. A., Goodwin, P. J., Clark, C. R., Armstrong, M. L., Harrison, D. G. (1989) Mechanisms of abnormal endothelium-dependent

vascular relaxation in atherosclerosis: implications for altered autocrine and paracrine functions of EDRF *Blood Vessels* **26,** 300-314
97. Forstermann, U. (1986) Properties and mechanisms of production and action of endothelium-derived relaxing factor *J. Cardiovasc. Pharmacol.* **8,** S45-S51
98. Carrier, S., Nagaraju, P., Morgan, D. M., Baba, K., Nunes, L., Lue, T. F. (1997) Age decreases nitric oxide-containing nerve fibers in the rat penis *J. Urol.* **157,** 1088-1092
99. Goldstein, I., Lue, T. F., Padma-Nathan, H., Rosen, R. C., Steers, W. D., Wicker, P. A. (1998) Oral sildenafil in the treatment of erectile dysfunction *N. Engl. J. Med.,* **338,** 1397-1404
100. Brock, G. B., Lue, T. F. (1993) Drug-induced male sexual dysfunction. An update *Drug Saf.* **8,** 414-426
101. Slag, M. F., Morley, J. E., Elson, M. K., Trence, D. L., Nelson, C. J., Nelson, A. E., Kinlaw, W. B., Beyer, H. S., Nuttall, F. Q., Shafer, R. B. (1983) Impotence in medical clinic outpatients *J. A. M. A.* **249,** 1736-1740
102. Weiss, R. J. (1991) Effects of antihypertensive agents on sexual function *Am. Fam. Physician.* **44,** 2075-2082
103. (1992) Drugs that cause sexual dysfunction: an update *Med. Lett. Drugs. Ther.* **34,** 73-78
104. (1987) Drugs that cause sexual dysfunction *Med. Lett. Drugs. Ther.* **29,** 65-70
105. Nakatsuka, M., Nakatsuka, K., Osawa, Y. (1998) Metabolism-based inactivation of penile nitric oxide synthase activity by guanabenz *Drug Metab. Dispos.* **26,** 497-501
106. Rosen, M. P., Greenfield, A. J., Walker, T. G., Grant, P., Dubrow, J., Bettmann, M. A., Fried, L. E., Goldstein, I. (1991) Cigarette smoking: an independent risk factor for atherosclerosis in the hypogastric-cavernous arterial bed of men with arteriogenic impotence *J. Urol.* **145,** 759-763
107. Mannino, D. M., Klevens, R. M., Flanders, W. D. (1994) Cigarette smoking: an independent risk factor for impotence? *American Journal of Epidemiology* **140,** 1003-1008
108. Shabsigh, R., Fishman, I. J., Schum, C., Dunn, J. K. (Cigarette smoking and other vascular risk factors in vasculogenic impotence *Urology* **38,** 227-231
109. Demady, D. R., Lowe, E. R., Everett, A. C., Billecke, S. S., Kamada, Y., Dunbar, A. Y., Osawa, Y. (2003) Metabolism-based inactivation of neuronal nitric-oxide synthase by components of cigarette and cigarette smoke *Drug Metab. Dispos.* **31,** 932-937
110. Xie, Y., Garban, H., Ng, C., Rajfer, J., Gonzalez-Cadavid, N. F. (1997) Effect of long-term passive smoking on erectile function and penile nitric oxide synthase in the rat *J. Urol.* **157,** 1121-1126
111. Mehta, S., Stewart, D. J., Langleben, D., Levy, R. D. (1995) Short-term pulmonary vasodilation with L-arginine in pulmonary hypertension *Circulation* **92,** 1539-1545
112. Celermajer, D. S., Adams, M. R., Clarkson, P., Robinson, J., McCredie, R., Donald, A., Deanfield, J. E. (1996) Passive smoking and impaired endothelium-dependent arterial dilatation in healthy young adults *N. Engl. J. Med.* **334,** 150-154
113. Bode-Boger, S. M., Boger, R. H., Kienke, S., Junker, W., Frolich, J. C. (1996) Elevated L-arginine/dimethylarginine ratio contributes to enhanced systemic NO

production by dietary L-arginine in hypercholesterolemic rabbits *Biochem. Biophys. Res. Commun.* **219,** 598-603
114. Cooke, J. P., Singer, A. H., Taso, P., Zera, P., Rowan, R. A., Billingham, M., E. (1992) Antiatherogenic effects of L-arginine in the hypercholesterolemic rabbit *J. Clin. Invest.* **90,** 1168-1172
115. Drexler, H., Zeiher, A. M., Meinzer, K., Just, H. (1991) Correction of endothelial dysfunction in coronary microcirculation of hypercholesterolaemic patients by L-arginine *Lancet* **338,** 1546-1550
116. Weyrich, A. S., Ma, X., Lefer, A. M. (1992) The role of L-arginine in ameliorating reperfusion injury after myocardial ischemia in the cat *Circulation* **86,** 279-288
117. Kakoki, M., Hirata, Y., Hayakawa, H., Suzuki, E., Nagata, D., Tojo, A., Nishimatsu, H., Nakanishi, N., Hattori, Y., Kikuchi, K., Nagano, T., Omata, M. (2000) Effects of tetrahydrobiopterin on endothelial dysfunction in rats with ischemic acute renal failure *J. Am. Soc. Nephrol.* **11,** 301-309
118. Heitzer, T., Brockhoff, C., Mayer, B., Warnholtz, A., Mollnau, H., Henne, S., Meinertz, T., Munzel, T. (2000) Tetrahydrobiopterin improves endothelium-dependent vasodilation in chronic smokers : evidence for a dysfunctional nitric oxide synthase *Circ. Res.* **86,** E36-E41
119. Heitzer, T., Krohn, K., Albers, S., Meinertz, T. (2000) Tetrahydrobiopterin improves endothelium-dependent vasodilation by increasing nitric oxide activity in patients with Type II diabetes mellitus *Diabetologia* **43,** 1435-1438
120. Mete, A., Connolly, S. (2003) Inhibitors of the NOS enzymes: A patent review *I. Drugs* **6,** 57-65
121. McMillan, K., Adler, M., Auld, D. S., Baldwin, J. J., Blasko, E., Browne, L. J., Chelsky, D., Davey, D., Dolle, R. E., Eagen, K. A., Erickson, S., Feldman, R. I., Glaser, C. B., Mallari, C., Morrissey, M. M., Ohlmeyer, M. H. J., Pan, G., Parkinson, J. F., Phillips, G. B., Polokoff, M. A., Sigal, N. H., Vergona, R., Whitlow, M., Young, T. A., Devlin, J. J. (2000) Allosteric inhibitors of inducible nitric oxide synthase dimerization discovered via combinatorial chemistry *Proc. Natl. Acad. Sci. U. S. A.* **97,** 1506-1511
122. Sennequier, N., Wolan, D., Stuehr, D. J., (1999) Antifungal imidazoles block assembly of inducible NO synthase into an active dimer *J. Biol. Chem.* **274,** 930-938
123. Abeles, R. H. (1983) Suicide enzyme inactivators *Chem. Eng. News* **61,** 48-56
124. Korsmeyer, K. K., Davoll, S., Figueiredo-Pereira, M. E., Correia, M. A. (1999) Proteolytic degradation of heme-modified hepatic cytochromes P450: A role for phosphorylation, ubiquitination, and the 26S proteasome? *Arch. Biochem. Biophys.* **365,** 31-44
125. Wang, H. F., Figueiredo-Pereira, M. E., Correia, M. A. (1999) Cytochrome P450 3A degradation in isolated rat hepatocytes: 26S proteasome inhibitors as probes *Arch. Biochem. Biophys.* **365,** 45-53
126. Tierney, D. J., Haas, A. L., Koop, D. R. (1992) Degradation of cytochrome P450 2E1: selective loss after labilization of the enzyme *Arch. Biochem. Biophys.* **293,** 9-16
127. Correia, M. A., Davoll, S. H., Wrighton, S. A., Thomas, P. E. (1992) Degradation of rat liver cytochromes P450 3A after their inactivation by 3,5-dicarbethoxy-2,6-

128. Correia, M. A., Yao, K., Wrighton, S. A., Waxman, D. J., Rettie, A. E. (1992) Differential apoprotein loss of rat liver cytochromes P450 after their inactivation by 3,5-dicarbethoxy-2,6-dimethyl-4-ethyl-1,4-dihydropyridine: a case for distinct proteolytic mechanisms? *Arch. Biochem. Biophys.* **294,** 493-503
129. Yang, M. X., Cederbaum, A. I. (1997) Characterization of cytochrome P450 2E1 turnover in transfected HepG2 cells expressing human CYP2E1 *Arch. Biochem. Biophys.* **341,** 25-33
130. Goasduff, T. Cederbaum, A. I. (1999) NADPH-dependent microsomal electron transfer increases degradation of CYP 2E1 by the proteasome complex: role of reactive oxygen species *Arch. Biochem. Biophys.* **370,** 258-270
131. Olken, N. M., Rusche, K. M., Richards, M. K., Marletta, M. A. (1991) Inactivation of macrophage nitric oxide synthase activity by NG-methyl-l-arginine *Biochem. Biophys. Res. Commun.* **177,** 828-833
132. Kone, B. C., Kuncewicz, T., Zhang, W., Yu, Z. (2003) Protein interactions with nitric oxide synthases: controlling the right time, the right place, and the right amount of nitric oxide *Am. J. Physiol. Renal Physiol.* **285,** F178-F190
133. Harrison, D. G. (1997) Cellular and molecular mechanisms of endothelial cell dysfunction *J. Clin. Invest.* **100,** 2153-2157
134. Cosentino, F., Patton, S., d'Uscio, L. V., Werner, E., Werner-Felmayer, G., Moreau, P., Malinski, T., Luscher, T. F. (1998) Tetrahydrobiopterin alters superoxide and nitric oxide release in prehypertensive rats *J. Clin. Invest.* **101,** 1530-1537
135. Liu, J., Hughes, T. E., Sessa, W. C. (1997) The first 35 amino acids and fatty acylation sites determine the molecular targeting of endothelial nitric oxide synthase into the Golgi region of cells: a green fluorescent protein study *J. Cell Biol.* **137,** 1525-1535
136. Michel, T., Feron, O. (1997) Nitric oxide synthases: which, where, how, and why? *J. Clin. Invest.* **100,** 2146-2152
137. Dawson, T. M., Steiner, J. P., Dawson, V. L., Dinerman, J. L., Uhl, G. R., Snyder, S. H. (1993) Immunosuppressant FK506 enhances phosphorylation of nitric oxide synthase and protects against glutamate neurotoxicity *Proc. Natl. Acad. Sci. U. S. A.* **90,** 9808-9812
138. Jaffrey, S. R., Snowman, A. M., Eliasson, M. J., Cohen, N. A., Snyder, S. H. (1998) CAPON: a protein associated with neuronal nitric oxide synthase that regulates its interactions with PSD95 *Neuron* **20,** 115-124
139. Tochio, H., Ohki, S., Zhang, Q., Li, M., Zhang, M. (1998) Solution structure of a protein inhibitor of neuronal nitric oxide synthase *Nat. Struct. Biol.* **5,** 965-969
140. Jaffrey, S. R., Snyder, S. H. (1996) PIN: an associated protein inhibitor of neuronal nitric oxide synthase *Science* **274,** 774-777
141. Kone, B. C. (2000) Protein-protein interactions controlling nitric oxide synthases *Acta Physiol. Scand.* **168,** 27-31
142. Kone, B. C., Kuncewicz, T. (1998) The Rho family GTPase Rac2 physically interacts with and activates inducible nitric oxide synthase *J. Am. Soc. Nephrol.* **9,** 463a

143. Abu Soud, H. M., Yoho, L. L., Stuehr, D. J. (1994) Calmodulin controls neuronal nitric oxide synthase by a dual mechanism *J. Biol. Chem.* **269,** 32047-32050
144. Salerno, J. C., Harris, D. E., Irizarry, K., Patel, B., Morales, A. J., Smith, S. M., Martasek, P., Roman, L. J., Masters, B. S., Jones, C. L., Weissman, B. A., Lane, P., Liu, Q., Gross, S. S. (1997) An autoinhibitory control element defines calcium-regulated isoforms of nitric oxide synthase *J. Biol. Chem.* **272,** 29769-29777
145. Nishida, C. R., de Montellano, P. R. (2001) Control of electron transfer in nitric-oxide synthases. Swapping of autoinhibitory elements among nitric-oxide synthase isoforms *J. Biol. Chem.* **276,** 20116-20124
146. Nishida, C. R., Ortiz de Montellano, P. R. (2000) Autoinhibition of endothelial nitric-oxide synthase. Identification of an electron transfer control element *J. Biol. Chem.* **274,** 14692-14698
147. Feron, O., Belhassen, L., Kobzik, L., Smith, T. W., Kelly, R. A., Michel, T. (1996) Endothelial nitric oxide synthase targeting to caveolae. Specific interactions with caveolin isoforms in cardiac myocytes and endothelial cells *J. Biol. Chem.* **271,** 22810-11814
148. Feron, O., Michel, J. B., Sase, K., Michel, T. (1998) Dynamic regulation of endothelial nitric oxide synthase: complementary roles of dual acylation and caveolin interactions *Biochemistry* **37,** 193-200
149. Feron, O., Saldana, F., Michel, J. B., Michel, T. (1998) The endothelial nitric-oxide synthase-caveolin regulatory cycle *J. Biol. Chem.* **273,** 3125-3128
150. Bucci, M., Gratton, J. P., Rudic, R. D., Acevedo, L., Roviezzo, F., Cirino, G., Sessa, W. C. (2000) In vivo delivery of the caveolin-1 scaffolding domain inhibits nitric oxide synthesis and reduces inflammation *Nat. Med.* **6,** 1362-1367
151. Sato, Y., Sagami, I., Shimizu, T. (2004) Identification of caveolin-1-interacting sites in neuronal nitric-oxide synthase: Molecular mechanism for inhibition of NO formation *J. Biol. Chem.* **279,** 8827-8836
152. Felley-Bosco, E., Bender, F., Quest, A. F. G. (2002) Caveolin-1-medieated post-transcriptional regulation of inducible nitric oxide synthase in human colon carcinoma cells *Biol. Res.* **35,** 169-172
153. Michel, J. B., Feron, O., Sacks, D., Michel, T. (1997) Reciprocal regulation of endothelial nitric-oxide synthase by Ca^{2+}-calmodulin and caveolin *J. Biol. Chem.* **272,** 15583-15586
154. Michel, J. B., Feron, O., Sase, K., Prabhakar, P., Michel, T. (1997) Caveolin versus calmodulin. Counterbalancing allosteric modulators of endothelial nitric oxide synthase *J. Biol. Chem.* **272,** 25907-25912
155. Bender, A. T., Silverstein, A. M., Demady, D. R., Kanelakis, K. C., Noguchi, S., Pratt, W. B., Osawa, Y. (1999) Neuronal nitric-oxide synthase is regulated by the Hsp90-based chaperone system in vivo *J. Biol. Chem.* **274,** 1472-1478
156. Garcia-Cardena, G., Fan, R., Shah, V., Sorrentino, R., Cirino, G., Papapetropoulos, A. Sess, W. C. (1998) Dynamic activation of endothelial nitric oxide synthase by Hsp90 *Nature* **392,** 821-824
157. Song, Y., Zweier, J. L., Xia, Y. (2001) Heat-shock protein 90 augments neuronal nitric oxide synthase activity by enhancing Ca^{2+}/calmodulin binding *Biochem. J.* **355,** 357-360

158. Billecke, S. S., Bender, A. T., Kanelakis, K. C., Murphy, P. J., Lowe, E. R., Kamada, Y., Pratt, W. B., Osawa, Y. (2002) Hsp90 is required for heme binding and activation of apo-neuronal nitric-oxide synthase: geldanamycin-mediated oxidant generation is unrelated to any action of hsp90 *J. Biol. Chem.* **277,** 20504-20509
159. Noguchi, S., Jianmongkol, S., Bender, A. T., Kamada, Y., Demady, D. R., Osawa, Y. (2000) Guanabenz-mediated inactivation and enhanced proteolytic degradation of neuronal nitric-oxide synthase *J. Biol. Chem.* **275,** 2376-2380
160. Bender, A. T., Demady, D. R., Osawa, Y. (2000) Ubiquitination of neuronal nitric oxide synthase in vitro and in vivo *J. Biol. Chem.* **275,** 17401-17411
161. Lee, M. H., Hyun, D. H., Jenner, P., Halliwell, B. (2001) Effect of proteasome inhibition on cellular oxidative damage, antioxidant defences and nitric oxide production *J. Neuro-chem.* **78,** 32-41
162. Felley-Bosco, E., Bender, F. C., Courjault-Gautier, F., Bron, C., Quest, A. F. (2000) Caveolin-1 down-regulates inducible nitric oxide synthase via the proteasome pathway in human colon carcinoma cells *Proc. Natl. Acad. Sci. U. S. A.* **97,** 14334-14339
163. Musial, A., Eissa, N. T. (2001) Inducible nitric-oxide synthase is regulated by the proteasome degradation pathway *J. Biol. Chem.* **276,** 24268-24273
164. Kolodziejski, P., Musial, A., Eissa, N. T. (2002) Ubiquitination of human inducible nitric oxide synthase is required for its degradation *Proc. Natl. Acad. Sci. U. S. A.* **99,** 12615-12320
165. Jiang, J., Cyr, D., Babbitt, R. W., Sessa, W. C., Patterson, C. (2003) Chaperone-dependent regulation of endothelial nitric-oxide synthase intracellular trafficking by the co-chaperone/ubiquitin ligase CHIP *J. Biol. Chem.* **278,** 49332-49341
166. Hershko, A., Ciechanover, A. (1998) The ubiquitin system *Annu. Rev. Biochem.* **67,** 425-479
167. Hochstrasser, M. (1996) Ubiquitin-dependent protein degradation *Annu. Rev. Genet.* **30,** 405-439
168. Chau, V., Tobias, J. W., Bachmair, A., Marriott, D., Ecker, D. J. (1989) A multiubiquitin chain is confined to specific lysine in a targeted short-lived protein *Science* **243,** 1576-1583
169. Pickart, C. M. (2001) Mechanisms underlying ubiquitination *Annu. Rev. Biochem.* **70,** 503-533
170. Herschko, A., Heller, H., Elias, S., Ciechanover, A. (1983) Components of ubiquitin-protein ligase system *J. Biol. Chem.* **258,** 8206-8214
171. Laney, D. J., Hochstrasser, M. (1999) Substrate targeting in the ubiquitin system *Cell* **97,** 427-430
172. Bachmair, A., Finely, D., Varshavsky, A. (1986) In vivo half-life of a protein is a function of its amino-terminal residue *Science* **234,** 179-186
173. Varshavsky, A. (1997) The N-end rule pathway of protein degradation *Genes Cells* **2,** 13-28
174. Glotzer, M., Murray, A. W., Kirschner, M. W. (1991) Cyclin is degraded by the ubiquitin pathway *Nature* **349,** 132-138
175. Page, A. M., Hieter, P. (1999) The anaphase-promoting complex: new subunits and regulators *Annu. Rev. Biochem.* **68,** 583-609

176. Deshaies, R. J. (1999) SCF and cullin/RING H2-based ubiquitin ligases *Annu. Rev. Cell. Dev. Biol.* **15,** 435-467
177. Koepp, D. M., Harper, J. W., Elledge, S. J. (1999) How the cyclin became a cyclin: regulated proteolysis in the cell cycle *Cell* **97,** 431-434
178. Goulet, C. C., Volk, K. A., Adams, C. M., Prince, L. S., Stokes, J. B. Snyder, P. M. (1998) Inhibition of the epithelial Na+ channel by interaction of Nedd4 with a PY motif deleted in Liddle's syndrome *J. Biol. Chem.* **273,** 30012-30017
179. Yaron, A., Gonen, H., Alkalay, I., Hatzubai, A., Jung, S., Beyth, S., Mercurio, F., Manning, A. M., Ciechanover, A., Ben-Neriah, Y. (1997) Inhibition of NF-kappa-B cellular function via specific targeting of the I-kappa-B-ubiquitin ligase *EMBO J. 16,* 6486-6494
180. Yaron, A., Hatzubai, A., Davis, M., Lavon, I., Amit, S., Manning, A. M., Andersen, J. S., Mann, M., Mercurio, F., Ben-Neriah, Y. (1998) Identification of the receptor component of the IkappaBalpha-ubiquitin ligase *Nature* **396,** 590-594
181. Spencer, E., Jiang, J., Chen, Z. J. (1999) Signal-induced ubiquitination of IkappaBalpha by the F-box protein Slimb/beta-TrCP *Genes Dev.* **13,** 284-294
182. Winston, J. T., Strack, P., Beer-Romero, P., Chu, C. Y., Elledge, S. J., Harper, J. W. (1999) The SCFbeta-TRCP-ubiquitin ligase complex associates specifically with phosphorylated destruction motifs in IkappaBalpha and beta-catenin and stimulates IkappaBalphan ubiquitination in vitro [erratum appears in (1999) *Genes Dev.* **13,** 1050] *Genes Dev.* **13,** 270-283
183. Aberle, H., Bauer, A., Stappert, J., Kispert, A., Kemler, R. (1997) beta-catenin is a target for the ubiquitin-proteasome pathway *EMBO J.* **16,** 3797-3804
184. Yoshida, Y., Chiba, T., Tokunaga, F., Kawasaki, H., Iwai, K., Suzuki, T., Ito, Y., Matsuoka, K. Yoshida, M., Tanaka, K, Tai, T. (2002) E3 ubiquitin ligase that recognizes sugar chains *Nature* **418,** 438-442
185. Kostova, Z., Wolf, D. H. (2003) For whom the bell tolls: protein quality control of the endoplasmic reticulum and the ubiquitin-proteasome connection *EMBO J.* **22,** 2309-2317
186. Johnson, P. R., Swanson, R., Rakhilina, L., Hochstrasser, M. (1998) Degradation signal masking by heterodimerization of MATalpha2 and MATa1 blocks their mutual destruction by the ubiquitin-proteasome pathway *Cell* **94,** 217-227
187. Peng, H. -M., Morishima, Y., Jenkins, G. J., Dunbar, A. Y., Lau, M., Patterson, C., Pratt, W. B., Osawa, Y. (2004) Ubiquitylation of neuronal nitric-oxide synthase by CHIP, a chaperone-dependent E3 ligase *J. Biol. Chem.* **279,** 52970-52977
188. Cyr, D. M., Hohfeld, J., Patterson, C. (2002) Protein quality control: U-box-containing E3 ubiquitin ligases join the fold *Trends Biochem. Sci.* **27,** 268-375
189. Jackson, P. K., Eldridge, A. G., Freed, E., Furstenthal, L., Hsu, J. Y., Kaiser, B. K., Reimann, J. D. R. (2000) The lore of the RINGs: substrate recognition and catalysis by ubiquitin ligases *Trends Cell Biol.* **10,** 429-439
190. Joazeiro, C. A. P., Weissman, A. M. (2000) RING finger proteins: mediators of ubiquitin ligase activity *Cell* **102,** 549-552
191. Murray, A. W. (2004) Recycling the cell cycle: cyclins revisited *Cell* **116,** 221-234
192. Brooks, C. L., Gu, W. (2003) Ubiquitination, phosphorylation and acetylation: the molecular basis for p53 regulation *Curr. Opin. Cell Biol.* **15,** 164-171

193. Kwon, Y. T., Kashina, A. S., Davydov, I. V., Hu, R. -G., An, J. Y., Seo, J. W., Du, F., Varshavsky, A. (2002) An essential role of N-terminal arginylation in cardiovascular development *Science* **297,** 96-99
194. Pickart, C. M. (2004) Back to the future with ubiquitin *Cell* **116,** 181-190
195. Werner, E. R., Gorren, A. C., Heller, G., Werner-Felmayer, G., Mayer, B. (2003) Tetrahydrobiopterin and nitric oxide: mechanistic and pharmacological aspects *Exp. Biol. Med.* **228,** 1291-1302
196. Gross, S. S., Levi, R. (1992) Tetrahydrobiopterin syntesis. An absolute requirement for cytokine-induced nitric oxide generation by vascular smooth muscle *J. Biol. Chem.* **267,** 25722-25729
197. Delgado-Esteban, M., Almeida, A., Medina, J. M. (2002) Tetrahydrobiopterin deficiency increases neuronal vulnerability to hypoxia *J. Neurochem.* **82,** 1148-1159

Chapter II

Tetrahydrobiopterin Protects Against Guanabenz-mediated Inhibition of Neuronal NO Synthase In Vitro and In Vivo

Summary

It is established that guanabenz inhibits neuronal NO-synthase (nNOS) and causes the enhanced proteasomal degradation of nNOS *in vivo*. Although the time- and NADPH- dependent inhibition of nNOS has been reported in studies where guanabenz was incubated with crude cytosolic preparations of nNOS, the exact mechanism for inhibition is not known. Moreover, even less is known about how the inhibition of nNOS triggers its proteasomal degradation. In the current study, we show with the use of purified nNOS that guanabenz treatment leads to the oxidation of tetrahydrobiopterin and formation of a pterin-depleted nNOS, which is not able to form NO. With the use of ^{14}C-labeled guanabenz, we were unable to detect any guanabenz metabolites or guanabenz-nNOS adducts, indicating that reactive intermediates of guanabenz likely do not play a role in the inhibition. Superoxide dismutase, however, prevents the guanabenz-mediated oxidation of tetrahydrobiopterin and inhibition of nNOS, suggesting the role of superoxide as an intermediate. Studies in rats show that administration of tetrahydrobiopterin prevents the inhibition and loss of penile nNOS due to guanabenz, indicating that the loss of tetrahydrobiopterin plays a major role in the effects of guanabenz *in vivo*. Our findings are consistent with the destabilization and enhanced

degradation of nNOS found after tetrahydrobiopterin depletion. These studies suggest that drug-mediated destabilization and subsequent enhanced degradation of protein targets will likely be an important toxicological consideration.

Introduction

Nitric oxide synthase (NOS) plays a key role in a variety of physiological processes, including neurotransmission and penile erection (1, 2). Clinical experience and several publications have linked prescribed drugs with sexual dysfunction (3, 4). The antihypertensive agents, in particular, are commonly associated with drug-induced impotence (4). Guanabenz, an antihypertensive agent associated with impotence (4, 5), inhibits NOS activity in penile tissue (6) and brain cortex (7) after administration of the drug to rats. Interestingly, the loss of activity is concomitant with the loss of immunodetectable nNOS in penile tissue (6). Consistent with this finding, guanabenz inhibits nNOS and enhances the proteasomal degradation of the enzyme in HEK 293 cells (8). Guanabenz causes the time- and NADPH- dependent inhibition of nNOS in an *in vitro* system containing penile cytosol (6, 8). It is noteworthy that other time- and NADPH- dependent inhibitors of nNOS, such as N^G-methyl-L-arginine and N^5-(1-iminoethyl)-L-ornithine, also enhance the proteasomal degradation of the enzyme in cells (8). The trigger is not due to the activity loss per se as reversible inhibitors, such as N^G-nitro-L-arginine and 7-nitroindazole, do not enhance degradation of nNOS and may actually stabilize the protein (6, 8).

We wondered how the time-dependent inhibition of nNOS renders the enzyme susceptible for degradation. Although guanabenz is well characterized with respect to

degradation of nNOS in cells and in rats, relatively little is known about how guanabenz inhibits nNOS. In the current study, we chose to address this question with the use of purified nNOS in the hopes of understanding what dysfunctional forms of nNOS are recognized for degradation. We found that guanabenz causes a tetrahydrobiopterin (BH_4)-deficient state of nNOS due to the oxidative destruction of the pterin that is facilitated by the presence of NADPH. The addition of BH_4 completely reactivates this dysfunctional form of the enzyme. The administration of BH_4 to rats completely protects from guanabenz-mediated inhibition of nNOS as well as the loss of nNOS protein, suggesting that the pterin deficiency plays a major role in the *in vivo* effects of guanabenz on nNOS.

Materials and Methods

Materials

Guanabenz was purchased from Research Biochemicals International (Natick, MA). Glucose-6-phosphate, glucose 6-phosphate dehydrogenase, $NADP^+$, N^G-nitro-L-arginine, L-arginine, D-arginine, dihydropteridine reductase from sheep liver, calmodulin, catalase, superoxide dismutase, and NADPH were purchased from Sigma Aldrich (St. Louis, MO). Male Wistar rats were purchased from Charles River Laboratories (Wilmington, MA). (6R)-5,6,7,8-tetrahydro-L-biopterin (BH_4) was purchased from Dr. Schirk's Laboratory (Jona, Switzerland). The affinity-purified rabbit IgG against brain NOS used for immunoblotting nNOS was from BD Biosciences Transduction Laboratories (Lexington, KY). [Benzylidene carbon ^{14}C]-labeled guanabenz (56 mCi/mmol) was custom synthesized by Du Pont NEN (Boston, MA). L-[^{14}C(U)]-

arginine (330.0 mCi/mmol) and ^{125}I-Labeled antibody against rabbit IgG were purchased from PerkinElmer Life and Analytical Sciences (Boston, MA).

Methods

In vitro inhibition assays – For studies on the inactivation of purified nNOS, we overexpressed the enzyme in insect cells and purified the nNOS as previously described (9). Purified nNOS (80 μg/ml) was added to a 'first reaction mixture' of 40 mM potassium phosphate, pH 7.4, containing 0.2 mM $CaCl_2$, 2500 unit/ml superoxide dismutase, 1250 units/ml catalase, 20 μg/ml pure calmodulin, 0.23 mg/ml bovine serum albumin, and an NADPH-regenerating system composed of 0.4 mM $NADP^+$, 10 mM glucose 6-phosphate, and 1 unit of glucose 6-phosphate dehydrogenase/ml, expressed as final concentrations, in a total volume of 180 μl. After incubation at 30°C, aliquots (10 μl) of the first reaction mixture were transferred to an 'oxyhemoglobin assay mixture' containing 200 μM $CaCl_2$, 250 μM L-arginine, 100 units/ml catalase, 10 μg/ml crude calmodulin, 25 μM oxyhemoglobin, and the NADPH-regenerating system, in a total volume of 180 μl of 40 mM potassium phosphate, pH 7.4. The oxyhemoglobin assay mixture was incubated at 37°C, and the rate of NO-mediated oxidation of oxyhemoglobin was monitored by measuring the absorbance at λ401 nm-411 nm with a microtiter plate reader (SpectraMax Plus, Molecular Devices Corp., Sunnyvale, CA). The rate was determined from the linear portion of the time dependent changes in absorbance. In studies where endothelial NOS was used, the enzyme was overexpressed and purified as described (10). The assay conditions were the same as nNOS, except that 200 μg/ml of the endothelial NOS was used in the first reaction mixture and 20 μl aliquots were taken for the oxyhemoglobin assay mixture.

SDS-resistant dimer analysis – In studies where the SDS-resistant dimer was measured, we examined the samples by low temperature SDS-PAGE (11). nNOS forms a very tight dimer that is resistant to SDS at low temperatures. By keeping the samples on ice and running the SDS-PAGE with a cooling unit, the stable dimeric species can be visualized. In these studies, an aliquot (10 μl) of the first reaction mixture containing purified nNOS was quenched with an equal volume of sample buffer containing 5 % SDS, 20 % glycerol, 100 mM dithiothreitol, 200 μM L-arginine and 0.02 % bromophenol blue in 125 mM Tris-HCl, pH 6.8. The samples were kept on ice and 10 μl of the quenched sample was loaded for analysis by 6 % SDS-PAGE. Proteins were then transferred to nitrocellulose membranes (0.2 μm, BioRad) and probed with 0.1 % anti-nNOS. The immunoblots were then incubated a second time with ^{125}I-conjugated goat anti-rabbit IgGs to visualize the immunoreactive bands. The membranes were dried and exposed to X-OMAT film for 1 h at –80°C. The nitrocellulose bands corresponding to nNOS were excised and the radioactivity quantified by the use of a gamma counter.

HPLC analysis – The alteration of the heme prosthetic group was measured by HPLC similar to that described (12). HPLC was performed with the use of a Waters 600S controller, 717 plus autosampler, and 996 photodiode array detector (Waters Corp., Milford, MA). Samples were injected onto a reverse phase HPLC column (C4 Vydac, 5 μm, 0.21 x 15 cm) equilibrated with solvent A (0.1% trifluoroacetic acid) at a flow rate of 0.3 ml/min. A linear gradient to 75% and 100 % solvent B (0.1% trifluoroacetic acid in acetonitrile) was run over 30 min and 5 min, respectively. Absorbance at 220 nm and 400 nm was monitored.

Quantification of BH_4 and BH_2 – The amounts of BH_4 and BH_2 in the reaction mixtures were determined by use of an HPLC fluorescence method as described by Klatt et al (13). The method involves oxidization of BH_4 and BH_2 to biopterin by treatment with KI/I_2 solution under acidic conditions. To give the specific amount of BH_2, the KI/I_2 oxidation is done in a basic solution where BH_4 and BH_2 are oxidized to pterin and biopterin, respectively. Specifically for oxidation under acidic conditions, a 40-µl aliquot of the first reaction mixture was treated with 10 mM I_2 and 50 mM KI in a total volume of 50 µL of 100 mM HCl for 1 hr at room temperature in the dark. The solution was neutralized with 5 µl of 1.0 M NaOH and then 5 µl of 0.2 M ascorbate was added. An aliquot (30 µl) of the resulting solution was injected onto a reverse phase HPLC column (C18 Vydac 5 mm, 4.6 x 250 mm) equilibrated with 20 mM NaH_2PO_4, pH 3, with 5% methanol at a flow rate of 1 ml/min. The pterins were eluted with the same mobile phase and detected by fluorescence at excitation and emission wavelengths of 350 and 418 nm, respectively. The HPLC and analysis of pterins was performed with the use of a Waters systems described above and an Applied Biosystems Spectroflow 980 fluorescence detector. To oxidize the pterins under basic conditions, the first reaction mixture was treated as above except that 100 mM NaOH replaced 100 mM HCl and the final solution was neutralized with 5 µl of 1 M HCl.

Treatment of nNOS with ^{14}C-guanabenz – The purified nNOS was treated as described above in a first reaction mixture, except that nNOS (1.5 µM) was treated with 50 µM guanabenz (56 mCi/mmol) for 60 min at 22ºC. An aliquot (75 µl) was injected onto a reverse phase HPLC column (C4 Vydac 5 µm, 2.1 x 150 mm) equilibrated with solvent A (0.1% TFA) at a flow rate of 0.3 ml/min. A linear gradient to 75% solvent B

(0.1% TFA in acetonitrile) was run over 45 min and then a linear gradient to 100% B was run over the next 5 min. The absorbance at 220 nm was monitored. The radioactivity in the eluent was measured by an on-line radiochemical detector (Radiomatic 500TR, Packard, Downers Grove, IL)

Treatment of animals, sample preparation, and activity assays – Guanabenz was dissolved in physiological saline and administrated to male Wistar rats (150-250 g) at the indicated doses by intraperitoneal injection at 9:00 A.M. and 6:00 P.M. BH_4 was dissolved in 0.1 % (w/v) ascorbic acid in physiological saline and injected in a total volume of 1 ml, 30 min before the injection of guanabenz. The controls were given the appropriate volumes of physiological saline or 0.1 % (w/v) ascorbic acid in physiological saline. Rats were sacrificed by decapitation 16 h after the last injection. Whole deskinned penis was removed, washed with ice-cold physiological saline, cut into 1-2 mm pieces and homogenized in 1 ml of ice-cold homogenization buffer (10 mM Hepes, pH 7.5, containing 320 mM sucrose, 100 μM EDTA, 1.5 mM DTT, 10 μg/ml trypsin inhibitor, 10 mg/ml of leupeptin, 2 μg/ml of aprotinin, 1 mg/ml phenylmethanesulphonyl fluoride, and 100 μM BH_4) with the use of a metal tissue mincer (SDT Tissumizer®, Tekmar, Cincinnati, OH). The homogenate was centrifuged at 245,000 x g for 10 min at 4°C. The supernatant fraction was collected and frozen in liquid nitrogen and stored at – 80°C for later analysis. Protein concentration of these samples was determined by the method of Bradford (Bio-Rad, Hercules, CA) with the use of bovine serum albumin as a standard.

The NOS activity of samples from the *in vivo* studies were determined by adding the supernatant fraction (0.6 mg) to a 'citrulline assay mixture' containing 1 mM $CaCl_2$, 1

mM NADPH, 30 μM [^{14}C]-arginine (60 mCi/mmol), 100 μM BH_4, 10 μg/ml calmodulin in a total volume of 200 μl of 40 mM potassium phosphate, pH 7.4. The assay mixture was incubated at 37°C for 10 min and the amount of [^{14}C]-citrulline was determined as previously described (6). The formation of [^{14}C]-citrulline was linear over the 10-min period. For experiments on the *in vitro* inactivation of cytosolic NOS, the supernatant fraction from untreated rats was loaded onto a Sephadex G-25 M column (PD-10, Pharmacia Biotech, Piscataway, NJ) preequilibrated in 10 mM Hepes, pH 7.5, containing 320 mM sucrose, 100 μM EDTA, 1.5 mM DTT, 10 μg/ml trypsin inhibitor, 10 mg/ml of leupeptin, 2 μg/ml of aprotinin, and 1 mg/ml phenylmethanesulphonyl fluoride to remove endogenous arginine and excess BH_4. An aliquot (1.2 mg) of the gel-filtered fraction was placed in a 'reaction mixture' containing 1 mM $CaCl_2$, 1 mM NADPH, 10 μg/ml calmodulin, and the desired concentration of guanabenz, in a total volume of 1 ml of 40 mM potassium phosphate, pH 7.4. Aliquots (150 μl) were taken from the reaction mixture and placed in the citrulline assay mixture and the activity was determined as described above.

SDS PAGE and Western blotting – The penile supernatant fraction (15 μg of protein) was analyzed with the use of SDS-PAGE (4-12% gradient gel) as previously described (6). The gels were blotted onto a nitrocellulose membrane (Schleicher & Schuell, Keene, NH), blocked with 0.2 mg/ml thimerosal in Blotto solution (Advanced Biotechnologies Inc., Columbia, MD), and probed (1:250) with a mouse monoclonal antibody against brain NOS (Transduction Laboratories, Lexington, KY). An anti-mouse IgG antibody (1:10,000) conjugated to peroxidase (Boehringer Mannheim, Indianapolis, IN) was used as a secondary antibody. An ECL reagent (Amersham Life Science Inc.,

Arlington Heights, IL) and X-OMAT film (Kodak, Rochester, NY) was used to detect the peroxidase conjugate, as described by the manufacturer. The intensity of the bands was evaluated by a laser densitometer (Molecular Dynamics, Sunnyvale, CA). Differing amounts of cytosol prepared from rat brains or insect cells overexpressing neuronal NOS were analyzed to insure that the density was linearly dependent on the amount of NOS over the relevant concentration range.

In vitro ubiquitylation of guanabenz-treated nNOS – We used an *in vitro* ubiquitylation system containing fraction II that has been established to ubiquitylate nNOS by an ATP- dependent process (14). The specific detection of nNOS-ubiquitin conjugates has also been established (14). Fraction II was prepared from rabbit reticulocyte lysates as previously described (15). The nNOS was treated with 100 μM guanabenz as described above and an aliquot (160 μl) of this first reaction mixture was incubated at 37°C in a total volume of 400 μl of 50 mM Tris-HCl, pH 7.4, containing 2 mM dithiothreitol, 15 μM ubiquitin, an ATP-regenerating system (2 mM ATP, 10 mM creatine phosphate, 5 mM $MgCl_2$, and 10 units/ml creatine phosphokinase), and 0.4 mg/ml of fraction II. An aliquot (20 μl) of the samples were quenched with 20 μl of sample buffer containing 5% SDS, 20% glycerol, 100 mM dithiothreitol, and 0.02% bromophenol blue in 125 mM Tris-HCl, pH 6.8. The samples were boiled for 5 min and an aliquot (30 μl) was submitted to 6% SDS-PAGE (10 x 8 cm). Proteins were then transferred to nitrocellulose membranes (0.2 μm, BioRad) and probed with 0.5% anti-ubiquitin (DAKO, Carpinteria, CA). The immunoblots were then incubated a second time with ^{125}I-conjugated goat anti-rabbit IgGs to visualize the immunoreactive bands. The membranes were dried and exposed to X-OMAT film for 1 h at -80°C. The bands

corresponding to nNOS-ubiquitin were excised and the radioactivity quantified by the use of a gamma counter.

Statistical analysis – All values are reported as the mean ± standard error (S.E.). An upaired *t* test was used to compare values. Statistical significance was considered to be achieved at a level of $p < 0.05$. PRISM statistical software (Graphpad, San Diego, CA) was used for analysis of the data sets.

Results

Guanabenz-mediated inhibition of purified nNOS — It is established that guanabenz inhibits nNOS and enhances the proteolytic turnover of nNOS protein in cells (8). Consistent with this, administration of guanabenz to rats decreases nNOS activity and protein (6, 7). Moreover, the time-dependent inhibition of nNOS due to guanabenz has been characterized in *in vitro* studies with the use of penile cytosol (6). To better understand the mechanism of how guanabenz inhibits nNOS and causes the enhanced turnover of the enzyme, we chose to conduct studies with purified nNOS. We established here, for the first time, that guanabenz causes a time-dependent inhibition of purified nNOS (Fig. 2.1A, *closed squares*). There is a loss of activity even in the absence of guanabenz (*open squares*), albeit slower, representing an autoinactivation reaction. The half-life of the activity loss was 5.0 ± 1.8 min and 22.1 ± 6.9 min for the guanabenz-treated and untreated samples, respectively. These values are statistically different ($p < 0.05$). The loss of nNOS activity beyond this autoinactivation is dependent on the concentration of guanabenz (Fig. 2.1B). Taken together, these results are highly similar to those found when the nNOS in penile cytosol was treated with guanabenz (6).

Moreover, guanabenz did not inhibit endothelial NOS, suggesting that the action of guanabenz is selective (Fig. 2.1B, *inset*). The autoinactivation of nNOS in the absence of substrate or guanabenz is time-, calmodulin-, and NADPH- dependent (16). The autoinactivation could be due to alteration of critical amino acid residues, the prosthetic heme group, or tetrahydrobiopterin (16).

The time-dependent inhibition of activity is thought to produce a dysfunctional, altered form of nNOS that is preferentially ubiquitylated and proteasomally degraded (8). Recently, it was found that destabilization of the dimeric functional form of nNOS correlates with recognition for proteasomal degradation (17). Thus, we asked if guanabenz destabilizes nNOS dimers. As shown in Fig. 2.2A, the untreated nNOS exists in part as SDS-resistant dimers, which are visualized after low-temperature SDS-PAGE and subsequent immunoblotting (11). We quantified the bands corresponding to the dimer and monomer from these studies (Fig. 2.2B). This assay is not a measure of the dimeric content under native conditions, but is a measure of the amount of stable dimer that is not dissociated by SDS and, thus, underestimates the total dimeric content. Moreover, it is likely that the transfer efficiency of the dimer is lower than that of the monomer, further leading to the underestimation of dimeric content. Thus, we cannot determine the absolute amounts of each form, but we can determine the relative changes in dimer and monomer.

As shown in Fig. 2.2B, we found that the SDS-resistant dimeric form of the untreated nNOS is unstable (*closed circles*), likely reflecting an autoinactivation reaction. Treatment with guanabenz further destabilizes the dimeric nNOS (*closed squares*) and gives an increase in the monomeric nNOS (*open squares*). As shown in Fig. 2.2C, the

destabilization of the dimeric nNOS (*closed triangles*) and the formation of monomeric nNOS (*open triangles*) is dependent on the concentration of guanabenz. Both the time- and concentration- dependence of the loss of dimeric nNOS reflects the loss of nNOS activity seen above. These results are entirely consistent with the notion that destabilization of the dimer by guanabenz generates some altered nNOS form that is more susceptible for proteasomal degradation. We next sought to determine how guanabenz destabilizes the nNOS dimer.

As shown in Fig. 2.3A, we first determined the cofactor dependence of the inhibition by treating nNOS under the indicated conditions for 20 min in the presence (*open bars*) or absence (*closed bars*) of 100 μM guanabenz. The greatest decrease in activity due to guanabenz occurs when both calmodulin and NADPH are present. Under these conditions, the L-isomer, but not the D-isomer, of arginine protects from the inhibition, suggesting an active site directed process. These findings are similar to those found for nNOS in penile cytosol (6). However, unlike the previous observations with crude cytosol, approximately one-half of the activity is lost even when purified nNOS is treated with guanabenz in the absence of exogenous NADPH. Even under this condition, calmodulin is necessary for guanabenz-mediated inhibition of nNOS (data not shown). We wondered why NADPH was necessary for inhibition of the crude cytosolic preparation of nNOS (6) but not for the purified enzyme. To better understand the inactivation process and why there are seemingly disparate findings, we further investigated both the mechanism of inactivation without NADPH as well as that found with NADPH. In the course of our studies, we discovered that the concentration of BH_4 in the first reaction mixture is a critical factor and that the presence of NADPH,

superoxide dismutase and catalase also has an effect on the guanabenz-mediated inhibition of nNOS. To dissect these effects, we initially investigated the effect of BH_4 on the guanabenz-mediated inhibition of nNOS in the absence of superoxide dismutase and catalase (Fig. 2.3B). Under these conditions, guanabenz in the presence of NADPH causes a nearly complete inactivation of nNOS and the addition of BH_4 during the treatment has a protective effect (*solid circles*). Interestingly, NADPH alone has a large inhibitory effect, but in this case, the addition of even small amounts of BH_4 protects from the loss of activity (*c.f. solid squares* with *open squares*). Low levels of BH_4 also protect the enzyme when nNOS is treated with guanabenz in the absence of NADPH (*open circles*). Overall, greater inhibition of nNOS is observed when NADPH and guanabenz are present over that when NADPH is omitted (*c.f. solid circles* with *open circles*). This clearly demonstrates how NADPH-dependent inactivation of nNOS could be observed depending on the BH_4 concentration, and this likely explains the seemingly disparate observation made in a previous study on NADPH dependence (6).

As shown in Fig. 2.3C, BH_4 completely protects the enzyme from inactivation when nNOS is treated with guanabenz and NADPH in the presence of superoxide dismutase and catalase (*c.f. solid triangles* with *open triangles*). Also, the presence of superoxide dismutase and catalase protects against the autoinactivation of nNOS that occurs in the presence of NADPH. As a control, we show that BH_4 does not affect the inhibition of nNOS due to N^G-nitro-L-arginine, a slowly reversible active site directed inhibitor (*X*). It is noteworthy that N^G-nitro-L-arginine stabilizes the SDS-resistant dimeric form of nNOS (17). Thus, guanabenz appears to inhibit nNOS by a process that is antagonized by BH_4. We will show below that a BH_4 deficient enzyme is formed.

Tetrahydrobiopterin depletion as a mechanism for guanabenz-mediated inhibition of purified nNOS — Initially, we investigated the guanabenz-mediated inhibition of nNOS in the absence of NADPH. As shown in Fig. 2.4A, the calmodulin- and guanabenz– dependent loss of activity occurs concomitantly with the loss of BH_4. Approximately 60 % of the loss of BH_4 is accounted for by the formation of dihydrobiopterin (BH_2). As shown in Fig. 2.4B, the activity loss seen when nNOS is incubated with calmodulin and guanabenz in the absence of NADPH is completely reversed by the addition of BH_4 in the oxyhemoglobin assay mixture. A concentration of 0.1 μM BH_4 is sufficient for complete reversal, consistent with the approximate loss of BH_4. The restoration of activity is rapid, as there is no incubation step with BH_4 before the activity is measured. The restoration is nearly complete, suggesting that the depletion of BH_4 is the major mechanism for the activity loss under these conditions. It is noteworthy that in previous studies with the cytosolic fraction containing nNOS (6), BH_4 was present in the assay mixture; therefore the NADPH-independent inhibition of nNOS by guanabenz would have been obscured. There is also a loss of BH_4 after inhibition of nNOS in the presence of NADPH (Fig. 2.4C). The addition of dihydropteridine reductase, which reduces BH_2 to BH_4, abolishes the inhibition of nNOS due to guanabenz (Fig. 4C), indicating that the oxidation of BH_4 to BH_2 and the subsequent formation of a BH_4-deficient nNOS is the cause of the nNOS inhibition. Consistent with this finding, BH_4 completely reverses the inhibition of nNOS even when NADPH is present (Fig. 2.4D). This is similar to that found above for the inhibition when NADPH was omitted. Thus, under all conditions examined here, BH_4 deficiency is the major mechanism of nNOS inhibition due to guanabenz.

Superoxide dismutase prevents the guanabenz-mediated loss of nNOS activity and tetrahydrobiopterin — A more detailed analysis of the dependence on catalase and SOD was performed (Fig. 2.5). As shown in Fig. 2.5A, superoxide dismutase protects against the loss of activity with nearly complete protection at 1,000 units/ml (*solid circles*). Catalase at concentrations up to 400 units/ml has no effect (*solid triangles*). In a previous study, 100 units/ml of catalase completely protected nNOS from the oxidative inactivation caused by agmatine (16). Superoxide dismutase alone is nearly as effective as superoxide dismutase in combination with catalase (*solid squares*). Thus, it appears that the nNOS-mediated superoxide formation is mainly responsible for the activity loss. Consistent with these findings, superoxide dismutase alone could completely protect against the guanabenz-mediated loss of BH_4 (Fig. 2.5B).

Studies with radiolabeled guanabenz — The purified nNOS was treated with radiolabeled guanabenz to determine if any adducts of guanabenz with nNOS or guanabenz metabolites could be detected. As shown in Fig. 2.6A, reverse phase HPLC analysis of the entire first reaction mixture containing nNOS and radiolabeled guanabenz but not calmodulin gives a major radiolabeled peak (solid line, G) corresponding to guanabenz. The peak at 37 min with absorbance at 220 nm corresponds to nNOS (dashed line, NOS). Treatment of nNOS with radiolabeled guanabenz in the presence of calmodulin (CAM) did not cause an observable change in the radioactivity profile. We were thus unable to detect the metabolism of guanabenz. These results are consistent with the notion that BH_4 deficiency is the major mechanism of nNOS inhibition.

Tetrahydrobiopterin protects against guanabenz-mediated inhibition of penile NOS activity in rats — We sought to determine if the inhibition and loss of nNOS protein

in vivo could be ameliorated by BH_4. We utilized a previously established procedure for treatment of rats with 5 mg/kg/day guanabenz for four days (6). As shown in Fig. 2.7A, guanabenz causes an approximately 50% reduction in NOS activity and nNOS protein in penile tissue, highly similar to that previously described (6). The concurrent administration of 200 mg/kg/day of BH_4 completely abrogates the inhibitory effect of guanabenz and prevents the loss of nNOS protein. The administration of the same dose of BH_4 alone has no effect on NOS activity or level of nNOS protein. The dose dependence of the protection by BH_4 is shown in Fig. 2.7B. The amounts required to see an effect on nNOS are higher than those used in rats in previous studies on vascular function, which for the most part reflects endothelial NOS activity (18, 19). The effects of BH_4 on nNOS are not as well characterized and we know of no studies in penile tissue. To further examine the role of BH_4 on the guanabenz-mediated inactivation and protein turnover, we prepared desalted cytosol from penile tissue of untreated rats for use in *in vitro* inactivation studies. As shown in Fig. 2.7C, 100 μM guanabenz decreases nNOS activity by approximately one-half after treatment for 15 min (*solid circles*). We found that the addition of BH_4 in the reaction mixture completely prevents the inactivation due to guanabenz, with a concentration of 1μM giving nearly complete protection. The concentration dependence of BH_4 found here is highly similar to the concentration dependence reported for the activation of nNOS in desalted rat cerebellar cytosol where 1 μM BH_4 was required for maximal activation of nNOS (20). The addition of BH_4 does not increase the activity of the untreated sample (*X*) nor protect against the inhibition by N^G-nitro-L-arginine (*open circles*), a slowly reversible active site-directed inhibitor. These results are highly similar to that found for the purified nNOS above.

In vitro ubiquitylation of guanabenz-treated nNOS – As shown in Fig. 2.8 upper panel, there is an ubiquitin conjugate that is readily visualized with anti-ubiquitin in the 160 kDa region. The identity of this band as a nNOS-ubiquitin conjugate has been previously established (14, 21). The band corresponding to nNOS-ubiquitin was quantified and plotted (Fig. 2.8, lower panel). There is an increase in the nNOS-ubiquitin conjugates found for guanabenz-treated nNOS (*lane 2*) over that for untreated nNOS (*lane 1*). When MG132, an inhibitor of the proteasome, is not present then the nNOS-ubiquitin conjugate due to guanabenz is greatly reduced (*lane 4*).

Discussion

Guanabenz is known to enhance the proteasomal degradation of nNOS (8). It is thought that this labilization of the protein for degradation involves some alteration of the structure of nNOS, such that it is recognized by cellular factors that in turn lead to nNOS ubiquitylation and degradation. In order to better understand how guanabenz causes the selective removal of nNOS by the proteasome, we chose in the current study to determine how guanabenz alters nNOS. We found that guanabenz causes a destabilization of the native dimeric structure of the purified enzyme. This destabilization was due to the guanabenz-mediated, nNOS-catalyzed destruction of BH_4, which stabilizes the active dimeric state of nNOS. Moreover, the treatment of rats with BH_4 completely protects from the guanabenz-mediated inhibition and loss of penile nNOS. Although this suggests that the loss of BH_4 is a mechanism for the inhibition and loss of nNOS *in vivo*, further studies on BH_4 are needed to fully understand the molecular mechanisms responsible.

Superoxide dismutase, but not catalase, prevents the loss of BH_4 from purified nNOS treated with guanabenz, indicating that nNOS-derived superoxide is responsible for the loss of BH_4. The reaction of superoxide with tetrahydrobiopterin has been previously reported and shown to form BH_2 (22). Dihydropteridine reductase, which reduces BH_2 to BH_4, completely protects against the guanabenz-mediated inhibition of nNOS activity and loss of BH_4, strongly suggesting that BH_4 is oxidized to BH_2. However, under *in vivo* conditions where L-arginine is present, it appears that other reactive metabolites such as peroxynitrite, which can form by the reaction of superoxide with NO, are more likely the actual agents responsible for BH_4 oxidation (23-25).

In the case of nNOS, BH_4 is known to stabilize the native dimeric state of the enzyme and thus the oxidation of the BH_4 would destabilize the dimeric form, consistent with our findings. This may be important as destabilization of the dimer has recently been shown to lead to the ubiquitylation of nNOS *in vitro* (17) and in cells (14). This notion is furthered by the finding that stabilization of the dimeric form of nNOS by N^G-nitro-L-arginine or 7-nitroindazole protects nNOS from proteasomal degradation (17).

Although dimer stabilization plays an important role, the actual signal or recognition site for degradation is not clear. The trigger may be due to exposure of a site that is normally hidden in the active dimeric form of nNOS, a general unfolding of nNOS after perturbation of the BH_4 site, or exposure of hydrophobic residues in the heme active site cleft (26). A recent report on the structure of a loose dimer of NOS with a partially exposed active center and destabilized subdomains is entirely consistent with this view (27). The cellular factors that recognize the dysfunctional altered nNOS are also not known. In this respect, we have recently found that CHIP (C-terminus of Hsc70

interacting protein), a chaperone assisted E3 ubiquitin ligase, ubiquitylates nNOS in cells, as well as in an *in vitro* system containing purified E1 ubiquitin activating enzyme, an E2 conjugating enzyme (UbcH5a), CHIP, GST-tagged ubiquitin, and an ATP-generating system (26). The addition of purified hsp70 and hsp40 to this *in vitro* system greatly enhances the amount of nNOS-ubiquitin conjugates, suggesting that CHIP is an E3 ligase for nNOS whose action is facilitated by, and possibly requires, its interaction with nNOS-bound hsp70. This raises the possibility that hsp70 directly mediates protein triage decisions by recognition of destabilized nNOS and recruiting ubiquitin ligase machinery that involves CHIP. It remains to be determined if the guanabenz-treated nNOS is preferentially recognized by the hsp70-based chaperones in this manner. However, we did demonstrate that guanabenz-inactivated nNOS was labilized for ubiquitylation in an *in vitro* system that contains a crude preparation of reticulocyte proteins, including hsp70. The molecular mechanism by which dysfunctional forms of nNOS are recognized must be a fundamental biological process that maintains the quality of the nNOS protein in cells. We describe here how guanabenz may perturb this regulatory process to cause a prolonged decrease in nNOS activity and protein levels. The xenobiotic-mediated redox regulation of BH_4 may be important in understanding how chemicals inhibit and cause the loss of nNOS *in vivo*. The interactions of drug molecules in protein quality control will likely be an important pharmacological and toxicological consideration in the development of safer and more effective drugs.

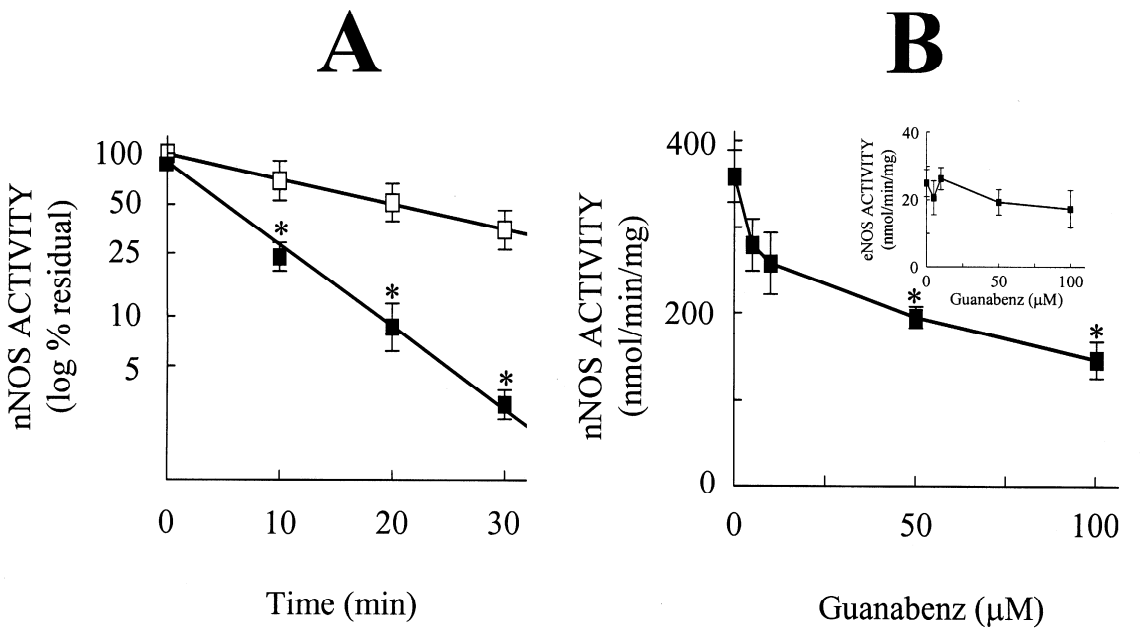

Fig. 2.1. **Guanabenz-mediated inactivation of purified nNOS.** *A,* indicates the time-dependent loss of nNOS activity due to guanabenz on a semi-log plot. Closed squares, treated with 100 μM guanabenz; open squares, untreated. The inactivation of nNOS activity was determined with the use of the modified first reaction mixture and oxyhemoglobin assay mixture as described in *Materials and Methods.* The half-life for each condition was calculated by least squares fitting of the semi-log plot. *denotes NOS activity was significantly ($p < 0.05$) lower for the guanabenz treated sample than that for control. *B,* indicates the effect of varying the concentration of guanabenz in the first reaction mixture. The amount of guanbenz is indicated and the activities were measured after 20 min of incubation. *Inset*, the endothelial NOS replaced nNOS and the effects of guanabenz were determined. *denotes significantly ($p < 0.05$) different from untreated. The values are the mean ± S.E. (n = 3).

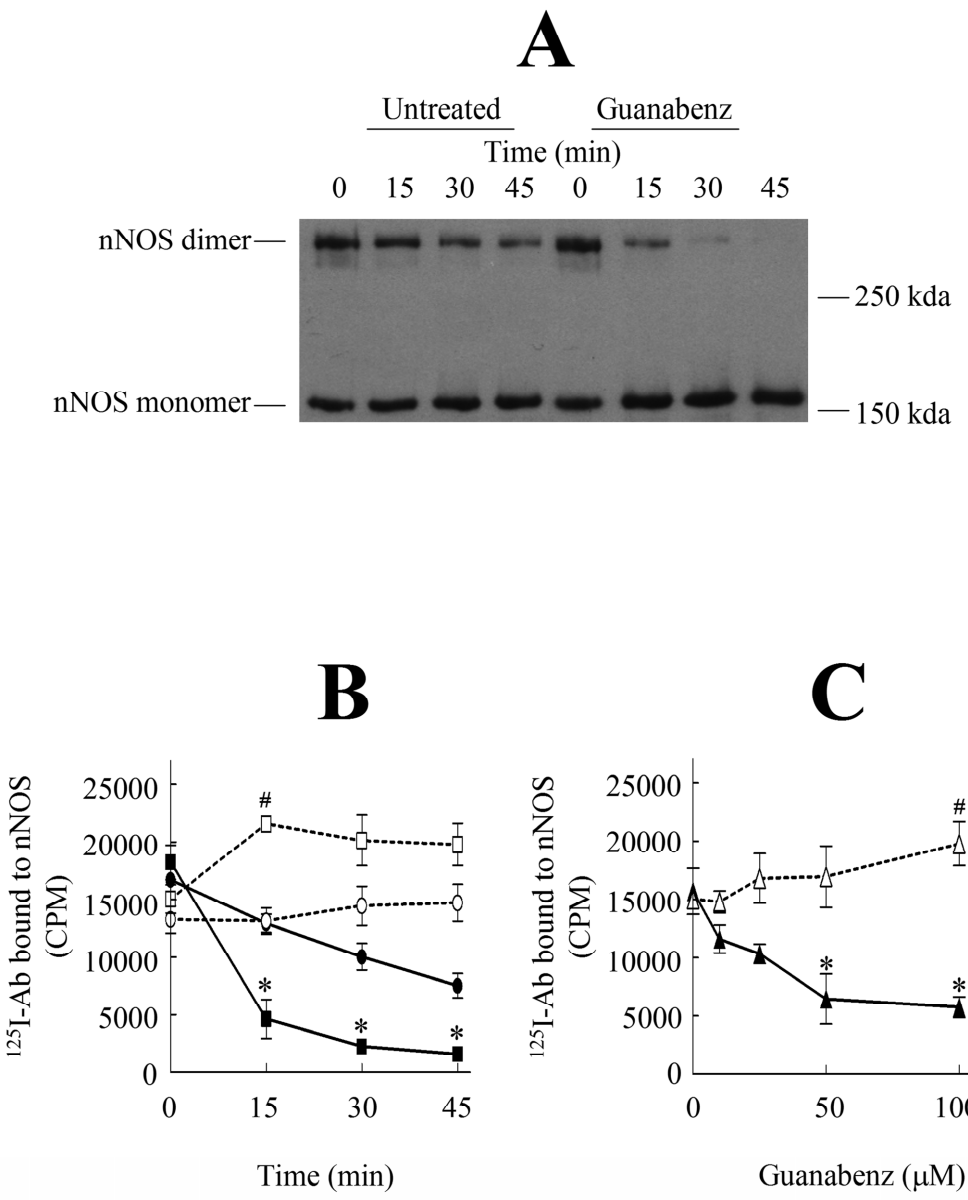

Fig. 2.2. **Effect of guanabenz on the amount of SDS-resistant dimer of nNOS**. The nNOS was treated with guanabenz as described and the amount of the SDS-resistant dimer (*nNOS dimer*) and the remainder of the nNOS that runs as a monomer (*nNOS monomer*) were measured. *A*, western blot of the reaction mixture of untreated nNOS (*Untreated*) or nNOS treated with guanabenz (*Guanabenz*) for 0, 15, 30, and 45 min. *B*, the bands corresponding to the nNOS dimer and monomer in *A* were quantified by the use of ^{125}I-labeled goat anti-rabbit IgG. Circles, untreated; squares, guanabenz-treated. The dimeric nNOS is represented by the closed symbols and the solid lines, and the monomeric nNOS is represented by the open symbols and the dashed lines. *denotes significantly ($p < 0.05$) lower dimer for guanabenz-treated versus untreated. #denotes significantly ($p < 0.05$) higher monomer for guanabenz treated over the untreated. *C*, the effect of varying the concentration of guanabenz on the amount of SDS-resistant dimer after treatment for 20 min. The bands were quantified as in B. Solid triangles, nNOS dimer; open triangles, monomeric nNOS. *denotes significantly ($p < 0.05$) lower dimer than untreated. #denotes significantly ($p < 0.05$) higher monomer than untreated. The values are the mean ± S.E. (n = 3).

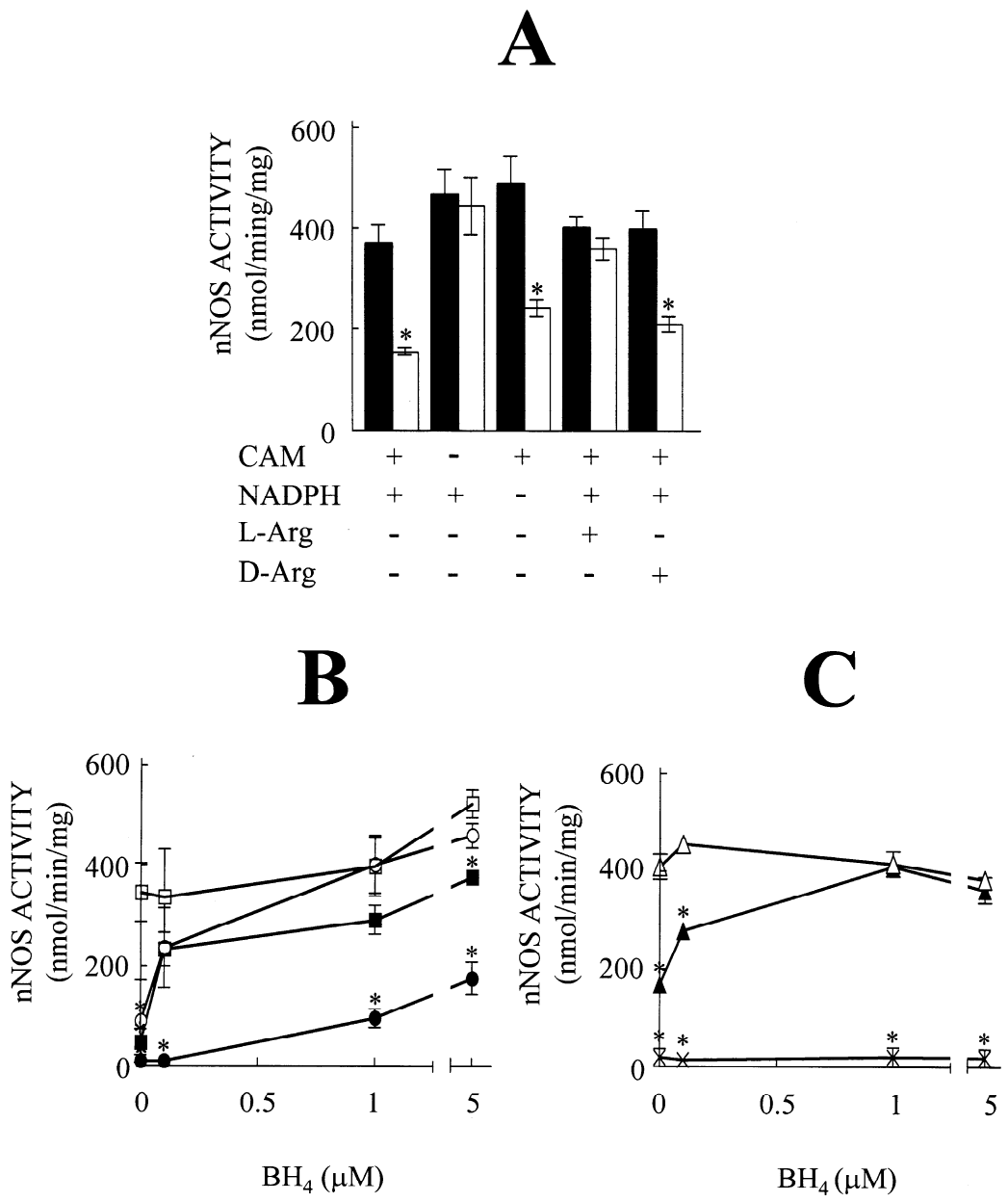

Fig. 2.3. **Effect of substrate, NADPH, tetrahydrobiopterin, and calmodulin, on the guanabenz-mediated inactivation of nNOS**. *A,* indicates the effect of calmodulin (CAM), NADPH, L-arginine (L-Arg), and D-arginine (D-Arg) on the extent of inhibition of nNOS after treatment for 20 min with 100 μM guanabenz (*open bars*) or untreated (*solid bars*). *B*, indicates the protective effect of BH_4 on the inhibition of nNOS caused by guanabenz when superoxide dismutase and catalase were omitted from the first reaction mixture described in *Methods*. nNOS was either treated with 100 μM guanabenz (*circles*) or untreated (*squares*). Open symbols, NADPH was omitted from the first reaction mixture; closed symbols, NADPH was present in the first reaction mixture. *C*, indicates the protective effect of BH_4 on the extent of inhibition of purified nNOS caused by 100 μM guanabenz (*closed triangles*), 10 μM N^G-nitro-L-arginine (*X*), or untreated (*open triangles*) in the first reaction mixture. This mixture contained superoxide dismutase, catalase, and NADPH. The values are the mean ± S.E. (n = 3). *denotes significantly ($p < 0.05$) lower activity for treated versus untreated.

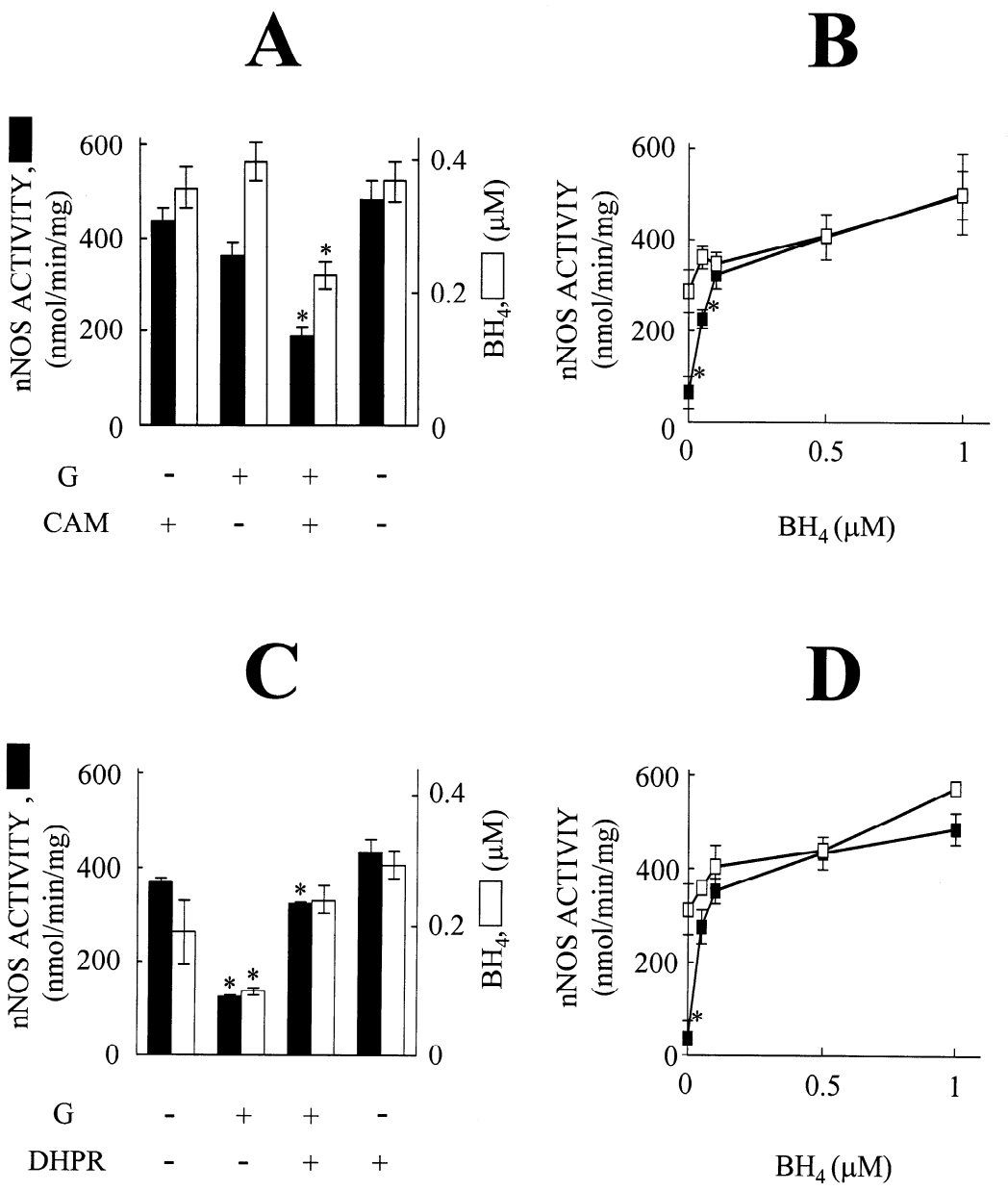

Fig. 2.4. **Guanabenz causes the loss of nNOS activity and tetrahydrobiopterin**. *A*, guanabenz causes the loss of BH_4. The nNOS was treated with 100 μM guanabenz for 20 min in the first reaction mixture as indicated in *Methods*, except that NADPH was omitted. The amount of BH_4 present in the first reaction mixture was measured by HPLC and compared to the nNOS activity. The presence of calmodulin and guanabenz are as indicated. *B,* the activity loss due to guanabenz is reversed by addition of BH_4 to the oxyhemoglobin assay mixture. The activity was measured by the oxyhemoglobin assay containing the indicated amounts of BH_4. Closed squares, nNOS treated with guanabenz; open squares, untreated nNOS. *C*, the conditions were as in A, except that NADPH was present in the first reaction mixture. All samples contained calmodulin and some samples contained 10 units/ml of dihydropteridine reductase (DHPR) as indicated. *D*, the conditions were as in B, except that NADPH was present in the first reaction mixture. The values are the mean ± S.E. (n = 3). *denotes significantly ($p < 0.05$) lower values for guanabenz treated versus untreated.

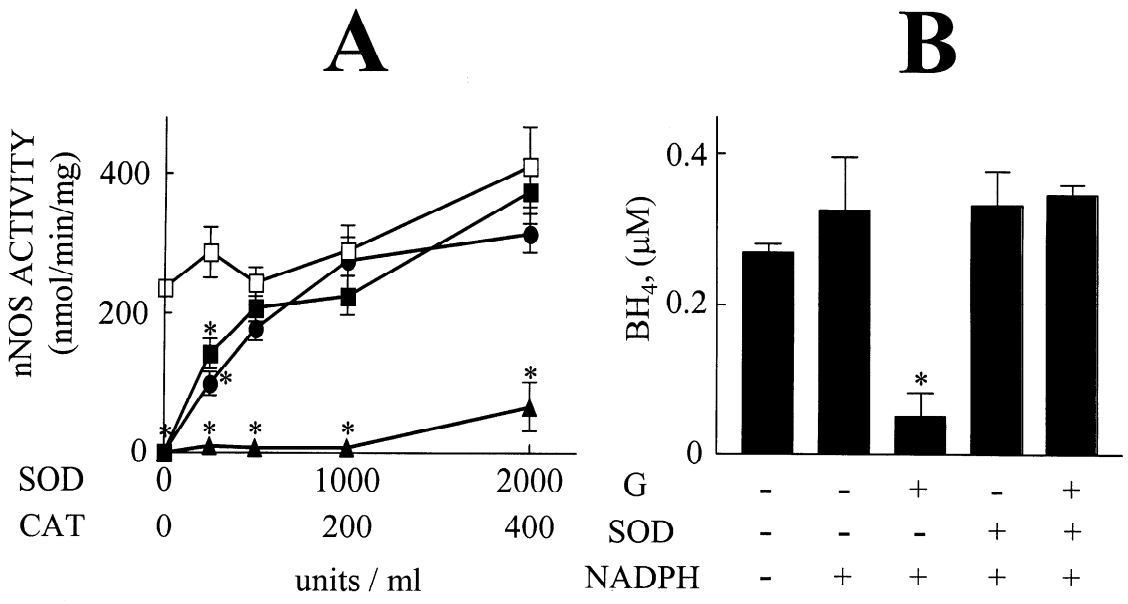

Fig. 2.5. **Effect of superoxide dismutase on the guanabenz-mediated loss of nNOS activity and tetrahydrobiopterin.** The nNOS was treated with guanabenz (100 μM) for 20 min and the nNOS activity and pterin were measured as described in *Methods*. *A,* nNOS activity. The amount of superoxide dismutase (SOD) or catalase (CAT) or both were varied in the reaction mixtures treated with guanabenz. Closed squares, a combination of SOD and CAT were added; closed circles, SOD was added; closed triangles, CAT was added. As a control, SOD and CAT were added to a reaction mixture not treated with guanabenz (*open squares*). *B*, tetrahydrobiopterin. The 100 μM guanabenz (G), 2,500 units/ml superoxide disumutase (SOD), or 1mM NADPH was omitted from the reaction mixtures as indicated. The values are the mean ± S.E. (n = 3). *denotes significantly ($p < 0.05$) lower values relative to untreated.

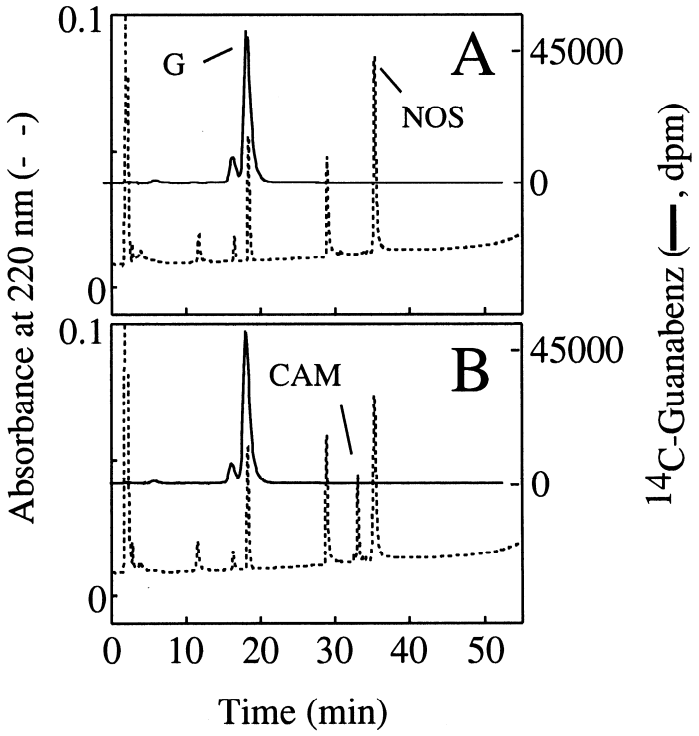

Fig. 2.6. **HPLC profile of nNOS treated with ^{14}C-labeled guanabenz in the absence or presence of calmodulin.** The nNOS was treated with radiolabeled guanabenz as described in *Methods. A,* indicates nNOS treated with guanabenz in the absence of calmodulin. *B,* indicates nNOS treated with guanabenz in the presence of calmodulin. The residual activity was 85% and 38% for the untreated and guanabenz treated sample, respectively. G, guanabenz; NOS, nNOS; CAM, calmodulin.

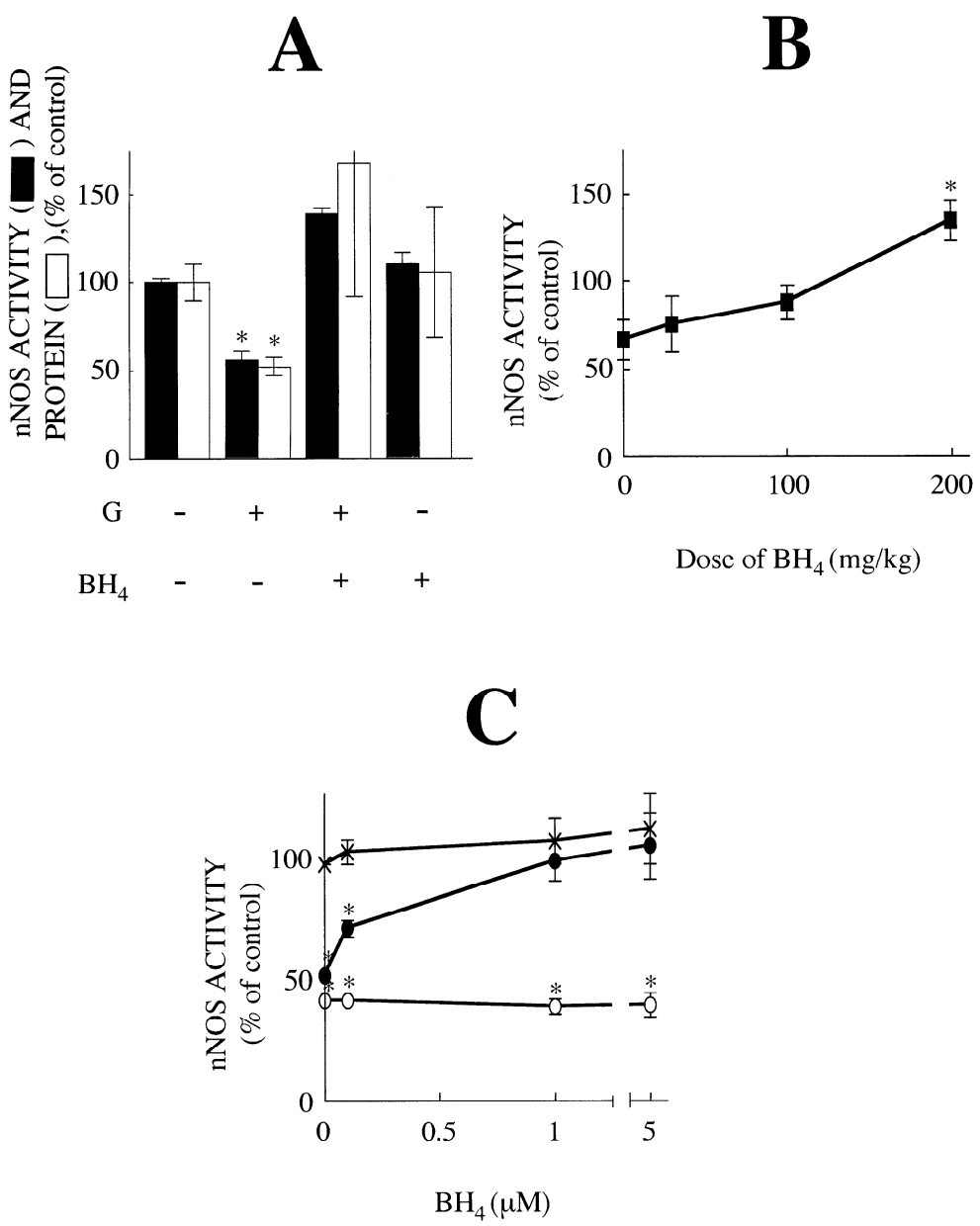

Fig. 2.7. **Tetrahydrobiopterin protects against guanabenz-mediated inactivation and loss of penile nNOS in rats.** *A,* indicates the effect of guanabenz (5mg/kg/day) and BH_4 (200 mg/kg/day) on penile NOS activity (*solid bars*) and penile nNOS protein (*open bars*) after treatment of rats for four days. The treatment of the rats and the measurement of activity by the citrulline assay are as described in *Methods.* *denotes significantly ($p < 0.05$) lower values relative to untreated. *B,* indicates the dose response of BH_4 on the penile nNOS activity under conditions of *A.* *denotes significantly ($p < 0.05$) higher activity relative to untreated. *C,* indicates the treatment of penile cytosol *in vitro* with guanabenz and BH_4. The inactivation of nNOS activity was determined with the use of the reaction mixture and citrulline assay mixture as described in *Methods.* The reaction mixture was incubated for 15 min in the presence of the following: closed circles, 100 μM guanabenz; open circles, 5 μM N^G-nitro-L-arginine; x, untreated. The indicated amounts of BH_4 were added to the reaction mixture. The values are the mean ± S.E. (n = 3). *denotes significantly ($p < 0.05$) lower activity relative to untreated.

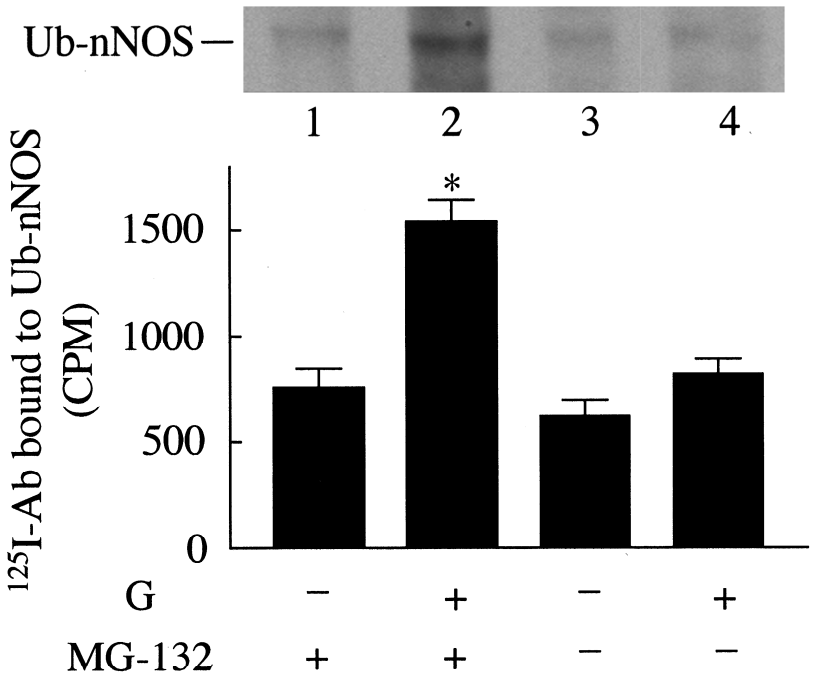

Fig. 2.8. **Guanabenz-treated nNOS is labilized for ubiquitylation in an in vitro system containing fraction II.** Purified nNOS was treated with 100 μM guanabenz (G) and then placed in a reaction mixture containing ubiquitin, ATP, and fraction II. The generation and detection of the nNOS ubiquitin conjugates are as described in *Methods*. The values are the mean ± S.E. (n = 3). *denotes significantly ($p < 0.05$) higher nNOS-Ub conjugates relative to untreated.

References

1. Moncada, S., Palmer, R. M. J., Higgs, E. A. (1991) Nitric oxide: Physiology, pathophysiology, and pharmacology *Pharmacol Rev* **43,** 109-142.
2. Burnett, A. L., Lowenstein, C. J., Bredt, D. S., Chang, T. S., Snyder, S. H. (1992) Nitric oxide: a physiological mediator of penile erection *Science* **257,** 401-403.
3. Slag, M. F., Morley, J. E., Elson, M. K., Trence, D. L., Nelson, C. J., Nelson, A. E., Kinlaw, W. B., Beyer, H. S., Nuttall, F. Q., Shafer, R. B. (1983) Impotence in medical clinic outpatients *JAMA* **249,** 1736-1740.
4. Brock, G. B., Lue, T. F. (1993) Drug-induced male sexual dysfunction. An update *Drug Saf.* **8,** 414-426.
5. Weiss, R. J. (1991) Effects of antihypertensive agents on sexual function *Am Fam Physician* **44,** 2075-2082.
6. Nakatsuka, M., Nakatsuka, K., Osawa, Y. (1998) Metabolism-based inactivation of penile nitric oxide synthase activity by guanabenz *Drug Metab Dispos* **26,** 497-501.
7. Dambrova, M., Kirjanova, O., Baumane, L., Liepinsh, E., Zvejniece, L., Muceniece, R., Kalvinsh, I., Wikberg, J. E. (2003) EPR investigation of in vivo inhibitory effect of guanidine compounds on nitric oxide production in rat tissues *J Physiol Pharmacol* **54,** 339-347.
8. Noguchi, S., Jianmongkol, S., Bender, A. T., Kamada, Y., Demady, D. R., Osawa, Y. (2000) Guanabenz-mediated inactivation and enhanced proteolytic. *J Biol Chem* **275,** 2376-2380.
9. Billecke, S. S., Draganov, D. I., Morishima, Y., Murphy, P. J., Dunbar, A. Y., Pratt, W. B., Osawa, Y. (2004) The Role of hsp90 in Heme-Dependent Activation of Apo-Neuronal Nitric-Oxide Synthase *J. Biol. Chem.* **279,** 30252-30258.
10. Lowe, E. R., Everett, A. C., Lee, A. J., Lau, M., Dunbar, A. Y., Berka, V., Tsai, A. L., Osawa, Y. (2005) Time-dependent inhibition and tetrahydrobiopterin depletion of endothelial nitric-oxide synthase caused by cigarettes *Drug Metab. Dispos.* **33,** 131-138.
11. Klatt, P., Schmidt, K., Lehner, D., Glatter, O., Bachinger, H. P., Mayer, B. (1995) Structural analysis of porcine brain nitric oxide synthase reveals a role for tetrahydrobiopterin and L-arginine in the formation of an SDS-resistant dimer *EMBO J.* **14,** 3687-3695.
12. Jianmongkol, S., Vuletich, J. L., Bender, A. T., Demady, D. R., Osawa, Y. (2000) Aminoguanidine-mediated inactivation and alteration of neuronal nitric oxide synthase *J Biol Chem* **275,** 13370-13376.
13. Klatt, P., Schmidt, K., Werner, E. R., Mayer, B. (1996) Determination of nitric oxide synthase cofactors: heme, FAD, FMN, and tetrahydrobiopterin *Methods Enzymol.* **268,** 358-365.
14. Kamada, Y., Jenkins, G. J., Lau, M., Dunbar, A. Y., Lowe, E. R., Osawa, Y. (2005) Tetrahydrobiopterin depletion and ubiquitylation of neuronal nitric oxide synthase *Molec Brain Res* **142,** 19-27.
15. Hershko, A., Heller, H., Elias, S., Ciechanover, A. (1983) Components of ubiquitin-protein ligase system. Resolution, affinity purification, and role in protein breakdown *J Biol Chem* **258,** 8206-8214.

16. Demady, D. R., Jianmongkol, S., Vuletich, J. L., Bender, A. T., Osawa, Y. (2001) Agmatine enhances the NADPH oxidase activity of neuronal NO synthase and leads to oxidative inactivation of the enzyme *Mol Pharmacol* **59,** 24-29.
17. Dunbar, A. Y., Kamada, Y., Jenkins, G. J., Lowe, E. R., Billecke, S. S., Osawa, Y. (2004) Ubiquitination and degradation of neuronal nitric-oxide synthase in vitro: dimer stabilization protects the enzyme from proteolysis *Mol Pharmacol* **66,** 964-969.
18. Hong, H. J., Hsiao, G., Cheng, T. H., Yen, M. H. (2001) Supplemention with tetrahydrobiopterin suppresses the development of hypertension in spontaneously hypertensive rats *Hypertension* **38,** 1044-1048.
19. Podjarny, E. Hasdan, G., Bernheim, J., Rashid, G., Green, J., Korzets, Z. (2004) Effect of chronic tetrahydrobiopterin supplementation on blood pressure and proteinuria in 5/6 nephrectomized rats *Nephrol Dial Tansplant* **19,** 2223-2227.
20. Nunokawa, Y., Ishihara, T., Kanai, T., Noguchi, T. (1992) (6R)-5,6,7,8-tetrahydro-L-biopterin modulates nitric oxide-associated soluble guanylate cyclase activity in the rat cerebellum *Arch Biochem Biophys* **298,** 726-730.
21. Bender, A. T., Demady, D. R., Osawa, Y. (2000) Ubiquitination of neuronal nitric oxide synthase in vitro and in vivo *J Biol Chem* **275,** 17407-17411
22. Vasquez-Vivar, J., Whitsett, J., Martasek, P., Hogg, N., Kalyanaraman, B. (2001) Reaction of tetrahydrobiopterin with superoxide: EPR-kinetic analysis and characterization of the pteridine radical *Free Radical Biol Med* **31,** 975-985.
23. Milstien, S., Katusic, Z. (1999) Oxidation of tetrahydrobiopterin by peroxynitrite: implications for vascular endothelial function *Biochem Biophys Res Commun* **263,** 681-684.
24. Laursen, J. B., Somers, M., Kurz, S., McCann, L., Warnholtz, A., Freeman, B. A., Tarpey, M., Fukai, T., Harrison, D. G. (2001) Endothelial regulation of vasomotion in apoE-deficient mice: implications for interactions between peroxynitrite and tetrahydrobiopterin *Circulation* **103,** 1282-1288.
25. Kuzkaya, N., Weissmann, N., Harrison, D. G., Dikalov, S. (2003) Interactions of peroxynitrite, tetrahydrobiopterin, ascorbic acid, and thiols: implications for uncoupling endothelial nitric-oxide synthase *J Biol Chem* **278,** 22546-22554.
26. Peng, H. –M., Morishima, Y., Jenkins, G. J., Dunbar, A. Y., Lau, M., Patterson, C., Pratt, W. B., Osawa, Y. (2004) Ubiquitylation of neuronal nitric-oxide synthase by CHIP, a chaperone-dependent E3 ligase *J Biol Chem* **279,** 52970-52977.
27. Pant, K., Crane, B. R.(2005) Structure of a loose dimer: an intermediate in nitric oxide synthase assembly *J Mol Biol* **352,** 932-940.

Chapter III

Tetrahydrobiopterin Depletion and Ubiquitylation of Neuronal Nitric Oxide Synthase

Summary

Tetrahydrobiopterin is a necessary cofactor for the synthesis of nitric oxide by the hemeprotein enzyme, NO-synthase (NOS). It is widely thought that inadequate levels of tetrahydrobiopterin lead to tissue injury and organ dysfunction due, in part, to formation of superoxide from pterin-deficient NOS. In the course of studies on the ubiquitylation of neuronal NOS, we have found that certain substrate analogs, such as N^G-nitro-L-arginine, stabilize the dimeric form of nNOS and protect the enzyme from ubiquitylation. Since tetrahydrobiopterin is known to bind near heme and confers stability to the active dimeric structure of nNOS, we wondered if the loss of tetrahydrobiopterin could be an endogenous signal for nNOS ubiquitylation and degradation. We show here that depletion of tetrahydrobiopterin in HEK293 cells stably transfected with nNOS by treatment with 2,4-diamino-6-hydroxypyrimidine leads to destabilization of the dimeric form and enhances ubiquitylation of nNOS. Sepiapterin, a precursor to tetrahydrobiopterin in the salvage pathway, completely reverses the effect of 2,4-diamino-6-hydroxypyrimidine on nNOS ubiquitylation. Consistent with that found in cells, the *in vitro* ubiquitylation of nNOS by reticulocyte proteins decreases when

tetrahydrobiopterin is present. Thus, inadequate amounts of tetrahydrobiopterin may lead to a sustained decrease in the steady state level of nNOS that is not readily reversed.

Introduction

Tetrahydrobiopterin is a cofactor of several amino acid metabolizing enzymes that are of importance in neurotransmitter synthesis. One of these enzymes is nitric oxide synthase (NOS), which requires tetrahydrobiopterin for metabolism of L-arginine to citrulline and NO. The importance of neuronal NOS (nNOS), inducible NOS, and endothelial NOS in neurotransmission, host defense, and vascular function, respectively, has brought much attention not only on the role of tetrahydrobiopterin deficit in a variety of diseases but also on the pharmacological supplementation of pterin (1). For example, numerous studies have described the improvement of vascular function and increased endothelial NOS activity when tetrahydrobiopterin levels are increased by pharmacological means (1). Conversely, the depletion of tetrahydrobiopterin has also been shown to decrease endothelial NOS activity and cause endothelial dysfunction (1). In the case of the inducible NOS, tetrahydrobiopterin depletion abrogates the ability of the enzyme to be upregulated by cytokines during an immune response (2). The effects of tetrahydrobiopterin depletion on nNOS have not been as well characterized as the other isoforms, although an increased vulnerability to hypoxia as well as nNOS dysfunction is observed in neurons (3). Overall, it is clear that an inadequate level of tetrahydrobiopterin is an important factor in a variety of pathological conditions involving NOS.

All the isoforms of NOS are ubiquitylated and proteasomally degraded (4-7). We have recently discovered that the heme-deficient monomeric form of nNOS is preferentially targeted (4, 8). Interestingly, N^G-nitro-L-arginine, a slowly reversible, active site directed, competitive inhibitor of nNOS stabilizes the heme-containing enzyme from ubiquitylation and degradation. Thus, it appears that some conformational effect related to the heme active site confers recognition for ubiquitylation. Since tetrahydrobiopterin is known to bind near heme and confers stability to the active dimeric structure of nNOS, we wondered if changes in tetrahydrobiopterin levels could be an endogenous signal for nNOS ubiquitylation and degradation.

We have directly examined this question in a HEK293 cell line that stably express nNOS as well as in an *in vitro* degradation model containing purified nNOS and partially purified reticulocyte proteins. In the current study, we found that decreased tetrahydrobiopterin levels enhance the ubiquitylation of nNOS in both models. Furthermore, tetrahydrobiopterin depletion in cells also leads to destabilization of the dimeric form of nNOS, but not to the loss of the prosthetic heme from nNOS. This indicates that a pool of inactive, heme-containing nNOS, which is not in a tightly associated homodimeric form, exists in cells. It appears that this pool of destabilized nNOS is labilized or susceptible to ubiquitylation and proteasomal degradation. Thus, the loss of nNOS protein should be considered as a long-term consequence of inadequate tetrahydrobiopterin levels in a variety of pathological and toxicological conditions.

Materials and Methods

Materials

Glucose-6-phosphate, glucose-6-phosphate dehydrogenase, 2,4-diamino-6-hydroxypyrimidine, calmodulin (crude, from bovine brain), horse heart myoglobin, anti-βtubulin antibody, L-arginine, leupeptin, NP40 (IGEPAL CA-630), A23187, ATP, ubiquitin, $MgCl_2$, creatine phosphokinase, hexokinase, and NADP+ were purchased from Sigma. (6R)-5,6,7,8-Tetrahydro-L-biopterin and sepiapterin were purchased from Dr. Schirck's Laboratory (Jona, Switzerland). The affinity-purified rabbit IgG against brain NOS used for immunoblotting nNOS was from Transduction Laboratories (Lexington, KY). ^{125}I-labelled goat antibody against rabbit IgG or mouse IgG were purchased from Perkin Elmer (Boston, MA). The affinity purified rabbit IgG used for Western blotting of ubiquitin was from DAKO Corporation (Carpinteria, CA). The rabbit antiserum used to immunoprecipitate nNOS was raised against rat neuronal NOS and was the generous gift of Dr. Lance Pohl (NHLBI, Bethesda). The antibody was affinity purified prior to use. Peroxidase conjugated anti-rabbit IgG antibody was from Boehringer Mannheim (Indianapolis, IN). Ubiquitin aldehyde was from Alexis Biochemicals (San Diego, CA). Untreated rabbit reticulocyte lysate was from Green Hectares (Oregon, WI). DE52 was purchased from Whatman Inc. (Fairfield, NJ). Cbz-leucine-leucine-leucinal (MG132) was purchased from BIOMOL (Plymouth Meeting, PA).

Methods

Cell culture and preparation of the cytosolic fraction - Human embryonic kidney 293 cells (HEK293) stably transfected with rat nNOS by Bredt et al. (9) were obtained

from Dr. Bettie Sue Masters (University of Texas Health Science Center, San Antonio, TX). HEK293 cells were cultured in Dulbecco's modified Eagle's medium (Life Technologies, Inc.) supplemented with 10% fetal bovine serum (Hyclone®), 20 mM Hepes, pH 7.4, and G418 (0.5 mg/mL, Geneticin®, Life Technologies, Inc.) as described previously (10). Prior to each experiment, the cells were cultured in DMEM containing 0.1 mM L-arginine (low arginine DMEM) for at least 12 hours. HEK cells were treated with 5.0 mM 2,4-diamino-6-hydroxypyrimidine (DP) and 100 μM sepiapterin (SP) similar to that previously used for other cells (2, 11). There was greater than 85% cell viability, as determined by trypan blue, for all conditions used in our studies. Cell viability was unaffected by DP or SP treatment. Sepiapterin was added in DMSO and the total concentration of DMSO did not exceed 0.2% in the medium. DMSO alone did not have any effects on the amount of monomeric or dimeric nNOS. HEK cells were harvested in their treatment medium, diluted 1:1 with ice-cold phosphate-buffered saline. The cells were then pelleted, washed 3-times with 5 mL of ice-cold phosphate-buffered saline, and pelleted again. The cell pellet was homogenized on ice with a Tenbroeck ground glass homogenizer in three-volumes of lysis buffer containing 50 mM Tris-HCl, pH 7.4, 1.0 mM EDTA, 1.0 mM DTT, 10 μg/mL trypsin inhibitor, 10 μg/mL leupeptin, 2 μg/mL aprotinin, and 5mM phenylmethylsulfonyl fluoride. Homogenates were centrifuged for 20 min at 16,000 x g and the supernatant was used for assays. For HPLC studies, the supernatant was removed and centrifuged for an additional 15 min at 100,000 x g to obtain a cytosolic fraction. For ubiquitin studies, the cell pellet was homogenized in HE lysis buffer containing 10 mM Hepes, pH 7.4, 0.32 M sucrose, 2.0 mM EDTA, 10 μg/mL trypsin inhibitor, 10 μg/mL leupeptin, 2 μg/mL aprotinin, 5 mM N-

ethylmaleimide (NEM), 10 mM Na_3VO_4, 1% NP40, and 6 mM phenylmethylsulfonyl fluoride. Homogenates were centrifuged for 20 min at 16,000 x g, the supernatant was used for assays.

Assay for SDS-resistant dimer of nNOS - To detect the SDS-resistant dimer of nNOS, we used a SDS-PAGE method previously described by Klatt *et al.* (12). Aliquots (50 μg) of the cytosol were added to 35 μl of ice-cold SDS sample buffer (250 mM Tris-HCl, pH 6.8, 10% SDS, 40% glycerol, 0.04% bromophenol blue, and 40 mM DTT) and resolved on 7% SDS-polyacrylamide gels. The samples were transferred to nitrocellulose membranes for 3 h at 850 mA. The electrophoresis and transfer were performed in a jacketed cooling system to insure that the samples were not warmed during the procedures. The membranes were probed with a 0.1% anti-nNOS polyclonal antibody from Transduction Laboratories. The immunoblots were then incubated a second time with ^{125}I-conjugated goat anti-rabbit IgGs to visualize the immunoreactive bands by X-ray film. For quantitation, each immunoreactive band was excised and counted by a gamma counter. As an internal control, the same procedure was used to quantify tubulin.

Detection of cellular ubiquitin-nNOS conjugates, immunoprecipitation, and western blotting - nNOS was immunoadsorbed from ~100 μg of HEK293 cytosol with 30 μl of anti-nNOS IgG and 20 μl of protein A Sepharose in a total volume of 400 μl of HE lysis buffer for 2 h at 4 ^{o}C. Immune pellets were boiled in SDS sample buffer and the proteins were resolved on 7% SDS-polyacrylamide gels and transferred to nitrocellulose membranes for 3 h at 850 mA. The membranes were probed with 0.1% anti-Ub polyclonal antibody. Prior to probing with the anti-Ub antibody, the nitrocellulose

membranes were autoclaved in distilled H_2O for 10 min. The immunoblots were then incubated a second time with ^{125}I-conjugated goat anti-rabbit IgGs for quantitation.

NOS activity assay - Aliquots (20 μL) of the cytosol were transferred to an 'oxyhemoglobin assay mixture' containing 200 μM $CaCl_2$, 100 μM L-arginine, 100 μM tetrahydrobiopterin, 100 units/ml catalase, 10 μg/ml calmodulin, 25 μM oxyhemoglobin, and an NADPH regenerating system consisting of 400 μM $NADP^+$, 10 mM glucose-6-phosphate, and 1 unit/ml glucose-6-phosphate dehydrogenase, expressed as final concentrations, in a total volume of 180 μl of 50 mM potassium phosphate, pH 7.4. The mixture was incubated at 37°C and the rate of NO-mediated oxidation of oxyhemoglobin was monitored by measuring the absorbance at λ401 nm - 411 nm with a microtiter plate reader (SpectraMax Plus, Molecular Devices, Sunnydale, CA) as previously described (13). The amount of nitrate and nitrite in the cell medium was assayed by the use of nitrate reductase and quantitation by the Griess method as described (14).

Heme assay - HPLC was performed with the use of a Waters 600S controller, 717 Plus autosampler and 996 photodiode array detector (Waters Corp., Milford, MA). Samples (100 μg of protein) were injected onto a reverse phase HPLC column (C4 Vydac, 5 μm, 0.21 x 15 cm) equilibrated with solvent A (0.1% trifluoroacetic acid) at a flow rate of 0.3 mL/min. A linear gradient was run to 75% solvent B (0.1% trifluoroacetic acid in acetonitrile) over 30 min and then to 100% solvent B over the next 5 min. Absorbance at 220 nm and 400 nm was monitored.

Tetrahydrobiopterin assay - The amount of BH_4 in the reaction mixtures was determined by use of an HPLC fluorescence method as described by Klatt et al. (15). The method involves oxidization of BH_4 and BH_2 to biopterin by treatment with KI/I_2

solution under acidic conditions. To give the specific amount of BH_2, the KI/I_2 oxidation is done in a basic solution where BH_4 and BH_2 are oxidized to pterin and biopterin, respectively. Specifically for oxidation under acidic conditions, a 30-µl aliquot of the sample was treated with 10 mM I_2 and 50 mM KI in a total volume of 60 µL of 100 mM HCl for 1 h at room temperature in the dark. The solution was neutralized with 5 µl of 1.0 M NaOH and then 5 µl of 0.2 M ascorbate was added. An aliquot (30 µl) of the resulting solution was injected onto a reverse phase HPLC column (C18 Vydac 5 mm, 4.6 x 250 mm) equilibrated with 20 mM NaH_2PO_4, pH 3, with 5% methanol at a flow rate of 1 ml/min. The pterins were eluted with the same mobile phase and detected by fluorescence at excitation and emission wavelengths of 350 and 418 nm, respectively. The HPLC and analysis of pterins was performed with the use of a Waters 600S system with a 717 autosampler and Applied Biosystems Spectroflow 980 fluorescence detector. To oxidize the pterins under basic conditions, the first reaction mixture was treated as above except that 100 mM NaOH replaced 100 mM HCl and the final solution was neutralized with 5 µl of 1 M HCl.

Expression and purification of holo-nNOS and apo-nNOS - nNOS was overexpressed in Sf9 insect cells as previously described (16). To express holo-nNOS, oxyhemoglobin (25 µM) was added as a source of heme during the last 24 h of expression. Cells were harvested and suspended in 1 volume of 10 mM Hepes, pH 7.5, containing 320 mM sucrose, 100 µM EDTA, 0.1 mM dithiothreitol, 10 µg/ml trypsin inhibitor, 1.0 µM leupeptin, 2 µg/ml of aprotinin, 6 mM phenylmethanesulphonyl fluoride, and 10 µM BH_4, and the suspended cells were ruptured by Dounce homogenization. Lysates from infected Sf9 cells (8×10^9) were centrifuged at 100,000 x

g for 1 h. The supernatant fraction was loaded onto a 2'5'-ADP Sepharose column (20 ml) and the nNOS was affinity purified as described (17), except that 10 mM 2' AMP in high salt buffer was used to elute the protein. The nNOS-containing fraction was concentrated with the use of a Centriplus YM-100 concentrator (Amicon, 100,000 MWCO) to 10 ml and loaded onto a Sephacryl S-300 HR gel filtration column (2.6 x 100 cm, Pharmacia Biotech) equilibrated with 50 mM Tris-HCl, pH 7.4, containing 100 mM NaCl, 10% glycerol, 0.1 mM EDTA, 0.1 mM dithiothreitol, and 5 μM BH_4. The proteins were eluted at a flow rate of 1.0 ml/min and 1.0 ml-fractions were collected and analyzed for protein content and NOS activity. The fractions containing NOS activity were pooled, supplemented with 10 μM BH_4 and concentrated with the use of a Centriplus YM-100 concentrator. This Sephacryl-purified nNOS preparation had a specific activity of approximately 1000 nmol/min/mg of protein and was stored at –80 ^{o}C. To prepare apo-nNOS, the procedure was the same as that for holo-nNOS except that oxyhemoglobin was omitted during expression and BH_4 was not added during purification. The specific activity of the apo-nNOS preparation was approximately 25 nmol/min/mg of protein.

In vitro ubiquitylation and degradation of apo-nNOS and holo-nNOS by fraction II - We used an *in vitro* degradation system, containing fraction II, that has been established to proteasomally degrade nNOS by an ubiquitin- and ATP- dependent process (8). Fraction II was prepared from rabbit reticulocyte lysates as previously described (18). The nNOS preparations (2 μg) were incubated at 37°C in a total volume of 120 μl of 50 mM Tris-HCl, pH 7.4, containing 2 mM dithiothreitol, 50 μM ubiquitin, an ATP-regenerating system (2 mM ATP, 10 mM creatine phosphate, 5 mM $MgCl_2$, and 10

units/ml creatine phosphokinase), and 2 mg/ml of fraction II. At indicated times, the samples were quenched with 25 µl of sample buffer containing 5% SDS, 20% glycerol, 100 mM dithiothreitol, and 0.02% bromophenol blue in 125 mM Tris-HCl, pH 6.8. The samples were boiled for 3 min and an aliquot (25 µl) was submitted to 6% SDS-PAGE (10 x 8 cm). Proteins were then transferred to nitrocellulose membranes (0.2 µm, BioRad) and probed with 0.1% anti-nNOS. The immunoblots were then incubated a second time with ^{125}I-conjugated goat anti-rabbit IgGs to visualize the immunoreactive bands. The membranes were dried and exposed to X-OMAT film for 1 h at -80°C. The bands corresponding to nNOS were excised and the radioactivity quantified by the use of a gamma counter. This method was quantitative up to 0.5 µg of nNOS with a linear relationship between the amount of nNOS and radioactivity ($r^2 = 0.99$). For studies where nNOS-ubiquitin conjugates were measured, nNOS was treated as above except that 38 µg of nNOS, 15 µM ubiquitin, and 0.4 mg/ml of fraction II were used. To inhibit deubiquitylation, 0.7 µM ubiquitin aldehyde was added. The nNOS-ubiquitin conjugates were detected as described for cellular nNOS-ubiquitin conjugates.

Results

Effect of 2,4-diamino-6-hydroxypyrimidine on nNOS dimer stability, nNOS activity, and tetrahydrobiopterin levels - An inhibitor of the rate-limiting enzyme in the *de novo* synthesis of tetrahydrobiopterin from guanosine triphosphate, 2,4-diamino-6-hydroxypyrimidine, has been used to decrease tetrahydrobiopterin levels in cells and in animals (2, 19, 20). Since tetrahydrobiopterin is known to stabilize the dimeric form of nNOS (1), we chose to first examine the effects of 2,4-diamino-6-hydroxypyrimidine on

the levels of nNOS dimer and monomer in HEK293 cells. We examined the samples by low temperature SDS-PAGE so that the SDS-resistant dimeric form of nNOS could be measured (12). This assay is not a measure of the dimeric content under native conditions, but is a measure of the amount of stable dimer that is not dissociated by SDS and thus underestimates the total dimeric content. Nonetheless, it is a convenient and reliable measure for effects on the stable dimeric state of nNOS. As shown in Fig. 3.1A, the nNOS in the HEK293 cells exists in part as a SDS-resistant dimer and treatment of the cells with 2,4-diamino-6-hydroxypyrimidine (*DP*) led to a decrease in the dimeric form over time relative to that found in the untreated cells (*Control*). As shown in Fig. 3.1B, the bands corresponding to the nNOS dimer (*upper, solid symbols*) and monomer (*lower, open symbols*) were quantified by gamma counting. By this analysis, we can clearly see that the treatment with 2,4-diamino-6-hydroxypyrimidine causes not only a time-dependent decrease in the nNOS dimer (*cf. solid circles* with *solid squares*) but also a concomitant increase in nNOS monomer (*cf. open circle* with *open square*). Moreover, the treatment of HEK293 cells with sepiapterin, a precursor to tetrahydrobiopterin synthesized by the pterin salvage pathway that involves dihydrofolate reductase, can circumvent the inhibition caused by 2,4-diamino-6-hydroxypyrimidine (2). Thus, when cells are treated with sepiapterin in addition to 2,4-diamino-6-hydroxypyrimidine, there is no change seen in the level of the nNOS dimer (*solid triangles*) from that of control cells (*solid squares*).

We next measured the cellular tetrahydrobiopterin levels and nNOS activity to verify the effects of 2,4-diamino-6-hydroxypyrimidine and sepiapterin. As shown in Fig. 3.2A, the treatment of cells with 2,4-diamino-6-hydroxypyrimidine decreases the

tetrahydrobiopterin levels to approximately one-quarter of that in control cells. The addition of sepiapterin increases the tetrahydrobiopterin levels by approximately 20-fold. The nNOS activity was determined by measuring nitrite and nitrate, which are the stable oxidation products of NO, released into the culture medium (21). As shown in Fig. 3.2B, the nNOS activity was decreased by one-half by 2,4-diamino-6-hydroxypyrimidine whereas sepiapterin had only a modest effect in counteracting the activity loss. Although this appears to be in conflict with the very high levels of tetrahydrobiopterin found, it is likely that the high levels of dihydrobiopterin that are also present (data not shown) compete with tetrahydrobiopterin and inhibit the nNOS enzyme (22). Thus in total, we have established in the HEK293 cells that 2,4-diamino-6-hydroxypyrimidine and sepiapterin have consistent effects on pterin and nNOS structure and function.

Effect of 2,4-diamino-6-hydroxypyrimidine on nNOS ubiquitylation - The major ubiquitin adduct to nNOS in HEK293 cells is the mono-ubiquitylated form, which can be detected by immunoprecipitation of nNOS and blotting with anti-ubiquitin (4). The nNOS-ubiquitin conjugates accumulate after treatment of cells with an inhibitor to the proteasome (4). As shown in Fig. 3.3A, treatment of HEK293 cells with 2,4-diamino-6-hydroxypyrimidine and MG132, a proteasome inhibitor, causes a time-dependent increase in the nNOS-ubiquitin conjugates over a 3 h period. The amount of conjugate was quantified in Fig. 3.3B and we see that after 3 h, the levels of nNOS-ubiquitin conjugates in the 2,4-diamino-6-hydroxypyrimidine-treated cells (*closed circles*) are approximately double that found in the control (*closed squares*) or sepiapterin–treated (*closed triangles*) cells. The major effect is on the extent of nNOS ubiquitylation, suggesting that we have increased the pool of nNOS that is susceptible for ubiquitylation.

Previous studies established that the heme-deficient apoprotein form of nNOS is rapidly ubiquitylated and proteasomally degraded (4, 8). To address if apoprotein is formed in the current studies when tetrahydrobiopterin is depleted, we chose to examine the heme content of the HEK293 cells. In the HEK293 cells, over 80% of the cytosolic heme is bound to nNOS (23). This is based on two observations. First, the transfected cells contain approximately 5-fold higher heme than non-tranfected cells. Second, treatment of transfected cells with N^G-amino-L-arginine, which is a suicide inactivator of nNOS that works by covalently altering and destroying the heme bound to nNOS, causes a loss of heme that is concomitant with the activity loss. This indicates that the heme that is in the cytosol must be from nNOS. As shown in Fig. 3.4A, the reverse phase HPLC profile at 400 nm of the cytosol from nNOS expressing cells gives one main peak corresponding to heme (solid line) that is approximately 5-fold higher than that in non-transfected cells. As shown in Fig. 3.4B, treatment of cells with 2,4-diamino-6-hydroxypyrimidine or sepiapterin does not affect the heme levels in the transfected nor non-transfected cells. The absence of a decrease in heme is interpreted as no loss of heme from nNOS. However, it is possible that heme is bound to some other protein in the cell after treatment with 2,4-diamino-6-hydroxypyrimidine. To directly address this point we have immunoprecipitated nNOS from untreated and 2,4-diamino-6-hydroxypyrimidine treated cells and measured heme levels due to nNOS. The nNOS-heme content in 2,4-diamino-6-hydroxypyrimidine treated cells is 95 ± 14 % of that found in untreated cells. Thus, we conclude that the nNOS-heme content is unchanged and we establish for the first time that tetrahydrobiopterin loss in cells destabilizes the

nNOS dimer but does not lead to heme loss and formation of apoprotein. Therefore, it appears that heme loss is not the initial trigger for enhanced ubiquitylation.

Effect of tetrahydrobiopterin on nNOS ubiquitylation and proteasomal degradation in vitro - Recently, an *in vitro* system of reticulocyte proteins was developed that mimics the cellular ubiquitylation and proteasomal degradation of nNOS (8). The effect of tetrahydrobiopterin has not been explored in this *in vitro* degradation system. As shown in Fig. 3.5A, the addition of 10 μM tetrahydrobiopterin greatly slows the rate of degradation of nNOS (*cf. closed circle* with *open circle*). As expected, the heme-deficient apo-nNOS (*closed squares*) is more rapidly degraded than heme-containing nNOS. Moreover, the addition of 10 μM tetrahydrobiopterin has very little effect on the degradation of apo-nNOS (*open squares*) consistent with tetrahydrobiopterin binding avidly to the heme-containing nNOS and not the apo-nNOS. The concentration-dependence on tetrahydrobiopterin was more closely examined in Fig. 3.5B. Greater than 20 μM tetrahydrobiopterin is needed for maximal protection of nNOS (*solid circles*) whereas even 40 μM tetrahydrobiopterin does not protect apo-nNOS (*solid squares*). Although there is clearly an effect on holo-nNOS and not on apo-nNOS, the concentration of tetrahydrobiopterin appears much higher than that needed for stabilization of the purified nNOS. We have observed, however, that nNOS in the presence of reticulocyte proteins and NADPH catalyzes the oxidation of tetrahydrobiopterin to dihydrobiopterin (data not shown). Therefore, the effective concentration of tetrahydrobiopterin during the assay is much lower. As shown in Fig. 3.5C, the effect of tetrahydrobiopterin on the *in vitro* ubiquitylation of nNOS was also examined. In these studies the nNOS-ubiquitin conjugates were detected by Western

blotting with anti-ubiquitin antibody. The major nNOS-ubiquitin conjugate *in vitro* is a mono-ubiquitylated form that is readily detected near the molecular mass of nNOS. We know it is a nNOS-ubiquitin conjugate as there is no such adduct in the absence of nNOS (*lane 6*) or of ubiquitin (*lane 7*). The addition of tetrahydrobiopterin to the reaction mixture decreases the nNOS-ubiquitin conjugate in a concentration-dependent manner. This is more clearly seen when the bands corresponding to the nNOS-ubiquitin adduct were quantified by gamma counting and plotted. The decreased proteolytic degradation and ubiquitylation caused by tetrahydrobiopterin seen in this *in vitro* system is entirely consistent with the effect of tetrahydrobiopterin depletion found in cells. Thus, tetrahydrobiopterin depletion does promote or labilize the nNOS for subsequent ubiquitylation and proteasomal degradation both *in vitro* as well as in cells.

Discussion

We have established that decreased tetrahydrobiopterin levels favor ubiquitylation of nNOS. The mechanism of how a pterin-depleted nNOS becomes recognized for ubiquitylation is not known. It is known that the absence of heme or suicide inactivation by substrate analogs that covalently alter the heme enhance the proteasomal degradation of nNOS (8, 21). Moreover, N^G-nitro-L-arginine, a slowly reversible inhibitor that binds to the heme of nNOS, was found to stabilize the dimeric form of nNOS and decrease nNOS ubiquitylation and degradation (8). Thus, it appears that conditions that perturb the heme binding pocket and lead to destabilization of the functional dimeric form of nNOS lead to ubiquitylation of nNOS whereas ligands that stabilize the pocket and the dimeric state of nNOS do not get ubiquitylated.

The ubiquitylation and proteasomal degradation of nNOS has been shown to involve hsp90 (16, 24). More recently, the role of hsp70 and the co-chaperone CHIP in nNOS ubiquitylation was established (25). Based on these findings, a notion that exposure of hydrophobic surfaces in the substrate binding cleft and recognition by hsp70 and hsp90 has been put forth as a mechanism for recognition of dysfunctional nNOS that leads to a protein-triage decision (25). In particular, it was proposed that hsp70 directs the ubiquitylation of nNOS through association with the E3 ubiquitin ligase, CHIP (25). Thus, it is possible that perturbations in the heme active site by covalent alteration of the heme by suicide inactivators or, in the current case, the loss of tetrahydrobiopterin, which is intimately associated with the prosthetic heme, may lead to exposure of hydrophobic regions in the active site of nNOS that are recognized by hsp70 and leads to ubiquitylation of nNOS. Alternatively, the destabilization of the dimeric nNOS may uncover a recognition site(s) that act as a signal for ubiquitylation. In support of this notion, heterodimerization of transcription factors, MATα2 and MATa1, is known to decrease the ubiquitin-proteasomal degradation of both factors (26). The destabilization of nNOS may be due to steric factors or perhaps to relaxation of the structural constraints, rendering the protein more flexible and/or disordered. It is noteworthy that destabilization of dimeric nNOS also leads to enhanced susceptibility to phosphorylation by protein kinase C (27) and hydrolysis by trypsin (28). However, in the case of iNOS, the monomer appears to be stable (29) and this suggests that perturbations of the active site may be a more important determinant for degradation. Deciphering the mechanism by which dysfunctional nNOS is recognized will certainly be important in the understanding of protein-triage decisions that control nNOS protein quality.

Since tetrahydrobiopterin oxidation has been implicated in a variety of diseases including hypertension, the findings here reveal the potential for long-term consequences of inadequate tetrahydrobiopterin levels on NO signal transduction processes. For example, cigarette smoking causes vascular dysfunction in man that is thought to be due to pterin-deficiency in the endothelial NOS (30). Moreover, in some cases the NOS activity is only partially reversed by tetrahydrobiopterin administration (30), possibly due to a loss of NOS protein. This notion is consistent with the observation that cigarette smoke causes a loss in endothelial NOS (31, 32) and nNOS proteins (33). Thus, our studies may aid in understanding the complex effects of tetrahydrobipterin deficiency.

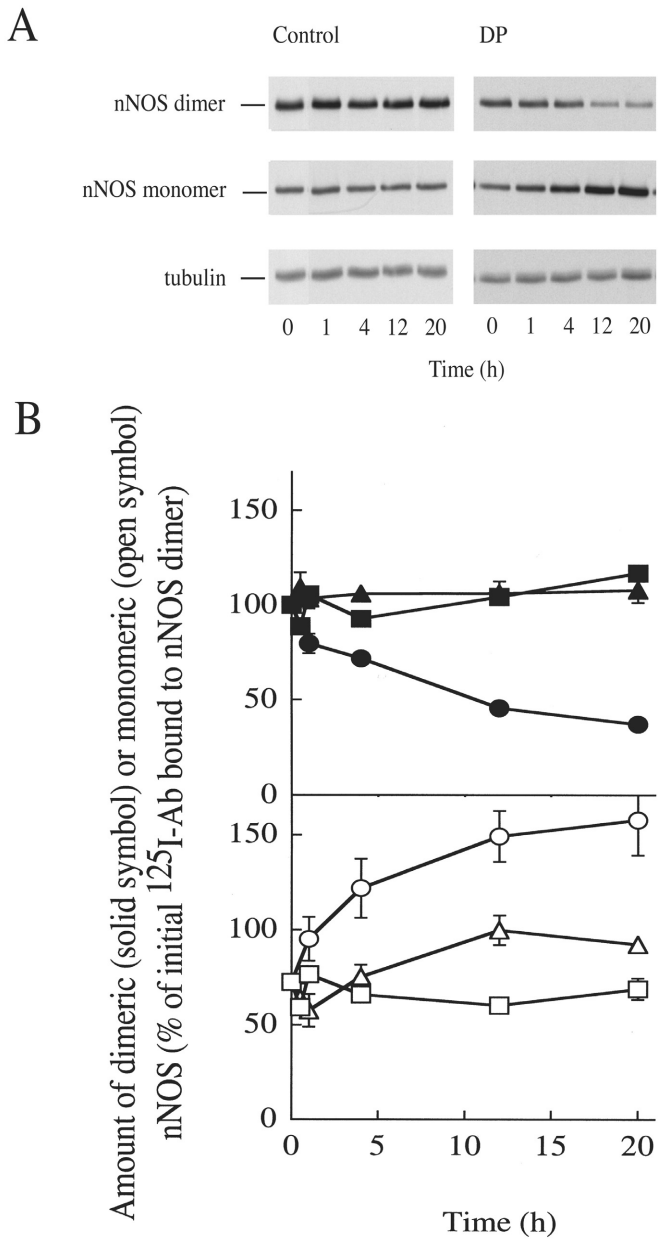

Fig. 3.1. **Effect of 2,4-diamino-6-hydroxypyrimidine and sepiapterin on the amount of SDS-resistant dimeric nNOS in HEK293 cells.** The HEK293 cells were treated with 2,4-diamino-6-hydroxypyrimidine, an inhibitor of BH_4 synthesis, and sepiapterin, a precursor to BH_4 via the pterin salvage pathway, so that the pterin levels could be manipulated. The monomeric and dimeric states of nNOS were measured by low temperature SDS-PAGE. *A*, 2,4-diamino-6-hydroxypyrimidine causes the loss of SDS-resistant dimer of nNOS. Immunoblots for dimeric and monomeric nNOS in cytosol from HEK293 cells treated with 5.0 mM 2,4-diamino-6-hydroxypyrimidine (*DP*) or untreated (*Control*) for the indicated times. Tubulin was blotted as an internal control. Bands were visualized by use of ^{125}I-antibody and autoradiography. *B,* quantitation of the effect of 2,4-diamino-6-hydroxypyrimidine and sepiapterin on the amount of SDS-resistant dimer. The amounts of SDS-resistant dimer (upper panel, solid symbols) and the band corresponding to the monomer (lower panel, open symbols) of nNOS was quantified by use of a gamma counter. Cells were untreated (squares) or treated with 5.0 mM 2,4-diamino-6-hydroxypyrimidine (circles) or with 5.0 mM 2,4-diamino-6-hydroxypyrimidine and 100 μM sepiapterin (triangles). The values are expressed as percentages of the raw counts. The values are the mean ± SE from 4 separate experiments.

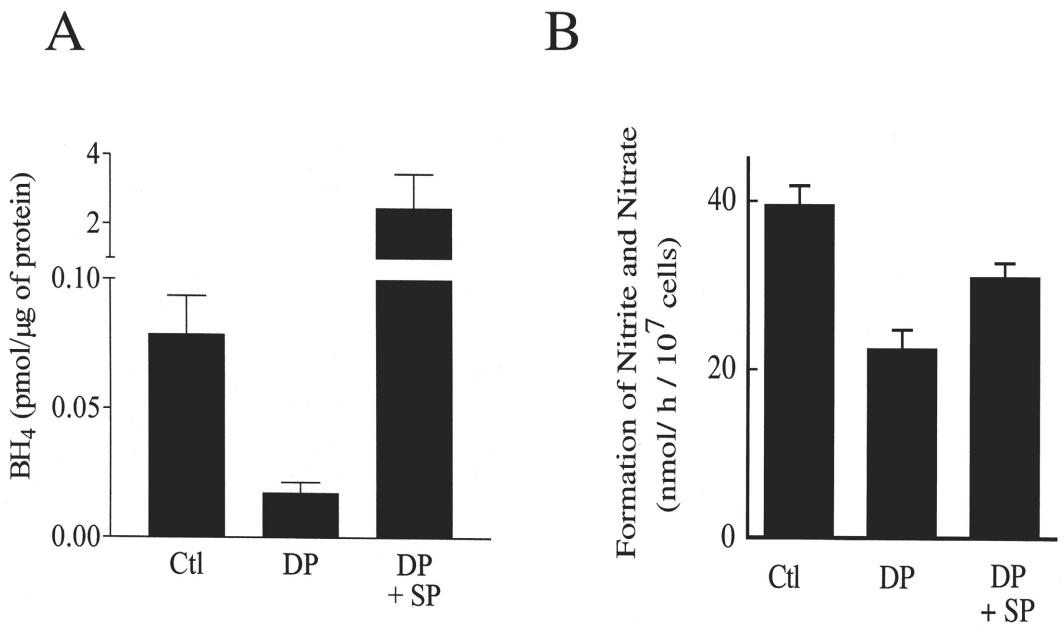

Fig. 3.2. **nNOS activity and tetrahydrobiopterin levels in HEK293 cells treated with 2,4-diamino-6-hydroxypyrimidine and sepiapterin**. *A,* tetrahydrobiopterin levels in cytosols of HEK293 cells treated with 2,4-diamino-6-hydroxypyrimidine and sepiapterin were measured as indicated in 'Materials and Methods'. The cells were untreated (Ctl) or treated with 5.0 mM 2,4-diamino-6-hydroxypyrimidine (DP) or with 5.0 mM 2,4-diamino-6-hydroxypyrimidine and 100 μM sepiapterin (DP+SP). Cells were harvested 20 h after initiating the treatment. The values are the mean ± SE from 4 separate experiments. *B*, nNOS activity in intact cells was measured after 20 h treatment with 2,4-diamino-6-hydroxypyrimidine and sepiapterin as in *A*. The nitrite and nitrate released into the medium over a period of 1 h after adding 10 μM calcium ionophore, A23187, was measured. The values are the mean ± SE from 5 separate experiments.

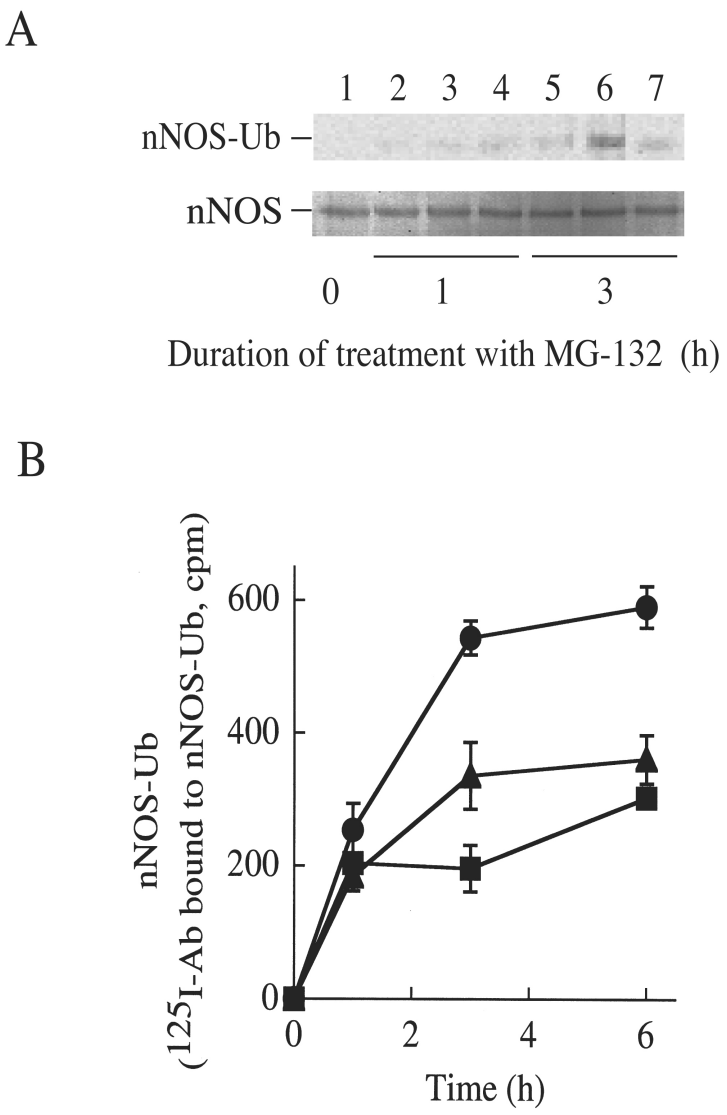

Fig. 3.3. **nNOS ubiquitylation is enhanced under conditions that favor loss of SDS-resistant dimer.** *A*, nNOS-ubiquitin conjugates (nNOS-Ub) were detected by SDS-PAGE after treatment with the proteasome inhibitor MG132. The cells were untreated (*lanes 1,2, and 5*) or treated with 5.0 mM 2,4-diamino-6-hydroxypyrimidine (*lanes 3 and 6*) or with 5.0 mM 2,4-diamino-6-hydroxypyrimidine and 100 μM sepiapterin (*lanes 4 and 7*). The cells were then treated with 10 μM MG132 for 1h (*lanes 2-4*) or 3h (*lanes 5-7*), the nNOS was immunoprecipitated from the cytosol and blotted for ubiquitin. There were no ubiquitin conjugates observed under any of the conditions without MG132. The amounts of immunoprecipitated nNOS are shown (nNOS) as a control. *B*, the relative amount of ubiquitin detected in *A* was quantified by gamma counting. Closed squares, untreated; Closed circles, 5.0 mM 2,4-diamino-6-hydroxypyrimidine; Closed triangles, 5.0 mM 2,4-diamino-6-hydroxypyrimidine and 100 μM sepiapterin. The values are the mean ± SE from 5 separate experiments.

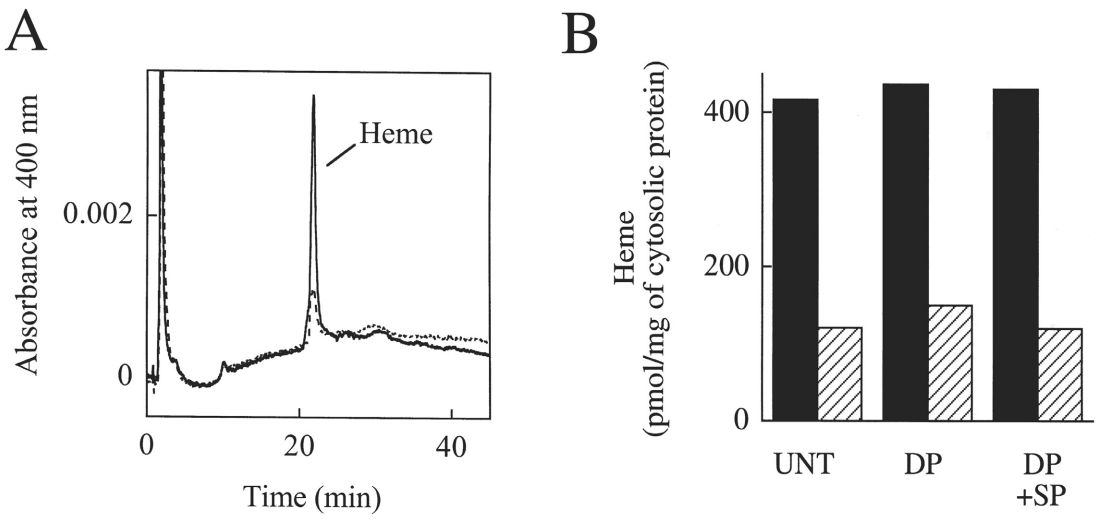

Fig. 3.4**. HPLC profiles of cytosol prepared from HEK293 cells treated with 2,4-diamino-6-hydroxypyrimidine and sepiapterin.** Cytosol from cells treated with sepiapterin and/or 2,4-diamino-6-hydroxypyrimidine for 22 h, as indicated in Fig.3.1, was analyzed by reverse phase HPLC. *A*, the HPLC profile at 400 nm of untreated nNOS-transfected cells (*solid line*) and untreated non-transfected cells (*dashed line*) are plotted. The major peak with elution time of 21.8 min corresponds to heme. *B,* the amount of heme was quantified with the use of myoglobin as a standard. The values from nNOS-transfected (*solid bars*) and non-transfected (*hatched bars*) are shown. *UNT*, untreated; *DP*, treated with 5.0 mM 2,4-diamino-6-hydroxypyrimidine; *DP+SP*, treated with 5.0 mM 2,4-diamino-6-hydroxypyrimidine and 100 μM sepiapterin.

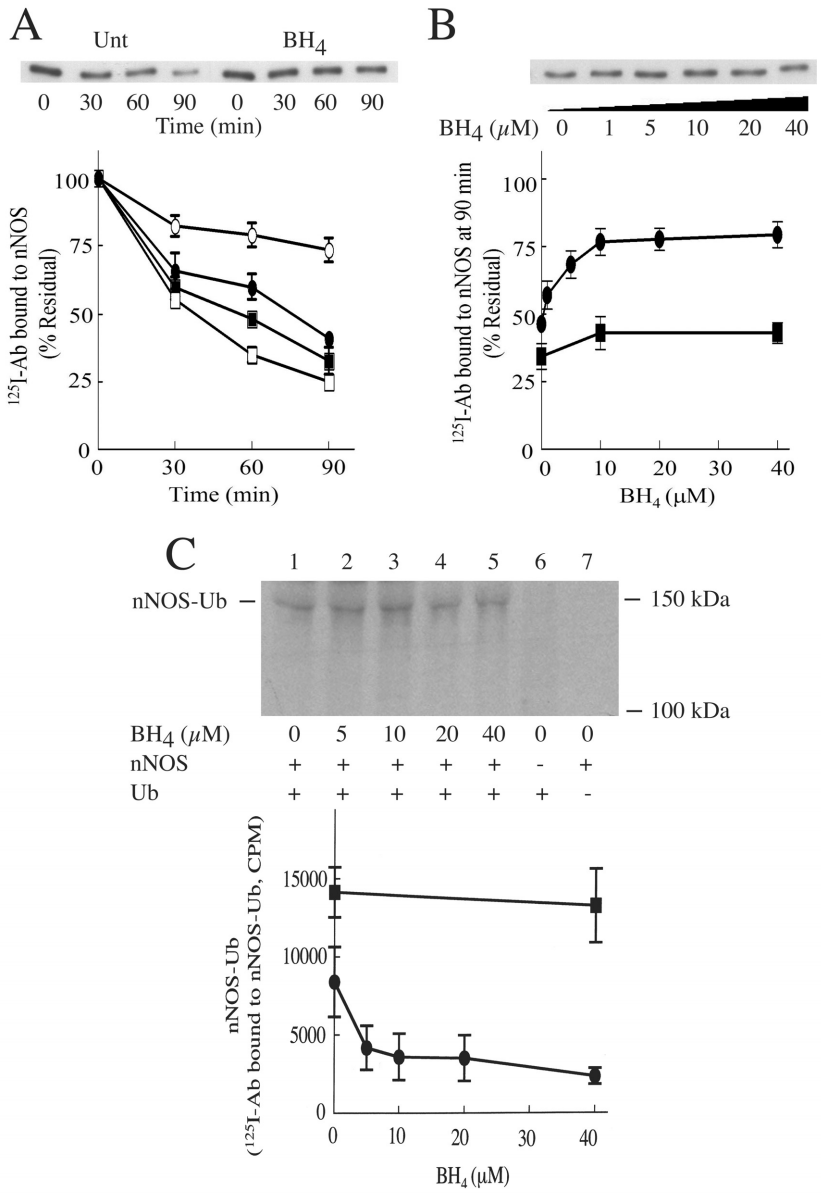

Fig. 3.5. **Effect of tetrahydrobiopterin on the ubiquitylation and degradation of purified nNOS in an *in vitro* system containing fraction II.** Purified nNOS (20 μg/ml) was incubated with fraction II, which contains ubiquitin ligases and proteasome that ubiquitylate and degrade nNOS. The effect of tetrahydrobiopterin on nNOS ubiquitylation and proteasomal degradation was determined. *A*, the time dependent loss of nNOS in the presence of fraction II. Closed squares, heme-deficient apo-nNOS; Open squares, heme-deficient apo-nNOS in the presence of 10 μM BH_4; Closed circles, heme-containing nNOS; Open circles, heme-containing nNOS in the presence of 10 μM BH_4. A representative blot for heme-containing nNOS in the absence (Unt) or presence (BH_4) of 10 μM BH_4 is also shown. *B,* the dependence on the concentration of BH_4 on the extent of degradation of nNOS. The residual amount of nNOS after 90 min of treatment with fraction II is shown for apo-nNOS (closed squares) and holo-nNOS (closed circles). A representative blot for holo-nNOS is also shown. *C*, the effect of BH_4 on the extent of nNOS ubiquitylation. Holo nNOS (closed circles) and apo-nNOS (closed squares) were treated with fraction II in the presence of 10 μM MG132 for 120 min as described in 'Materials and Methods'. Different amounts of tetrahydrobiopterin were added and nNOS-ubiquitin conjugates were quantified as in Fig. 3.3. A representative blot of the ubiquitinated holo-nNOS is also shown. The values in all graphs are the mean ± SE from 3 separate experiments.

References

1. Werner, E. R., Gorren, A. C., Heller, R., Werner-Felmayer, G., Mayer, B. (2003) Tetrahydrobiopterin and nitric oxide: mechanistic and pharmacological aspects, *Experimental Biology & Medicine* **228,** 1291-1302.
2. Gross, S. S., Levi, R. (1992) Tetrahydrobiopterin synthesis. An absolute requirement for cytokine-induced nitric oxide generation by vascular smooth muscle *J. Biol. Chem.* **267,** 25722-25729.
3. Delgado-Esteban, M., Almeida, A., Medina, J. M. (2002) Tetrahydrobiopterin deficiency increases neuronal vulnerability to hypoxia *J. Neurochem.* **82,** 1148-1159.
4. Bender, A. T., Demady, D. R., Osawa, Y. (2000) Ubiquitination of neuronal nitric oxide synthase in vitro and in vivo *J. Biol. Chem.* **275,** 17407-17411.
5. Felley-Bosco, E., Bender, F. C., Courjault-Gautier, F., Bron, C., Quest, A. F. (2000) Caveolin-1 down-regulates inducible nitric oxide synthase via the proteasome pathway in human colon carcinoma cells *Proc. Natl. Acad. Sci. U.S.A.* **97,** 14334-14339.
6. Jiang, J., Cyr, D., Babbitt, R. W., Sessa, W. C., Patterson, C. (2003) Chaperone-dependent Regulation of Endothelial Nitric-oxide Synthase Intracellular Trafficking by the Co-chaperone/Ubiquitin Ligase CHIP *J. Biol. Chem.* **278,** 49332-49341.
7. Musial, A., Eissa, N. T. (2001) Inducible nitric-oxide synthase is regulated by the proteasome degradation pathway *J. Biol. Chem.* **276,** 24268-24273.
8. Dunbar, A. Y., Kamada, Y., Jenkins, G. J., Lowe, E. R., Billecke, S.S., Osawa, Y. (2004) Ubiquitination and degradation of neuronal nitric-oxide synthase in vitro: dimer stabilization protects the enzyme from proteolysis *Mol. Pharmacol.* **66,** 964-969.
9. Bredt, D. S., Hwang, P. M., Glatt, C. E., Lowenstein, C., Reed, R. R., Snyder, S.H. (1991) Cloned and expressed nitric oxide synthase structurally resembles cytochrome P-450 reductase *Nature* **351,** 714-718.
10. McMillan, K., Bredt, D. S., Hirsch, D. J., Snyder, S. H., Clark, J. E., Masters, B. S. S. (1992) Cloned, expressed rat cerebellar nitric oxide synthase contains stoichiometric amounts of heme, which binds carbon monoxide *Proc. Natl. Acad. Sci. U.S.A.* **89,** 11141-11145.
11. Sakai, N., Kaufman, S., Milstein, S. (1993) Tetrahydrobiopterin is required for cytokine-induced nitric oxide production in a murine macrophage cell line (RAW 264) *Mol. Pharmacol.* **43,** 6-10.
12. Klatt, P., Schmidt, K., Lehner, D., Glatter, O., Bachinger, H. P., Mayer, B. (1995) Structural analysis of porcine brain nitric oxide synthase reveals a role for tetrahydrobiopterin and L-arginine in the formation of an SDS-resistant dimer, *EMBO J.* **14,** 3687-3695.
13. Feelisch, M., Kubitzek, D., Werringloer, J. (1996) The oxyhemoglobin assay Feelisch, M. and Stamler, J. S. (Eds.) *Methods in Nitric Oxide Research* Wiley, New York, 455-478.
14. Schmidt, H. H., Warner, T. D., Nakane, M., Forstermann, U., Murad, F. (1992) Regulation and subcellular location of nitrogen oxide synthases in RAW264.7

macrophages [published erratum appears in (1992) *Mol Pharmacol* **42**, 174] *Mol. Pharmacol.* **41**, 615-624.
15. Klatt, P., Schmidt, K., Werner, E. R., Mayer, B. (1996) Determination of nitric oxide synthase cofactors: heme, FAD, FMN, and tetrahydrobiopterin *Methods Enzymol.* **268,** 358-365.
16. Bender, A. T., Silverstein, A. M., Demady, D. R., Kanelakis, K. C., Noguchi, S., Pratt, W. B., Osawa, Y. (1999) Neuronal nitric oxide synthase is regulated by the hsp90-based chaperone system in vivo *J. Biol. Chem.* **274,** 1472-1478.
17. Roman, L. J., Sheta, E. A., Martasek, P., Gross, S. S., Liu, Q., Masters, B. S. (1995) High-level expression of functional rat neuronal nitric oxide synthase in Escherichia coli *Proc. Natl. Acad. Sci. U.S.A.* **92,** 8428-8432.
18. Hershko, A., Heller, H., Elias, S., Ciechanover, A. (1983) Components of ubiquitin-protein ligase system. Resolution, affinity purification, and role in protein breakdown *J. Biol. Chem.* **258,** 8206-8214.
19. Cotton, R.G. (1986) A model for hyperphenylalaninaemia due to tetrahydrobiopterin deficiency *Journal of Inherited Metabolic Disease* **9,** 4-14.
20. Suzuki, S., Watanabe, Y., Tsubokura, S., Kagamiyama, H., Hayaishi, O. (1988) Decrease in tetrahydrobiopterin content and neurotransmitter amine biosynthesis in rat brain by an inhibitor of guanosine triphosphate cyclohydrolase *Brain Res.* **446,** 1-10.
21. Noguchi, S., Jianmongkol, S., Bender, A. T., Kamada, Y., Demady, D. R., Osawa, Y. (2000) Guanabenz-mediated inactivation and enhanced proteolytic *J Biol Chem* **275**, 2376-2380.
22. Vasquez-Vivar, J., Martasek, P., Whitsett, J., Joseph, J., Kalyanaraman, B. (2002) The ratio between tetrahydrobiopterin and oxidized tetrahydrobiopterin analogues controls superoxide release from endothelial nitric oxide synthase: an EPR spin trapping study *Biochem J.* **362,** 733-739.
23. Vuletich, J. L., Lowe, E. R., Jianmongkol, S., Kamada, Y., Kent, U. M., Bender, A. T., Demady, D. R., Hollenberg, P. F., Osawa, Y. (2002) Alteration of the heme prosthetic group of neuronal nitric-oxide synthase during inactivation by N^G-amino-L-arginine in vitro and in vivo *Mol. Pharmacol.* **62,** 110-118.
24. Osawa, Y., Lowe, E. R., Everett, A. C., Dunbar, A. Y., Billecke, S. S. (2003) Proteolytic degradation of nitric oxide synthase: effect of inhibitors and role of hsp90-based chaperones *J. Pharmacol. Exp. Ther.* **304,** 1-5.
25. Peng, H. -M., Morishima, Y., Jenkins, G. J., Dunbar, A. Y., Lau, M., Patterson, C., Pratt, W. B., Osawa, Y. (2004) Ubiquitylation of neuronal nitric-oxide synthase by CHIP, a chaperone-dependent E3 ligase *J. Biol. Chem.* **279,** 52970-52977.
26. Johnson, P. R., Swanson, R., Rakhilina, L., Hochstrasser, M. (1998) Degradation signal masking by heterodimerization of MATalpha2 and MATa1 blocks their mutual destruction by the ubiquitin-proteasome pathway *Cell* **94,** 217-227.
27. Okada, D. (1998) Tetrahydrobiopterin-dependent stabilization of neuronal nitric oxide synthase dimer reduces susceptibility to phosphorylation by protein kinase C in vitro *FEBS Lett.* **434,** 261-264.
28. Panda, K., Rosenfeld, R. J., Ghosh, S., Meade, A. L., Getzoff, E. D., Stuehr, D. J. Distinct (2002) Dimer Interaction and Regulation in Nitric-oxide Synthase Types I, II, and III *J. Biol. Chem.* **277,** 31020-31030.

29. Sennequier, N., Wolan, D., Stuehr, D. J. (1999) Antifungal imidazoles block assembly of inducible NO synthase into an active dimer *J. Biol. Chem.* **274**, 930-938.
30. Heitzer, T., Brockhoff, C., Mayer, B., Warnholtz, A., Mollnau, H., Henne, S., Meinertz, T., Munzel, T. (2000) Tetrahydrobiopterin improves endothelium-dependent vasodilation in chronic smokers: evidence for a dysfunctional nitric oxide synthase *Circ.Res.* **86,** E36-41.
31. Ma, L., Chow, J. Y., Cho, C. H. (1999) Cigarette smoking delays ulcer healing: role of constitutive nitric oxide synthase in rat stomach *Am. J. Physiol.* **276,** G238-G248.
32. Su, Y., Han, W., Giraldo, C., De Li, Y., Block, E. R. (1998) Effect of cigarette smoke extract on nitric oxide synthase in pulmonary artery endothelial cells *Am. J. Respir. Cell Mol. Biol.* **19,** 819-825.
33. Xie, Y., Garban, H., Ng, C., Rajfer, J., Gonzalez-Cadavid, N. F. (1997) Effect of long-term passive smoking on erectile function and penile nitric oxide synthase in the rat *J.Urol.* **157,** 1121-1126.

Chapter IV

Degradation of Neuronal NO-Synthase is Regulated by Ubiquitination in the Calmodulin Binding Region of the Enzyme

Summary

It is established that neuronal NO-synthase (nNOS) is ubiquitinated and proteasomally degraded. Certain forms of dysfunctional nNOS, such as the heme deficient apo-protein and the suicide-inactivated enzyme, are selectively targeted by the ubiquitin-proteasome system for degradation. Both poly- and mono-ubiquitinated forms of nNOS have been detected in cells and *in vitro*. While mono-ubiquitination can signal for many different processes including proteasomal degradation, the fate of mono-ubiquitinated nNOS has not been determined. The location of the ubiquitin adduct on nNOS that targets the enzyme for proteasomal degradation has also not been identified. In the current study, we show with the use of methylated ubiquitin and purified nNOS that mono-ubiquitination of nNOS can signal for proteasomal degradation *in vitro*. We also discovered, with the use purified nNOS, that ubiquitination in the calmodulin binding region provides the signal for proteasomal degradation *in vitro*. Specifically, direct blocking of the region by calmodulin was shown to greatly inhibit the ubiquitination of nNOS. Furthermore, mutant nNOS protein that has the lysines in the calmodulin binding region mutated to arginines was found to be resistant to both

ubiqutination and proteasomal degradation *in vitro*. Restoration of single native lysine residues in the calmodulin binding region was sufficient to reverse the resistance. The location of the residue within the calmodulin binding region was not critical, as all three sites tested were able to restore function. To directly map the ubiquitination site, nNOS-ubiquitin conjugates from a large scale *in vitro* reaction mixture (180 mg total protein) containing his-tagged ubiquitin were isolated, proteolyzed with trypsin, and analyzed by CapLC-MS/MS for amino acid sequence using data dependent scanning. Trypsin cleavage of an ubiquitinated peptide leaves a signature diglycine tag on the conjugated lysine residue that also results in a missed cleavage at the modification site. Using these criteria, the MS/MS spectra were analyzed using Turbo Sequest to identify any possible ubiquitinated peptides from the calmodulin binding region of nNOS. A potential candidate peptide was identified, mapping to amino acid residues 752-756, with the site of ubiquitin adduction at lysine residue 754. This data supports the results found in the mutagenesis studies, which determined that nNOS proteasomal degradation can be regulated by ubiquitination of the enzyme in the calmodulin binding region. Knowledge of the exact site of ubiquitination is an important first step in determining the process by which a protein becomes recognized and degraded by the ubiquitin-proteasome system.

Introduction

Neuronal NO-synthase (nNOS) is a highly regulated enzyme that is degraded by the ubiquitin-proteasome system (1). It is known that certain dysfunctional forms of nNOS are selectively targeted for degradation (2, 3). The ubiquitin-proteasome system is the major pathway for the degradation of many proteins. In this pathway, a protein is selectively recognized and conjugated to the conserved 76-residue polypeptide ubiquitin through the sequential action of activating (E1), conjugating (E2), and ligating (E3) enzymes (4). It is clear that the recognition of substrates for ubiquitination is a highly selective process that is initiated by the availability of an ubiquitinatable lysine residue (5) and the presence and accessibility of ubiquitination signals in the substrate that are recognized by E3 ligases (6). It is also known that both mono- and polyubiquitination can occur, with monoubiquitination being linked to many functional outcomes (6). While polyubiquitination of 4 or more ubiquitin monomers linked through lysine residue 48 on ubiquitin is the most commonly reported signal for proteasomal degradation, mono-ubiquitination can also signal for proteasomal degradation (7).

While it was determined that certain dysfunctional forms of nNOS are selectively targeted for ubiquitination (2, 3) and that C-terminal Hsc70 Interacting Protein (CHIP) can serve as an E3 ligase for nNOS (20), both the ubiquitin binding site on nNOS and the length of the ubiquitin chain responsible for signaling the proteasomal degradation of the enzyme are not known. Both poly- and mono-ubiquitination of nNOS have been detected, but the major ubiquitin adduct to nNOS detected in HEK293 cells and *in vitro* is the mono-ubiquitinated form (1). In this study, we first sought to determine whether mono-ubiquitination could serve as a signal for the proteasomal degradation of nNOS.

To address this question, we used purified nNOS and methylated ubiquitin (Methyl-Ub) in an *in vitro* ubiquitination system containing rabbit reticulocyte lysate proteins (2). Methyl-Ub was chosen, since it is methylated at lysine residue 48 and is therefore unable to form the classic polyubiquitin chain. We found that Methyl-Ub was able to conjugate to nNOS and facilitate its proteasomal degradation, suggesting that the monoubiquitinated form of nNOS could be the signal for nNOS proteasomal degradation.

We also wanted to determine which region on nNOS, specifically which lysine residue(s), was conjugated to ubiquitin to aid in understanding what areas must be accessible in dysfunctional nNOS protein that selectively target it for proteasomal degradation. To address this question, we used purified heme-deficient monomeric nNOS (apo-nNOS), which is known to be selectively ubiquitinated and degraded *in vitro* (1). We found that the binding of calmodulin, a necessary cofactor for nNOS activity, to apo-nNOS greatly reduced its ubiquitination *in vitro*. Experiments using separate nNOS oxygenase and reductase domains, as well as nNOS mutants where the lysine residues in the calmodulin binding region were converted to arginines, supported the finding that the calmodulin binding region is the locus of ubiquitin conjugation to nNOS. To directly map the ubiquitination site, purified ubiquitinated nNOS was trypsinized and analyzed by CapLC-MS/MS for amino acid sequence determination. A candidate ubiquitinated peptide mapping to the calmodulin binding region was detected, with the site of ubiquitination being at lysine residue 754. The direct mapping data are consistant with the mutagenesis data showing that the ubiquitin conjugate responsible for signaling for the proteasomal degradation of nNOS *in vitro* occurs in the calmodulin binding region.

Materials and Methods

Materials

Untreated rabbit reticulocyte lysate was from Green Hectares (Oregon, WI). The affinity-purified rabbit IgG for Western blotting of the oxygenase domain of nNOS (raised against residues 251-270), Protein A-Sepharose, ubiquitin, ATP, creatine phosphokinase, EGTA, and $MgCl_2$ were purchased from Sigma-Aldrich (St. Louis, MO). The affinity-purified rabbit polyclonal antibody raised against nNOS residues 37-56 used to immunoprecipitate the oxygenase domain was from Santa Cruz Biotechnology, Inc. (Santa Cruz, CA). The affinity-purified rabbit IgG raised against the C-terminus of nNOS (residues 1095-1289) used for Western blotting was from Transduction Laboratories (Lexington, KY). The affinity-purified IgG used for Western blotting of ubiquitin was from DakoCytomation (Denmark). ^{125}I-Labeled antibody against rabbit IgG was purchased from PerkinElmer Life and Analytical Sciences (Boston, MA). TPCK treated trypsin was from Promega (Madison, WI). MG-132 was purchased from Biomol (Plymouth Meeting, PA). The cDNA for rat neuronal NOS was kindly provided by Dr. Solomon Snyder (Johns Hopkins Medical School, Baltimore, MD). The cDNA for His-HA-tagged ubiquitin was generously given by Dr. Yi Sun (University of Michigan). Ubiquitin aldehyde and methylated ubiquitin were from Boston Biochem (Cambridge, MA). ^{125}I-Ubiquitin was purchased from Amersham Pharmacia (Buckinghamshire, England). Creatine phosphate was from Fluka (Switzerland). Nickel-nitriloacetic acid-agarose was from Qiagen, Inc. (Valencia, CA). DE52 was purchased from Whatman (Clifton, NJ).

Methods

Expression and purification of nNOS - nNOS was overexpressed in Sf9 insect cells in the absence of heme to produce the heme-deficient, monomeric apo-protein as previously described (9). Cells were harvested and suspended in 1 volume of 10 mM Hepes, pH 7.5, containing 320 mM sucrose, 100 μM EDTA, 1 mM dithiothreitol, 10 μg/ml trypsin inhibitor, 1.0 μM leupeptin, 2 μg/ml of aprotinin, and 6 mM phenylmethanesulphonyl fluoride, and the suspended cells were ruptured by Dounce homogenization. Lysates from infected Sf9 cells (8×10^9) were centrifuged at 100,000 x g for 1 h. The supernatant fraction was loaded onto a 2'5'-ADP Sepharose column (20 ml) and the nNOS was affinity purified as described (10), except that 10 mM 2' AMP was used to elute the protein. The nNOS-containing fraction was concentrated with the use of a Centriplus YM-100 concentrator (Amicon, 100,000 MWCO) to 10 ml and loaded onto a Sephacryl S-300 HR gel filtration column (2.6 x 100 cm, Pharmacia Biotech) equilibrated with 50 mM Tris-HCl, pH 7.4, containing 100 mM NaCl, 10% glycerol, 0.1 mM EDTA, and 1 mM dithiothreitol. The proteins were eluted at a flow rate of 1.0 ml/min and 1.0 ml-fractions were collected and analyzed for protein content. The fractions containing nNOS were pooled and concentrated with the use of a Centriplus YM-100 concentrator. The concentrated nNOS was stored at –80 ^{o}C.

Expression and purification of nNOS domains and mutant nNOS proteins - pCWoxy-CaM containing the oxygenase domain (residues 1-756) was constructed as described (11) with a 6xHis-tag attached to the C-terminus. pCWred containing the reductase domain (residues 746-1429) was constructed as described (11) with a 6xHis-tag attached to the N-terminus. We mutated all 7 lysine residues present in the calmodulin

binding region of nNOS (residues 725, 732, 733, 739, 743, 751, and 754) to arginine residues using QuikChange Multi Site-Directed Mutagenesis Kits (Stratagene, La Jolla, CA). The three 5'- phosphorylated primers used were 5'-CCCCCACGAGGCGGCGAG CTATCGGCTTTAGGAGATTGGCAGA-3', 5'-GGCCGTCAGGTTCTCAGCCAGGC TAATGGGACAG-3', and 5'-GCCATGGCCAGGAGGGTCAGGGCGACCATTCTCT AC-3' (codons for arginine are underlined). The template was pCWnNOS. The plasmid with the desired mutation was confirmed by sequencing and digested with *Pfl*M1 to liberate the 1863 bp fragment, then subcloned into *Pfl*M1 sites of the wt-pCWnNOS vector. The resultant construct was designated as pCW7R. We also created mutants to restore individual native lysine residues 733, 739, and 754. Three distinct mutants were constructed with the use of a QuikChange II XL Site-Directed Mutagenesis Kit (Stratagene, La Jolla, CA). The template was pcDNA7R. The plasmid with the desired mutation was confirmed by sequencing. The plasmid was then digested with Sbf1 and Blp1 to liberate the 3271 bp fragment and subcloned into the wt-pCWnNOS vector. The resultant mutants were designated 6R733K, 6R739K, and 6R754K.

The nNOS mutants (including a wild type as control) were bacterially expressed using the pCW vector and BL21 (DE3) competent cells (Stratagene), according to the manufacturer's recommendations. Cells from 1L-cultures were harvested 48 h after induction with IPTG, and ruptured by french press at 1500 PSI. The lysates were processed and purified as above for the Sf9 cells, except that a PD-10 gel filtration column (GE Healthcare) was used instead of the Sephacryl S-300 HR gel filtration column. The samples were concentrated with the use of a Centriplus YM-100 concentrator and stored at –80 ^{o}C

In vitro ubiquitination and degradation of nNOS by fraction II - Fraction II was prepared from rabbit reticulocyte lysate as previously described (12). In studies where nNOS degradation was measured, purified nNOS (2 μg) was incubated at 37°C in a total volume of 120 μl of 50 mM Tris-HCl, pH 7.4, containing 2 mM dithiothreitol, 50 μM ubiquitin, an ATP-regenerating system (2 mM ATP, 10 mM creatine phosphate, 5 mM $MgCl_2$, and 10 units/ml creatine phosphokinase), and 2 mg/ml of fraction II. At indicated times, a 25 μl aliquot of each sample was taken and quenched with 25 μl of sample buffer containing 5% SDS, 20% glycerol, 100 mM dithiothreitol, and 0.02% bromophenol blue in 125 mM Tris-HCl, pH 6.8. The samples were boiled for 3 min and an aliquot (25 μl) was submitted to 6% SDS-PAGE (10 x 8 cm). Proteins were then transferred to nitrocellulose membranes (0.2 μm, BioRad) and probed with 0.1% anti-nNOS IgG. The immunoblots were then incubated a second time with ^{125}I-conjugated goat anti-rabbit IgGs to visualize the immunoreactive bands. The membranes were dried and exposed to a phosphor imaging screen for 4 hours, digitized using a Typhoon™ imaging system. Individual nNOS bands were selected, baseline corrected, and quantified using ImageQuant™ software. For studies where nNOS-ubiquitin conjugates were measured, nNOS was treated as above except that 38 μg of nNOS, 15 μM ubiquitin, and 0.4 mg/ml of fraction II were used. To inhibit deubiquitination, 0.7 μM ubiquitin aldehyde was added. The nitrocellulose membranes were autoclaved in distilled H_2O for 10 min and probed with 0.2% anti-ubiquitin polyclonal antibody. In some studies, Methyl-Ub was substituted for ubiquitin.

Limited trypsinolysis of nNOS and isolation of the resultant oxygenase and reductase domains – Purified nNOS protein (0.32 mg/ml) was incubated with 2 units/ml TPCK trypsin for 12 min at room temperature in a total volume of 200 µl of 50 mM Tris, pH 7.6, containing 1 mM DTT. An aliquot (86 µl) of the reaction was added to the *in vitro* ubiquitination mixture described above. After 60 min of incubation, an aliquot (60 µl) was immunoadsorbed with 3 mg Protein-A Sepharose and 30 µl of anti-nNOS IgG specific for the oxygenase domain. An additional aliquot (60 µl) was affinity purified with 3 mg ADP-Sepharose. The samples were both incubated for 3 h at 4^{o}C in a total volume of 340 µl HE lysis buffer containing 10 mM Hepes, pH 7.4, 0.32 M sucrose, 2.0 mM EDTA, 10 µg/mL trypsin inhibitor, 10 µg/mL leupeptin, 2 µg/mL aprotinin, 5 mM N-ethylmaleimide, 10 mM Na_3VO_4, 1% NP40, 6 mM phenylmethylsulfonyl fluoride, and 0.9 mg/ml BSA. The samples were centrifuged for 10 min and the supernatant discarded. The pellets were washed three times with HE lysis buffer and then boiled in 60 µl SDS sample buffer. The proteins were resolved on 6% SDS-polyacrylamide gels and transferred to nitrocellulose membranes for 2.5 h at 850 mA. The membranes were dried and exposed to X-ray film to visualize the ^{125}I-ubiquitin conjugates. To visualize the reductase domain, the membranes were probed with 0.05% nNOS mAb antibody (Transduction Laboratories) followed by 0.01% goat anti-mouse IgG antibody conjugated to peroxidase (Boehringer Mannheim, Indianapolis, IN). An ECL reagent (Amersham Life Science Inc., Arlington Heights, IL) and X-OMAT film (Kodak, Rochester, NY) were used to detect the peroxidase conjugate, as described by the manufacturer. The blots were re-probed with 0.04% nNOS pAb (Sigma) as above to visualize the oxygenase domain.

Expression and purification of his-tagged ubiquitin (His-Ub) - The full length human ubiquitin (pcDNA3.1-ub), kindly provided by Dr. Yi Sun, was modified by PCR with the forwarding primer containing an *NdeI* site (underlined) and a polyhistidine tag: 5'-ATATACATATGAAGCTTATGAGACATCACCATCACCATCACCAGATCTTCG TG-3' and the reverse primer containing a *BamHI* site (underlined): 5'-TTAAGCTTGGT ACCGGTACCGAGCTCGGATCCTT-3'. The resulting 300 bp PCR fragment was digested with *NdeI* and *BamHI*, ligated to similarly digested pET-11a, then transformed in *E. coli* BL21 (DE3) cells. The entire coding region of ubiquitin was confirmed by sequencing and the resulting construct was designated pHis-Ub.

His-Ub was bacterially expressed using the pET-11a vector and BL21 (DE3) competent cells (Stratagene), according to the manufacturer's recommendations. Cells from 1L-cultures were harvested 19 h after induction with IPTG, and ruptured by french press at 1500 PSI in lysis buffer containing 300 mM KCl, 20 mM Imidazole, 10% glycerol, 1 mM phenylmethanesulphonyl fluoride, and Complete Mini protease inhibitor cocktail (Roche) in 50 mM potassium phosphate pH 7.5. The lysates were centrifuged at 100,000 x g for 30 min, the cytosol removed and loaded on a Ni-NTA agarose (Qiagen) column. The column was washed and the His-Ub eluted using the manufacturer's recommended buffers (non-denaturing conditions). The His-Ub was loaded onto a PD-10 gel filtration column (GE Healthcare) equilibrated with 50 mM Tris, pH 7.5, 10 % glycerol, and 100 mM NaCl. The His-Ub was stored at –80 ^{o}C.

Purification of His-Ub-nNOS – The apo-nNOS was ubiquitinated as described above except His-Ub was used instead of native ubiquitin, the fraction II concentration was 4 mg/ml, ubiquitin aldehyde was omitted, and the total reaction volume was 40 ml. .

The nNOS was purified from the ubiquitination reaction using an ADP-sepharose column as described above. This ADP-Sepharose purified nNOS was immediately treated with N-ethylmalemide (10 mM) to inhibit de-ubiquitinating enzymes and inactivate the remaining dithiothreitol. The nNOS conjugated to His-Ub (His-Ub-nNOS) was then purified from the sample by Ni-NTA agarose (Qiagen) according the manufacturer's suggestions (denaturing conditions). The sample was concentrated with the use of a Centriplus YM-100 concentrator and stored at –80 ^{o}C.

CapLC-MS/MS Analysis – Purified His-Ub-nNOS was digested with trypsin (1:100 w:w) at room temperature for 2 hours. The digest was separated and analyzed using a Waters CapLC system (Waters Corp., Milford, MA) interfaced to an LTQ Linear Ion Trap (Thermo Finnigan). The trypsinized His-Ub-nNOS (100 μg of protein) was injected onto a reverse phase CapLC column (C18 Vydac, 5 μm, 0.05 x 15 cm, 350 A) equilibrated with solvent A (0.05% trifluoroacetic acid, 0.05% formic acid) at a flow rate of 5 μL/min. A linear gradient was run to 50% solvent B (0.05% trifluoroacetic acid, 0.05% formic acid, in acetonitrile) over 95 min and then to 100% solvent B over the next 5 min. Absorbance at 220 nm was monitored using the CapLC UV detector, and the eluted peptides were detected, isolated and fragmented on the LTQ ion trap using data dependent scanning.

Turbo Sequest Peptide Mapping Search Conditions – All MS/MS spectra were searched against the human ubiquitin and rat nNOS sequences from the non-redundant protein database (nr.fasta) using TurboSequest software. Variable modifications were allowed for the following mass shifts (in Daltons): ubiquitinated lysine (-GG, +114.1), ubiquitinated lysine with 1 missed trypsin cleavage on ubiquitin (-LRGG, +384.5), NEM

modified cysteine (+124.13), oxidized methionine (+16), phosporylated tyrosine (+79.98), and N-terminal acetylation (+42). Mass shifts for ubiquitinated lysine were obtained from Peng, et al (13). Sequest search criteria were as follows: Dta Generation – MW Range 0-10,000, Threshold 10,000. Dta Search – Enzyme Trypsin, # of internal cleavage sites 6, Database ratnNOS.fasta and ub.fasta (derived from nr.fasta). Tolerance & Limits for Dta Generation – Precursor Mass 1.4, Minimum Ion Count 1. Tolerance & Limits for Dta Search – Peptide 2.00, Fragment Ions 0.70, Results Scored 1000. Only peptides with and Xcorr value greater than 1.5, 2.0 and 2.5 for +1, +2 and +3 charge states, respectively, were reported.

Statistical analysis – All values are reported as the mean ± standard error (S.E.). Dunnett's Multiple Comparison Test was used with one-way ANOVA data to compare values. Statistical significance was considered to be achieved at a level of $p < 0.05$. PRISM statistical software (Graphpad, San Diego, CA) was used for analysis of the data sets.

Results

Mono-ubiquitination is a Sufficient Signal for the Proteasomal Degradation of nNOS – To address if mono-ubiquitinated nNOS plays a role in signaling for proteasomal degradation, we conducted studies with methylated ubiquitin (Methyl-Ub), which cannot form polyubiquitin chains (23, 24). For these studies, we used an *in vitro* reaction system, containing fraction II, which has been established to ubiquitinate and proteasomally degrade nNOS by an ATP-dependent process (2). The nNOS was incubated in the reaction mixture with ubiquitin or Methyl-Ub and aliquots were taken

and Western blotted with ubiquitin antibody. As shown in Fig. 4.1A, nNOS incubated for 60 min with ubiquitin (*lane 10*) shows a strong ubiquitin band detected at the bottom of the blot (160 kDa) corresponding to mono-ubiquitinated nNOS (nNOS-Ub), and a smear of higher molecular weight conjugates corresponding to polyubiquitinated nNOS. There is an increase in both ubiquitin species over time for the ubiquitin samples (*lanes 1, 4, 7 and 10*), that is not seen in the control sample where no ubiqutin was added (*lanes 3, 6, 9 and 12*). As expected, when Methyl-Ub (*lanes 2, 5, 8, and 11*) was substituted for ubiquitin, there is an increase in the mono-ubiquitinated nNOS over time, but not in the polyubiquitin conjugates, confirming that Methyl-Ub can conjugate to nNOS, but cannot form polyubiquitin chains. The intense ubiquitin band seen on the bottom of the blot was previously identified as mono-ubiquitinated nNOS (1, 8). There is also some background mono-ubiquitinated nNOS detected (*lanes 1-3*), which is due to the presence of a small amount of ubiquitinated nNOS in our purified nNOS preparation. The time-dependent accumulation of mono-ubiquitinated nNOS (*nNOS-Ub*) was quantified and plotted (Fig. 4.1B). There is a time-dependent increase in the mono-ubiquitinated nNOS in the presence of Methyl-Ub (*closed squares*) over that of the no ubiquitin control (*closed triangles*). While there appear to be lower levels of mono-ubiquitinated nNOS in the Methyl-Ub (*closed squares*) as compared to the ubiquitin (*closed circles*) samples, there was no statistical difference between the levels.

In Fig. 4.1C, we incubated nNOS in fraction II in the presence of ubiquitin (Ub) or Methyl-Ub and Western blotted for nNOS to determine the proteasomal degradation of the protein, as previously established (2). The band corresponding to nNOS was quantified, and the loss of the protein over time was plotted (Fig. 4.1D). As shown in

Fig. 4.1D, there was a time-dependent loss of nNOS when ubiquitin was present (*closed circles*). In the absence of added ubiquitin, there is a loss of nNOS for the first 40 min (*solid triangles*), which is likely attributed to the presence of trace ubiquitin in fraction II, as previously described (2). In the presence of Methyl-Ub, there is a loss of nNOS comparable to that found with ubiquitin (*cf. closed squares and closed circles*). We establish here, for the first time, that mono-ubiquitination of nNOS is a sufficient signal for the proteasomal degradation of the enzyme.

Ubiquitination of nNOS Domains – Next we chose to investigate what site(s) on nNOS is ubiquitinated. Using limited trypsinolysis, which selectively cleaves at Lys 727 (15), we generated the oxygenase and reductase domains of nNOS. This trypsin-treated nNOS was then directly used for ubiquitination studies. In Fig. 4.2A, we compared the ubiquitination of full length nNOS (*lane 1*) and trypsinized nNOS (*lane 2*) in fraction II utilizing ^{125}I-ubiquitin. As a control, an ubiquitination reaction mixture where nNOS was omitted (*lane 3*) was included. After ubiquitination, the mixtures were immunoprecipitated with an antibody recognizing the oxygenase domain (IP) or affinity purified by ADP-Sepharose (ADP) which binds to the NADPH binding region in the reductase domain of nNOS. Immunoprecipitation of the ubiquitination reaction mixture containing the trypsinized nNOS showed an immunodetectable nNOS band at 85 kDa (*oxygenase*) only when blotted with the antibody specific for the oxygenase domain of nNOS (*left panel, IP, lane 2*). Conversely, the ADP-Sepharose affinity purification showed an immunodetectable nNOS band at 77 kDa (*reductase*) only when blotted with the reductase specific antibody (*center panel, ADP, lane 2*). Both purifications were able to isolate the 160 kDa full length nNOS (*nNOS*) from the ubiquitination reaction (*left and*

center panels, lane 1). Direct exposure of the blot to x-ray film detected an ^{125}I-ubiquitin signal for the trypsin derived reductase fragment (*Red 1-Ub; right panel, ADP, lane 2*) and the full length nNOS controls (*nNOS-Ub*; *right panel, lane 1*). The Red 1-Ub signal was ~8 kDa higher (84 kDa) than the immuodetectable nNOS band (*reductase*) found in the sample (*compare right panel, ADP, lane 2 with center panel, ADP, lane 2*), which is consistant with the addition of one ubiquitin monomer (8.5 kDa) to the protein. The lack of immunodetectable nNOS signal for the ubiquitin band is attributed to the relative sensitivities of the assays. It is also possible that the accessibility of the antibody recognition sequence may be hindered by the bound ubiquitin. The ^{125}I-ubiquitin signal seen at 160 kDa for full length nNOS (*right panel, lane 1*) is the same as the immunodetectable nNOS bands (*left and center panels, lane 1*), which is also consistant with the mono-ubiquitination of nNOS.

The oxygenase (Oxy-CaM; residues 1-756) and reductase (residues 746-1429) domains were generated directly by recombinant expression and purification, and used as substrates for ubiquitination by fraction II. As shown in Fig.4.2B top panel, incubations with the purified Oxy-CaM show a time-dependent increase in the ubiquitin band at ~90 kDa, corresponding to ubiquitinated Oxy-CaM (Oxy-CaM-Ub). Studies with the purified reductase domain show a very faint ubiquitin band found at ~75 kDa corresponding to ubiquitinated reductase (Red 2-Ub). The accumulation of Oxy-CaM-Ub is much greater than that seen for Red-2-Ub, and this difference is not due to variable protein levels, as shown by Amido Black staining of the membrane (*bottom panel*).

Fig.4.3 shows a schematic of the recombinant nNOS domains (Oxy-CaM and Red 2), and the predicted nNOS domains resulting from limited trypsinolysis (Oxy 1 and Red

1). The sites of recognition for the antibodies used to detect the oxygenase (Anti-Oxy) and reductase (Anti-Red) domains in Fig.4.2A are also shown. It is interesting to note that the site of trypsin cleavage is located in the calmodulin binding site (residues 720-756), a linker region between the two domains. Bound calmodulin is required for proper electron transfer to the active site, and is a necessary co-factor for nNOS activity. The purified Oxy-CaM domain (residues 1-756) contains amino acid residues 728-756 that are not found in the Oxy 1 domain (residues 1-727) generated from limited trypsinolysis. The presence of these amino acid residues appears to be sufficient for ubiquitination of the oxygenase domain. Taken together with the fact that the recombinant Red 2 (residues 746-1429) was not ubiquitinated and the Red 1 domain (residues 728-1429) generated from limited trypsinolysis was detected as the main ubiquitinated domain, the critical residues for this apparent switching of ubiquitination between domains seem to be in the calmodulin binding region.

Bound Calmodulin Hinders nNOS Ubiquitination – We sought to determine if the binding of calmodulin to nNOS could block the formation of nNOS-Ub conjugates in the ubiquitination reaction mixture. The mono-ubiquitination of nNOS was measured with $CaCl_2$ (200 μM) and calmodulin added to the in the reaction mixture. As shown in Fig.4.4A upper panel, the mono-ubuiquitinated nNOS band (nNOS-Ub) decreases as the concentration of calmodulin increases (*cf. lanes 1-4*). This effect is partially reversed in the presence of 10 mM EGTA (*cf. lanes 4 and 5*), which will sequester the calcium, a necessary factor for calmodulin binding to nNOS. To analyze the differences, the bands corresponding to nNOS-Ub were quantified and graphed (Fig.4.4B). The nNOS-Ub levels when 150 or 500 μg/ml calmodulin was added to the reaction were statistically

lower than found when no calmodulin was added. The calmodulin protection of nNOS from ubiquitination at 500 μg/ml was partially reversed by the addition of EGTA, resulting in nNOS-Ub levels that were not statistically different than the no calmodulin added control.

Mutagenesis Studies on the Calmodulin Binding Region of nNOS, and Ubiquitination of the Mutant Proteins – The ability of calmodulin to block the ubiquitination of nNOS supported the idea that the site of ubiquitin attachment to nNOS is in the calmodulin binding region. Since ubiquitin is covalently bound to a lysine residue on the target protein, we decided to construct a mutant nNOS (7R) that replaced the seven lysine residues found within the calmodulin binding region with arginine residues (Fig. 4.5). Arginine was chosen because it will maintain the charge, and should not significantly alter the structure or folding of the enzyme. All seven lysine residues were mutated because ubiquitination of a target protein can be very promiscuous, and the ubiquitin adduct could form with another available lysine residue in the same region if the primary site is mutated. The mutant was tested and found to be as active as the wild type with activities of 323 and 371 nmol NO/min/mg protein, respectively.

In Fig.4.6A top panel, we compared the ubiquitination of 7R with wild type nNOS (WT) using the *in vitro* ubiquitination mixture containing fraction II. As seen previously, we detect a time-dependent increase in the immunodetectable mono-ubiquitinated nNOS band (nNOS-Ub) and the higher molecular weight polyubiquitin smear in the case of the wild type protein. The time-dependent increase in ubiquitin conjugates is seen for the 7R mutant as well, but the signal for mono-ubiquitinated nNOS appears to be less intense than that found for the wild type. The band corresponding to

mono-ubiquitinated nNOS was quantified and plotted to compare the levels of ubiquitination (Fig.4.6B). The level of nNOS-Ub for the 7R mutant (*closed squares*) was statistically different than WT (*closed circles*), with an approximately six-fold difference in the mean values at 60 min. To determine if we could recover some, or all, of the loss in signal by the introduction of a native lysine residue back into the 7R, we created three "6R" mutants 6R733K, 6R739K and 6R754K that have the indicated lysine residue restored. These native lysine residues map to the N-terminal, middle, and C-terminal sections of the calmodulin binding region of nNOS, respectively (see Fig.4.5). The 6R mutants were tested for activity, and were shown to be equivalent to wild type (*data not shown*). The ubiquitination of the 6R733K, 6R739K and 6R754K mutants was tested using the *in vitro* ubiquitination mixture containing fraction II. Fig.4.6A (*lower panel*) shows that we can detect a time-dependent increase in the immunodetectable mono-ubiquitinated nNOS band (nNOS-Ub) and the higher molecular weight polyubiquitin smear for all the 6R mutants. These levels appear to be at least at the level of WT, and the time-dependent accumulation of mono-ubiquitinated nNOS was quantified and plotted (Fig.4.6B). The nNOS-Ub levels for 6R733K (*closed triangles*), 6R739K (*closed diamonds*), and 6R754K (*open circles*) were all higher than that seen for 7R (*closed squares*), and were not statistically different than WT (*closed circles*). It appears that the restoration of a single lysine residue to 7R was able to restore the time-dependent ubiquitination back to the levels of wild type, despite their various locations within the calmodulin binding region.

Degradation of the 7R and 6R nNOS Mutants – While we detected much lower levels of ubiquitination in the 7R mutant as compared to wild type (Fig.4.6),

ubiquitination of a target protein can serve as a signal for many processes besides proteasomal degradation. To determine if ubiquitination in the calmodulin binding region could serve as a signal for degradation, we measured the *in vitro* proteasomal degradation of the 7R mutant as compared with wild type (WT) in Fig.4.7A. The immunodetectable nNOS signal for WT decreases over time, while the signal for the 7R sample remains stable. The nNOS bands were quantified (Fig.4.7B). The time-dependent loss of nNOS protein was greater for WT (closed circles) as compared to 7R (closed squares), with the 7R only losing 3% of its initial protein level over 40 min, and only 10% over 80 min. The *in vitro* proteasomal degradation was also measured for 6R733K, 6R739K and 6R754K (Fig.4.7A). The immunodetectable nNOS signal appears to decrease over time for all samples. As shown in Fig.4.7B, the time-dependent loss of nNOS protein for 6R733K (*closed triangles*), 6R739K (*closed diamonds*), and 6R754K (*open circles*) was greater than that found for 7R (*closed squares*), and was not statistically different from WT (*closed circles*). In that the degradation data parallel the ubiquitination data for the mutants tested, ubiquitination in the calmodulin binding region must be a signal for selective degradation by the proteasome.

Generation and Purification of the His-tagged-ubiquitin nNOS conjugate (His-Ub-nNOS) – The mutation data show that lysine residues contained in the nNOS calmodulin binding region can serve as targets for ubiquitination that leads to proteasomal degradation. While the 6R733K, 6R739K and 6R754K mutants were able to be ubiquitinated and degraded by the proteasome, it is not known which lysine residue is the primary site of ubiquitin attachment in the wild type protein. To determine the exact site(s) of ubiquitination on wild type nNOS and to confirm that nNOS can indeed be

ubiquitinated in the calmodulin binding region, we decided to use a direct mapping technique that detects ubiquitinated peptides after trypsinolysis using MS/MS sequencing (13). To identify an ubiquitinated nNOS peptide by this method, we needed to purify ubiquitinated nNOS. Using his-tagged ubiquitin and purified nNOS (12 mg), we generated his-tagged-ubiquitin nNOS conjugate (His-Ub-nNOS) using the *in vitro* ubiquitination reaction mixture containing fraction II. The reaction was scaled to 40 mL total volume, and the His-Ub-nNOS was enriched by ADP-Sepharose followed by Ni-NTA agarose. Samples were taken at each step of the enrichment process to determine the purity and stability of the His-Ub-nNOS, and Western blotted for ubiquitin and nNOS. As shown in Fig.4.8, the initial ubiquitination reaction contains large amount of ubiquitin conjugates (*wb:Ub, lane 1*). The sample also has a large amount of nNOS protein (*wb:nNOS, lane 1*). When this mixture is purified by ADP-Sepharose, most of the ubiquitin signal is found in the unbound fraction (*lane 2*) while most of the nNOS signal is bound (*lane 3*). There is still a strong ubiquitin signal above 100 kDa present in the bound fraction (*wb:Ub, lane 3*). The material bound to the ADP-sepharose was eluted and purified by Ni-NTA agarose. The vast majority of nNOS is unbound (*lane 4)*, whereas the ubiquitin signal is found only in the bound fraction (*lane 5*). The small amount of nNOS seen in the Ni-NTA bound fraction (*wb:nNOS, lane 5*) has a corresponding ubiquitin band with very little background (*wb:Ub, lane 5*). This final Ni-NTA bound nNOS is highly enriched for nNOS-Ub (~100 μg), and is representative of approximately 1% of the total nNOS used. This material (His-Ub-nNOS) was eluted and used as the substrate for the direct mapping studies.

Peptide Mapping Using Trypsin and CapLC-MS/MS – The His-Ub-nNOS was trypsinized for 2 hr at 37^{o}C and analyzed by CapLC-MS/MS to obtain a peptide map of the modified protein. The separation produced well over 50 distinct peptides by UV absorbance at 220 nm (Fig. 4.9, A), and many more as seen by total ion current (TIC) on the LTQ Linear Ion Trap (Fig. 4.9, B). The MS/MS data was analyzed using Turbo Sequest as described in "Methods." The peptide mapping data was searched for nNOS peptides containing the signature –GG (+114 Da) modification identifying an ubiquitinated lysine residue as described by Peng, et al (13). The search identified one peptide in the calmodulin binding region with an acceptable XCorr value (2.1) that met these criteria with a parent m/z of 894.52 with a +2 charge state (Fig. 4.10A). This ion had a mass (MH +) of 1789.04, and is consistent with the theoretical mass of the trypsin-derived nNOS peptide with the following sequence: RVKATILYATETGK. To confirm this sequence, MS/MS analysis was performed (Fig.410B). The peptide was found to contain the following modifications: acetylation (]), -GG tag (*, +114 Da), and phosphorylation (~) as depicted (Fig. 4.10B, *top panel*). The signature diglycine (-GG) indicating an ubiquitinated lysine resulted in a missed trypsin cleavage as predicted. Cleavage at the peptide backbone in the LTQ linear ion trap would result in the predicted fragment ion masses shown (*b*- and *y*-type ions). Fig.4.10B *bottom panel* shows the fragmentation pattern (MS/MS spectrum) acquired that identified the peptide in Fig.4.10B, *top panel*. The *b*- and *y*- ions for only the singly charged species are labeled for simplicity, and the *b*-ion fragmentation pattern is depicted at the top for reference. The ions below m/z 600 m/z were magnified 3x to help visualize the site of ubiquitin conjugation (b2 – b3). This nNOS peptide is found in the calmodulin binding region

(residues 752-765), with the –GG tag assigned to lysine residue 754. These data are consistant with the notion that wild type nNOS proteasomal degradation is regulated by mono-ubiquitination in the calmodulin binding region, as shown by the mutagenesis studies previously described.

Discussion

nNOS is known to be regulated by the ubiquitin proteasome system (1). Certain dysfunctional forms of the protein are selectively targeted for degradation (2-3). It is thought that these dysfunctional, or labilized, forms of the protein are selectively targeted due to the recognition of some change in structure of nNOS that is recognized by cellular control factors that facilitate the recruitment of the ubiquitination machinery. In the case of nNOS, it is has been shown that the monoubiquitinated form is the main species detected both in HEK293 cells and *in vitro* (1, 8). To better understand the ubiquitination process, and what structural features of dysfunctional nNOS are available for recognition by cellular factors, we chose to determine if mono-ubiquitination can signal for the proteasomal degradation of nNOS, and to identify the site(s) of ubiquitination. We found that monoubiquitinated nNOS is a substrate for proteasomal degradation, and that lysine residues in the calmodulin binding region can be ubiquitinated and signal for proteasomal degradation *in vitro*.

Ubiquitin that is methylated on lysine residue 48 is unable to form the classical polyubiquitin chain. When used in the *in vitro* ubiquitination system derived from rabbit reticulocyte lysate, this methylated ubiquitin was able to conjugate to nNOS. As expected, the ubiquitination patterns were different than seen with native ubiquitin, with a

distinct ubiquitin band at the same gel mobility of nNOS (160 kDa) detected in both the methylated ubiquitin and ubiquitin containing reactions but higher molecular weight polyubiquitin conjugates detected only in the ubiquitin containing sample. This data confirms the previously published work labeling this ubiquitin band a mono-ubiquitinated nNOS conjugate (1, 8). Furthermore, methylated ubiquitination was sufficient to target nNOS for degradation by the proteasome in the *in vitro* degradation reaction mixture. Taken together, these data show that the monoubiquitination of nNOS can indeed signal for proteasomal degradation. Monoubiquitination is known to target membrane proteins for lysosomal degradation, and monoubiquitination is also involved in transcriptional regulation (16). While monoubiquitination is not the standard form degraded by the proteasome (17), recent work on monoubiquitination of Pax3 (7) shows that it is possible for monoubiquitination to localize a protein to the proteasome, and to be sufficient for proteasomal degradation (18, 19).

In the case of nNOS, it is known that the stability of the dimer plays a role in the ubiquitination and degradation of the enzyme. In particular, destabilization of the enzyme has been shown to enhance the ubiquitination of nNOS *in vitro* (2) and in cells (8), whereas stabilization using reversible inhibitors protects the protein from proteasomal degradation (2). The stability of the dimer plays an important role, but the specific signal or structural recognition site for degradation is not known. It has been suggested that destabilization of the dimeric form of nNOS could lead to the exposure of hydrophobic residues normally hidden in the active form of the protein (20). These hydrophobic residues could serve as a "degradation signal" that is recognized by the ubiquitin-proteasome system when they are exposed, consistent with that found for the

heterodimerization of the MATa1 and Matα1 transcription factors in yeast (21). An E3 ubiquitin ligase CHIP (C-terminus of Hsc70 interacting protein) has also been shown to coimmunoprecipitate with nNOS and to facilitate its ubiquitination (20). However, the exact ubiquitin binding site on nNOS was not known. We chose to directly map the ubiquitination site on nNOS to provide information on what region of nNOS has to be accessible to the cellular factors recognizing dysfunctional nNOS for degradation. The mutagenesis data showing decreased ubiquitination and degradation of the 7R mutant strongly suggests that the calmodulin binding region is a site that, when ubiquitinated, can lead to the degradation of nNOS. This is even more apparent given the fact that the restoration of just one of the lysines in this region (6R733K, 6R739K or 6R754K) can fully restore ubiquitination and degradation back to the levels seen with native nNOS. To confirm that nNOS can form an ubiquitinated conjugate in the calmodulin binding region, we conducted peptide mapping studies using purified nNOS-ubiquitin conjugates that were proteolyzed by trypsinized and analyzed by CapLC-MS/MS. The mapping studies identified a candidate peptide located in the calmodulin binding region (residues 752-765) with the ubiquitin modification located on lysine residue 754, supporting the finding that mono-ubiquitination in the calmodulin binding site can indeed lead to the proteasomal degradation of nNOS.

Given the fact that NO is a very short lived molecule that cannot be stored or released from vesicles, its steady state levels are due soley to the levels of active NOS. Therefore, the molecular mechanism of how dysfunctional nNOS protein is selectively recognized for degradation is a basic cellular process that is directly involved in controlling the steady state levels of NO produced. These studies provide a first glimpse

into the complicated signaling process involved in cellular protein regulation. Due to the fact that the 7R mutant is not rapidly degraded, it can be used in future studies as a powerful tool to investigate the cellular factors that recognize, and form complexes with, dysfunctional nNOS. These studies may not otherwise be possible since dysfunctional native nNOS is rapidly degraded by the proteasome.

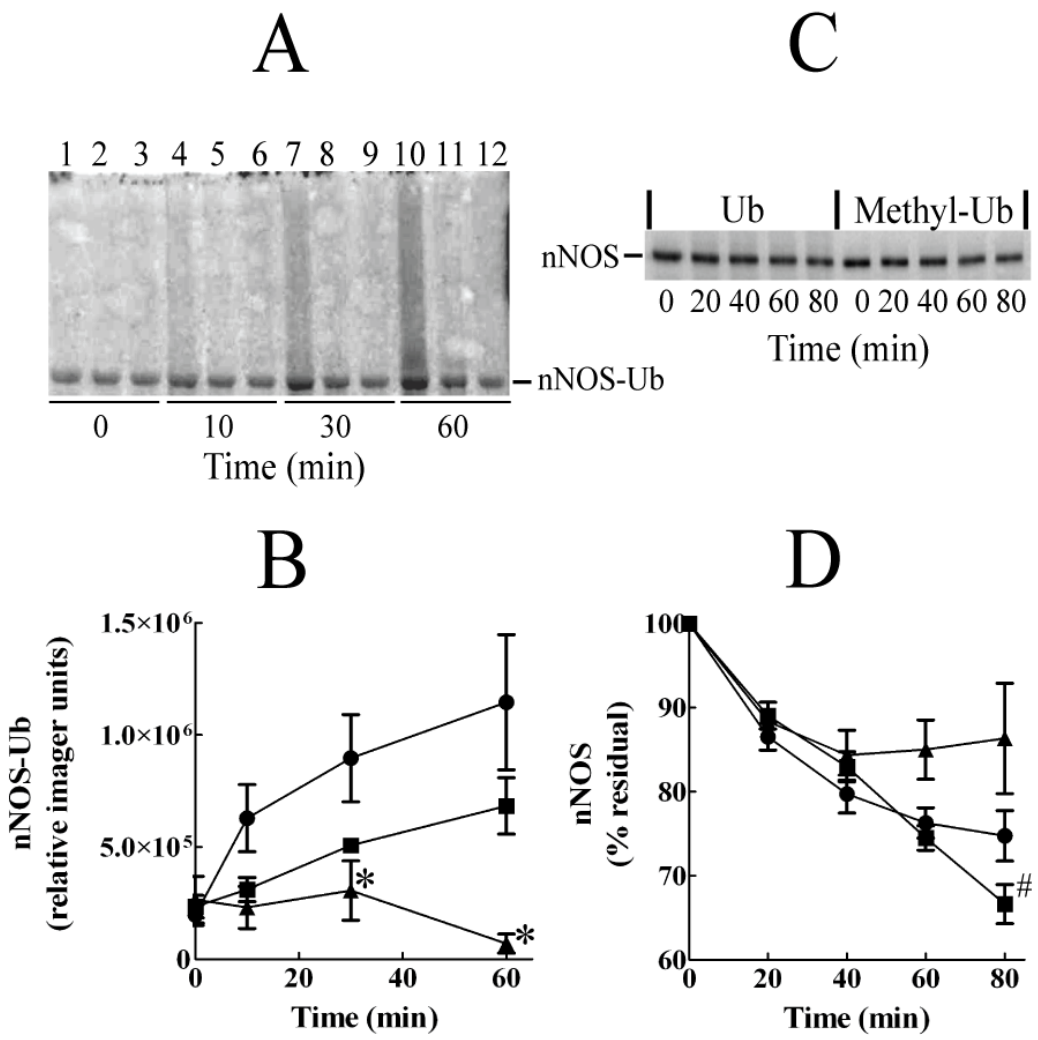

Fig. 4.1. **Effect of Methyl-Ub on the ubiquitination and degradation of nNOS by fraction II.** The ubiquitination and degradation of nNOS catalyzed by fraction II in the presence of ubiquitin or Methyl-Ub was examined, as described in "Methods." *A,* nNOS-ubiquitin conjugates (nNOS-Ub) were detected by Western blot. nNOS was incubated in fraction II without added ubiquitin (*lanes 3, 6, 9 and 12)*, with ubiquitin (*lanes 1, 4, 7 and 10*), or with Methyl-Ub (*lanes 2, 5, 8 and 11)*. *B*, the nNOS-Ub band shown in *A* was quantified by the use of phosphor imaging, as described in "Methods." Closed circles, ubiquitin; closed squares, methylated ubiquitin; closed triangles, no ubiquitin added. *C,* nNOS protein was detected by Western blot. nNOS was incubated in fraction II with ubiquitin (Ub) or Methyl-Ub for the times indicated. *D*, the nNOS band shown in *C* was quantified by the use of phosphor imaging, as described in "Methods." Closed circles, ubiquitin; closed squares, Methyl-Ub; closed triangles, no ubiquitin added. The values presented on the graphs are the means ± S.E. (n = 3). * denotes significantly ($p < 0.05$) lower nNOS-Ub conjugates relative to fraction II with ubiquitin. # denotes significantly ($p < 0.05$) lower nNOS levels relative to no ubiquitin added.

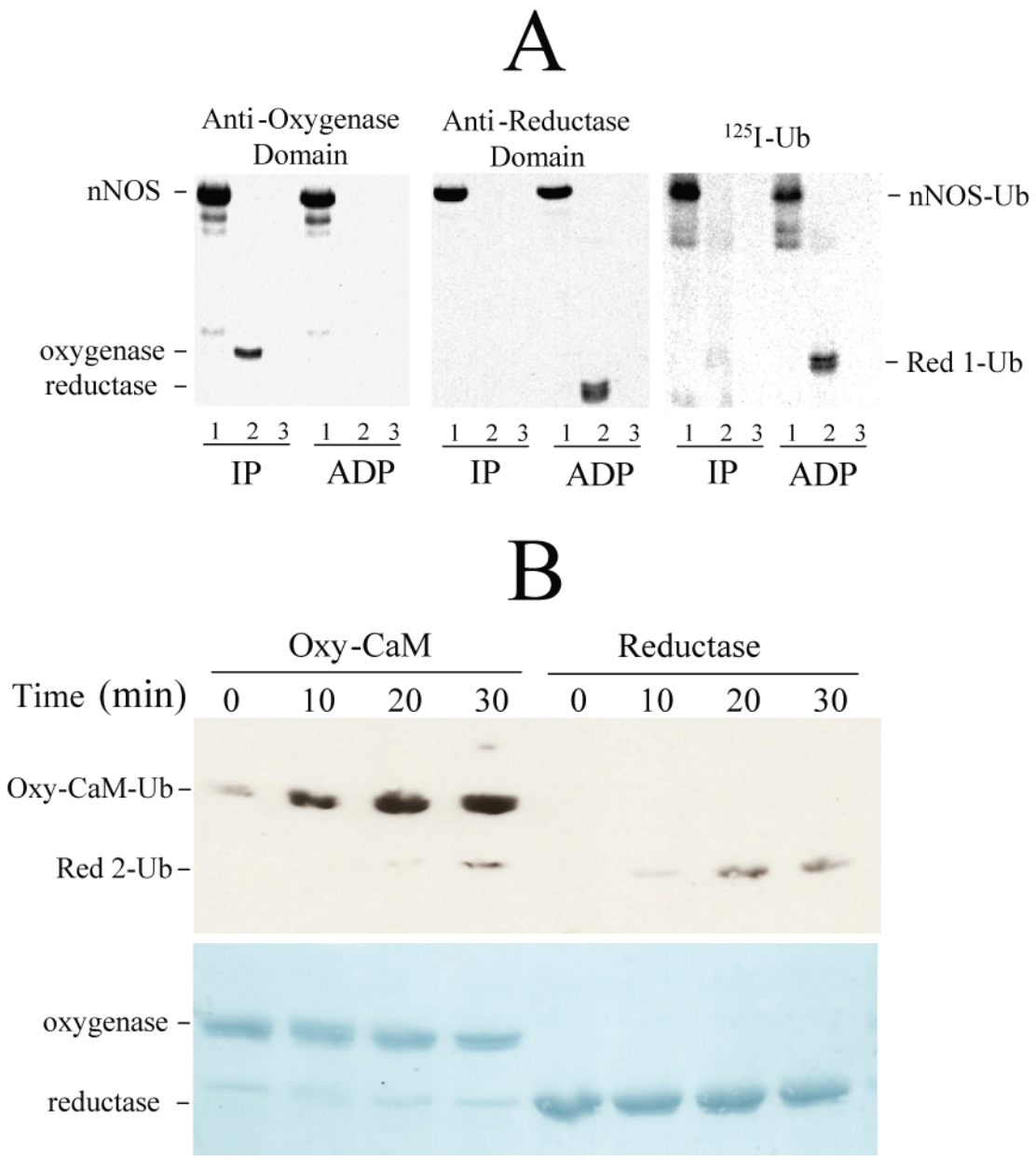

Fig. 4.2. **Ubiquitination of the oxygenase and reductase domains of nNOS by fraction II.** *A,* ubiquitination of the oxygenase and reductase domains, which were generated by limited typsinolysis of nNOS. Lane 1, full length nNOS; lane 2, trypsin-treated nNOS; lane 3, control where nNOS was omitted. The nNOS was treated with trypsin and then placed in the ubiquitination reaction mixture as described in "Methods." After ubiquitination, nNOS was immunoprecipitated with an antibody recognizing the oxygenase domain (*IP*) or was adsorbed to ADP sepharose (*ADP*). Samples were analyzed by Western Blot, using antibody specific for the oxygenase domain (*left panel),* the reductase domain (*center panel*), or by exposing the blot directly to x-ray film to visualize the ^{125}I-labeled ubiquitin (*right panel)*. *B*, ubiquitination of the recombinant oxygenase (Oxy-CaM, amino acid residues 1-756) and reductase (amino acid residues 746-1429) domains of nNOS by fraction II. *Upper panel,* ubiquitin adducts to Oxy-CaM (Oxy-CaM-Ub) and reductase (Red 2-Ub) were detected by Western blot. *Lower panel,* the protein levels of the oxygenase and reductase domains were determined by Amido Black staining.

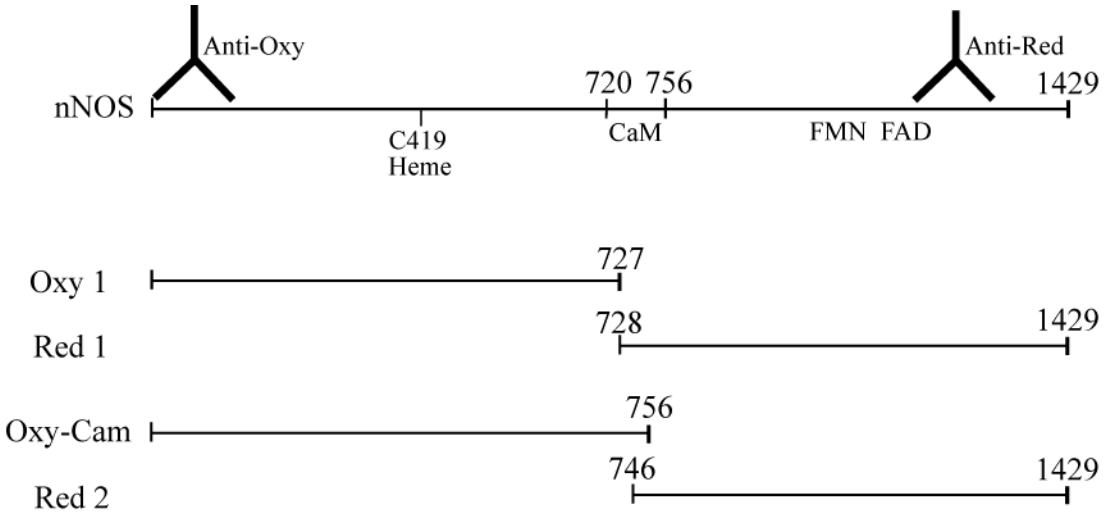

Fig. 4.3. **Schematic map of the nNOS domains used in the ubiquitination studies.** The resultant domains from limited trypsin cleavage of nNOS (Oxy and Red 1) and the recombinant nNOS domains (Oxy-CaM and Red 2) are shown.

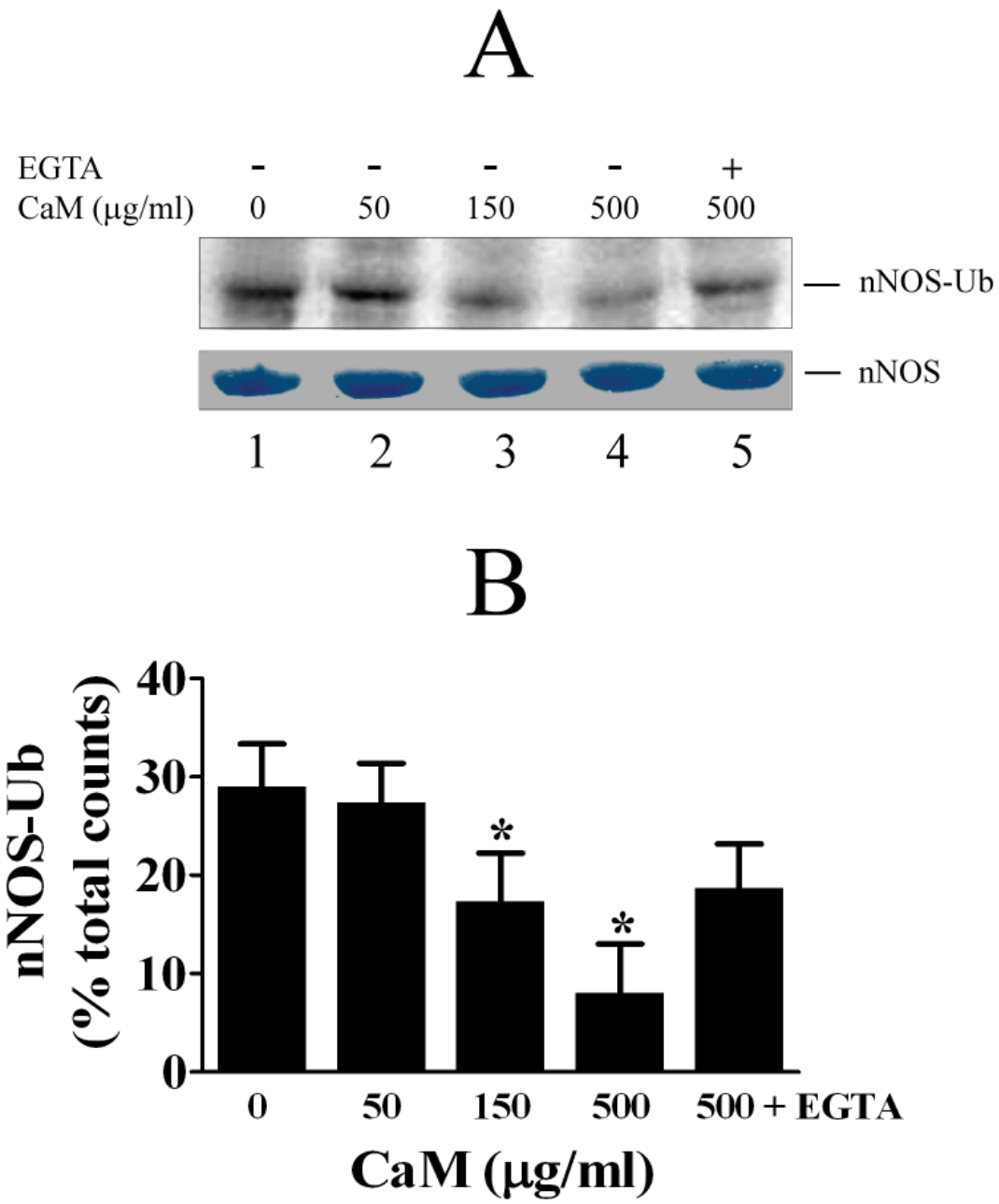

Fig. 4.4. **Calmodulin hinders ubiquitination of nNOS by fraction II.** The ubiquitination of nNOS catalyzed by fraction II was examined as described in "Methods," except that 200μM calcium chloride and calmodulin were added. EGTA (10mM) was added where indicated. *A, Upper panel,* nNOS-ubiquitin conjugates (nNOS-Ub) were detected by Western blot. *Lower panel,* the nNOS protein (nNOS) levels were determined by Amido Black staining. *B,* the relative amount of nNOS-Ub detected in *A* was quantified by phosphor imaging, as described in "Methods." The quantified nNOS-Ub bands were reported as a percentage of the sum of the counts for all the nNOS-Ub bands in the blot (% total counts). The values are the mean ± S.E. (n = 3). * denotes significantly ($p < 0.05$) lower nNOS-Ub conjugates relative to the 0 μg/ml CaM condition.

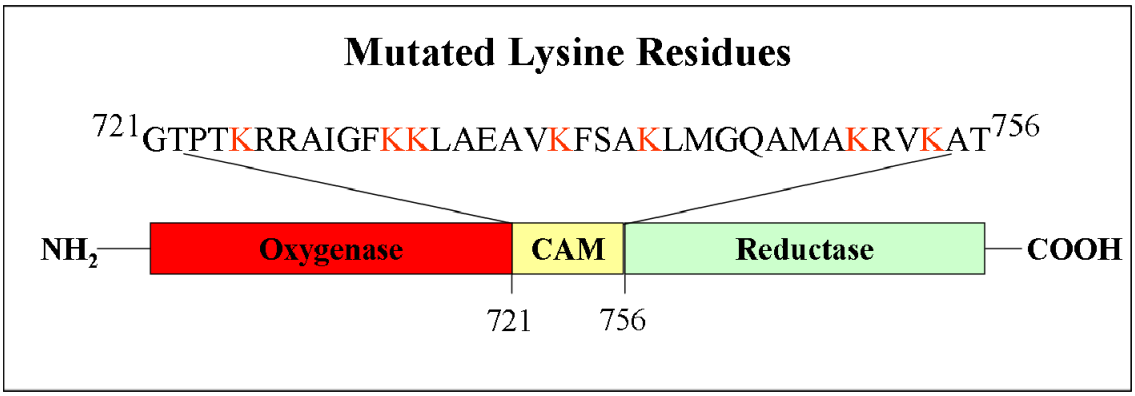

Fig. 4.5. **Creation of the 7R nNOS mutant.** The 7 lysine residues found within the calmodulin binding region were mutated to arginines.

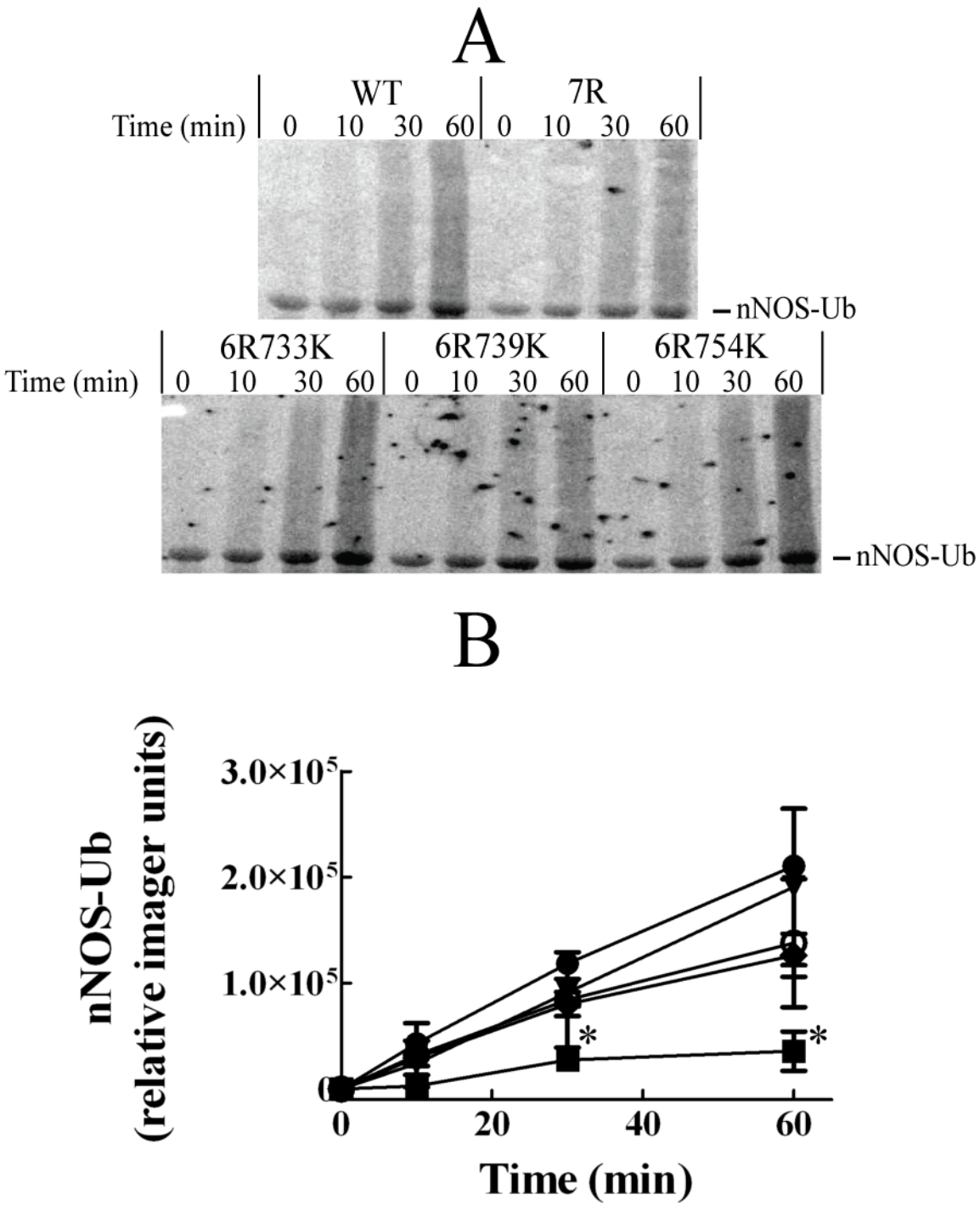

Fig. 4.6. **Ubiquitination of the 7R and 6R nNOS mutants.** The ubiquitination of the 7R and 6R mutants catalyzed by fraction II was examined, as described in "Methods." *A,* nNOS-ubiquitin conjugates (nNOS-Ub) were detected by Western blot. *B,* the nNOS-Ub band shown in *A* was quantified by the use of phosphor imaging, as described in "Methods." Closed circles, wild type; closed squares, 7R; closed triangles, 6R733K; closed diamonds, 6R739K; open circles, 6R754K. The values are the mean ± S.E. (n = 3). * denotes significantly ($p < 0.05$) lower nNOS-Ub conjugates relative to the wild type control.

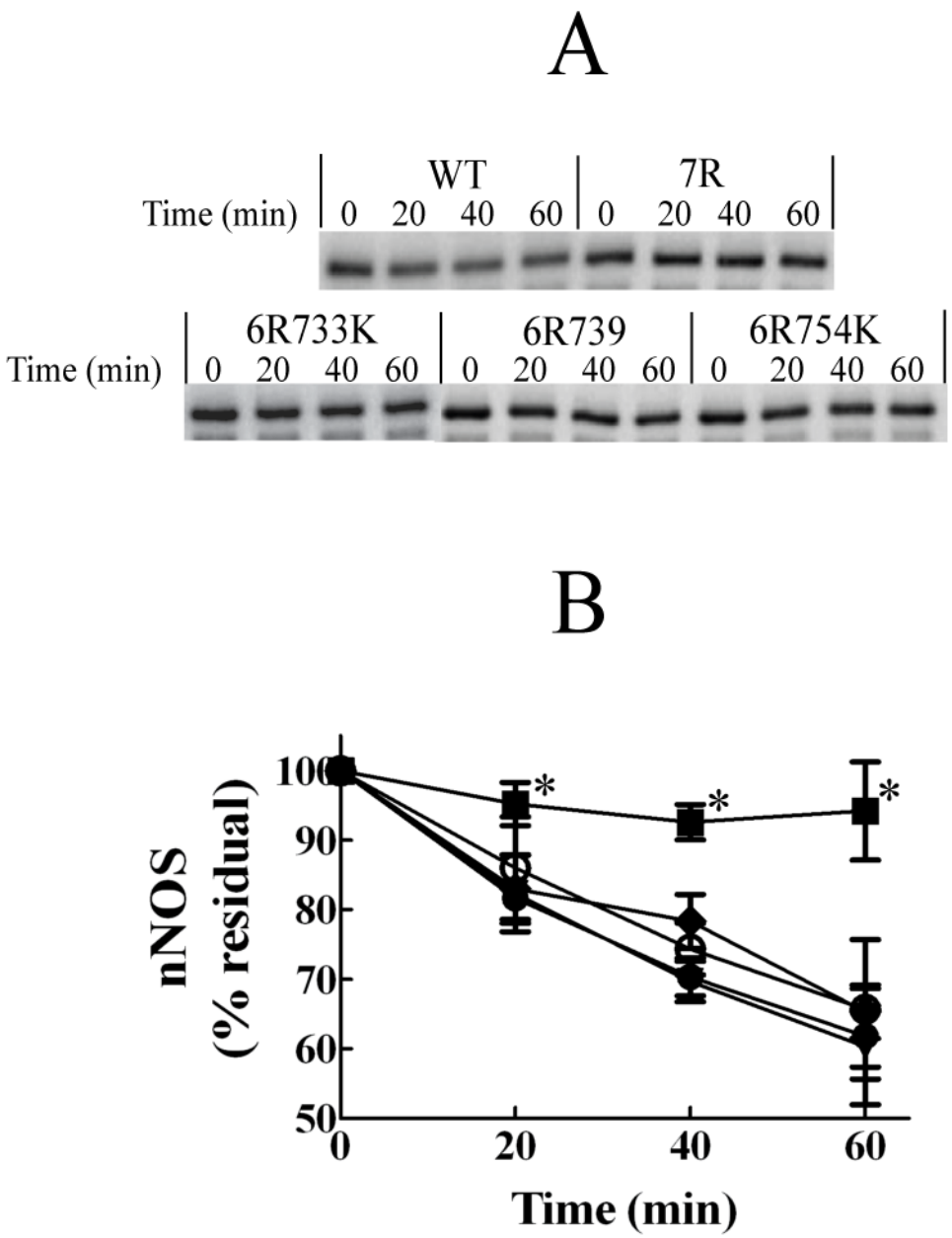

Fig. 4.7. **Degradation of the 7R and 6R nNOS mutants.** The degradation of nNOS catalyzed by fraction II was examined, as described in "Methods." *A,* nNOS protein was detected by Western blot. *B,* the nNOS band shown in *A* was quantified by the use of phosphor imaging, as described in "Methods." Closed circles, wild type; closed squares, 7R; closed triangles, 6R733K; closed diamonds, 6R739K; open circles, 6R754K. The values are the mean ± S.E. (n = 3). * denotes significantly ($p < 0.05$) higher nNOS protein relative to the wild type control.

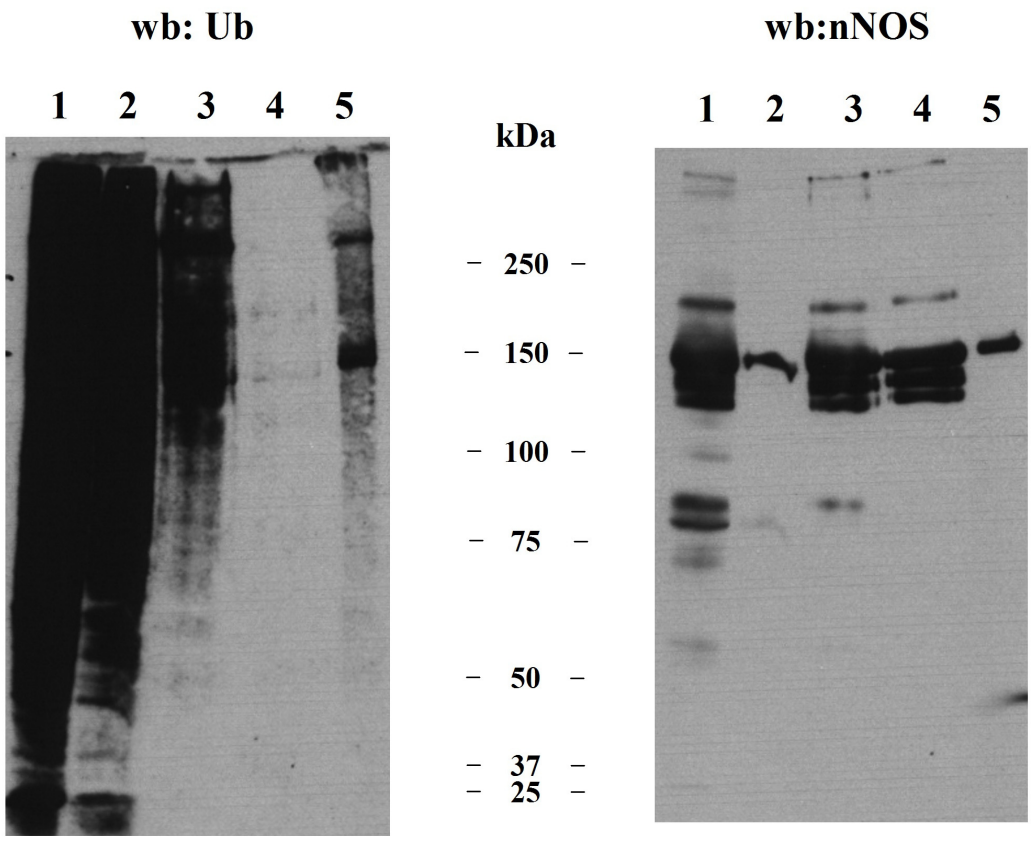

Fig. 4.8. **Purification of His-Ub-nNOS.** The large scale ubiquitination of nNOS catalyzed by fraction II in the presence of his-tagged ubiquitin was performed as described in "Methods." The nNOS in the ubiquitination reaction was purified by ADP-Sepharose. The his-tagged ubiquitin-nNOS conjugates (His-Ub-nNOS) were isolated from this ADP-Sepharose bound nNOS using Ni-NTA agarose. Aliquots were taken at each step and were analyzed by Western blot for ubiquitin (*Left pane1, wb:Ub)* and nNOS protein (*right panel, wb:nNOS)* Samples are: Ubiquitination reaction (*lane 1*), ADP-Sepharose unbound fraction (*lane 2*), ADP-Sepharose Eluant (*lane 3*), Ni-NTA agarose unbound fraction (*lane 4*), and Ni-NTA Eluant (lane 5). Samples were loaded in equal amounts as determined by percentage total volume.

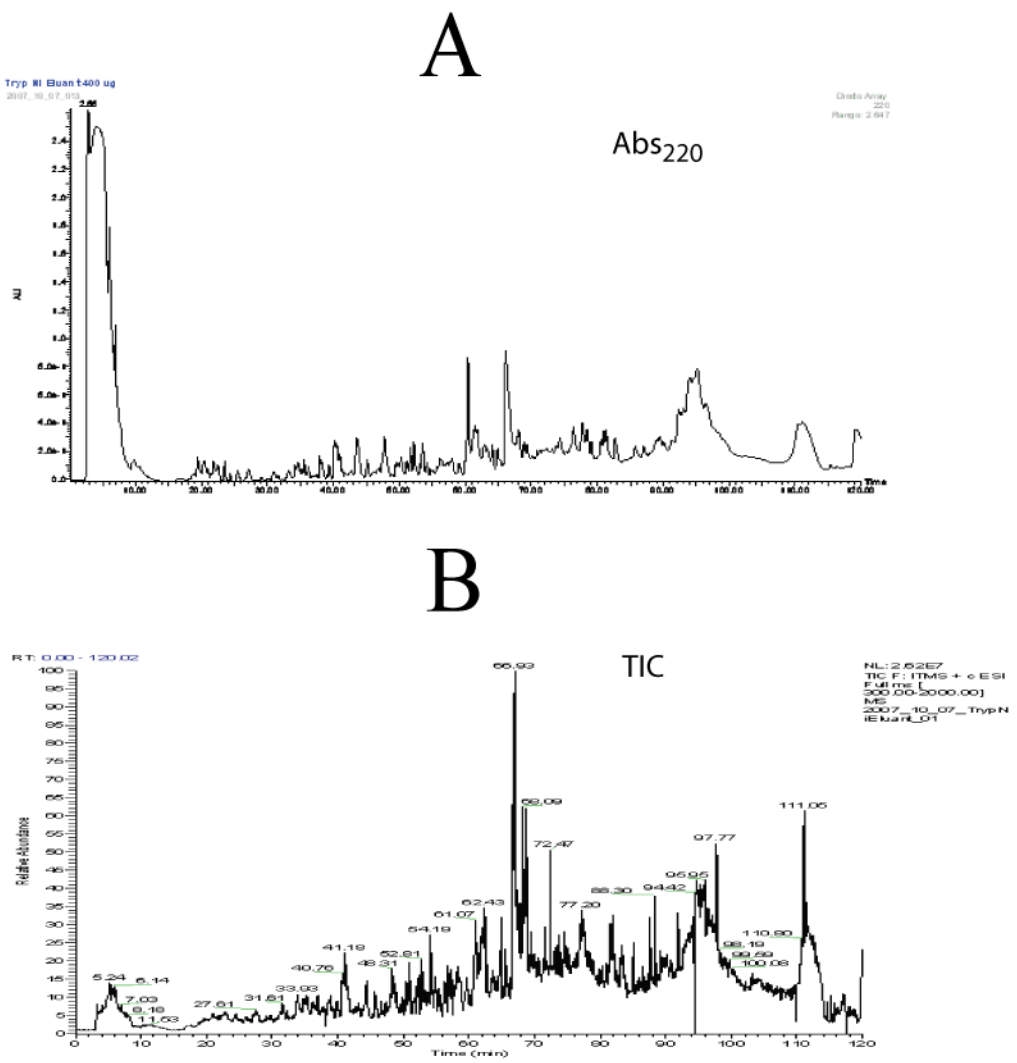

Fig. 4.9. **HPLC and CapLC-MS/MS profiles of His-Ub-nNOS treated with trypsin.** His-Ub-nNOS was trypsinized and analyzed by reverse phase CapLC-MS/MS as described in "Methods." *A*, HPLC profile (reverse phase, Abs_{220}) of trypsinized His-Ub-nNOS. *B*, total ion current (TIC) profile of the HPLC separated trypsinized His-Ub-nNOS digest on the Finnigan LTQ linear ion trap.

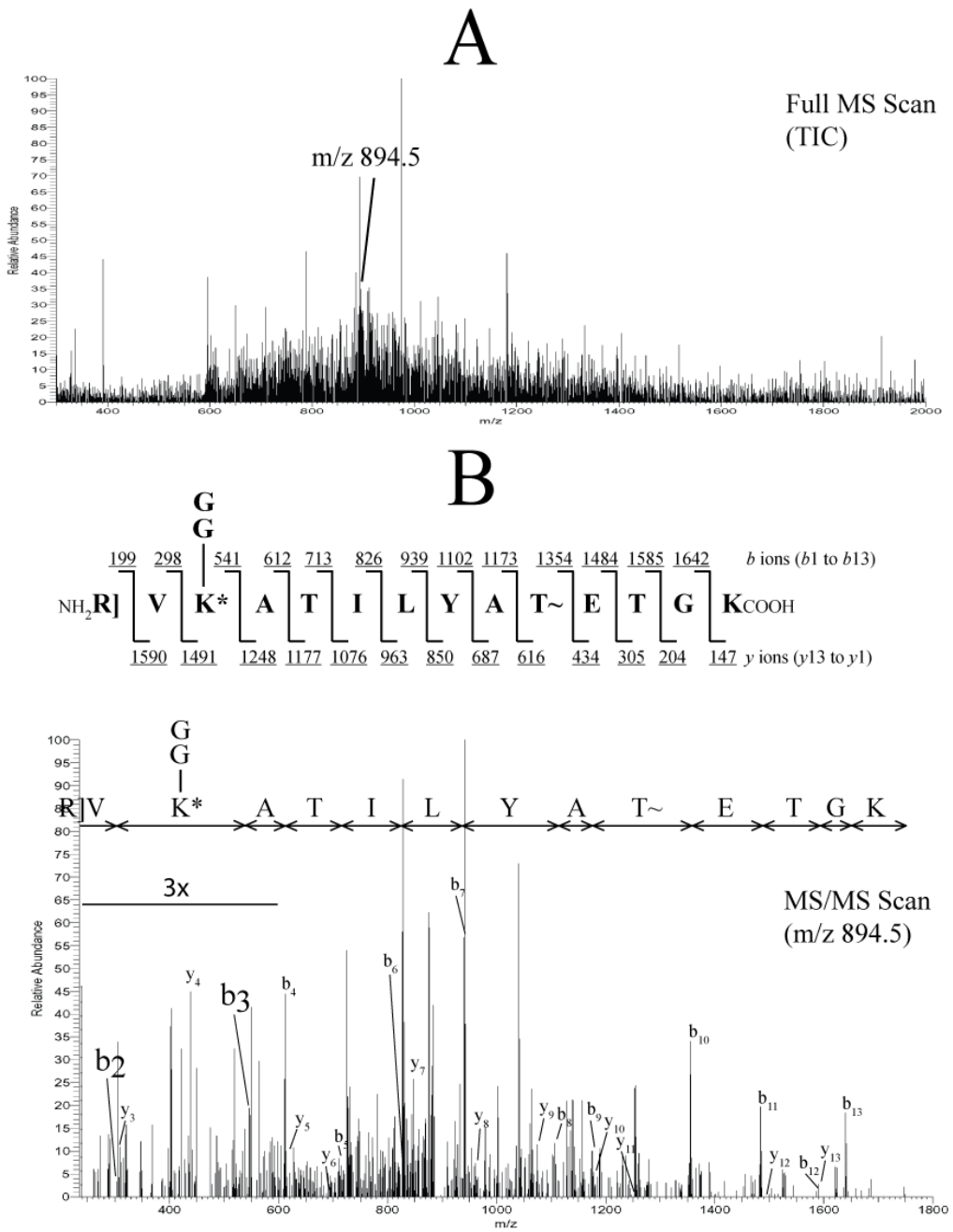

Fig. 4.10. **Ubiquitinated nNOS peptide identified by TurboSequest analysis of CapLC-MS/MS spectra.** All MS/MS spectra obtained from the data dependent CapLC-MS/MS analysis of trypsinized His-Ub-nNOS were searched against the rat nNOS sequence obtained from the nr.fasta database as described in "Methods." A peptide from the calmodulin region containing an ubiquitinated lysine (-GG) was identified (residue 754) by TurboSequest with an XCorr value of 2.1. *A,* full scan event (TIC) that identified the potential ubiquitinated peptide (m/z 894.5). *B, top panel*, sequence of the trypsin cleaved His-Ub-nNOS peptide identified (residues 752-765). Cleavage at the peptide backbone would result in the predicted fragment ion masses shown (*b*- and *y*-type ions) with the intact diglycine (-GG) modification. Phosporylation (~) and N-terminal acetylation (]) were also seen. *B, bottom panel,* MS/MS fragmentation pattern of m/z 894.5 detected in *A,*with the signal below m/z 600 amplified 3x. Only singly charged ions are labeled for simplicity. The individual *b*- and *y*- ions are labeled, and the site of ubiquitination is highlighted in a larger font (b_2 - b_3) The predicted b-ion fragmentation pattern is shown at the top for reference.

References

1. Bender, A. T., Demady, D. R., Osawa, Y. (2000) Ubiquitination of neuronal nitric oxide synthase in vitro and in vivo *J. Biol. Chem.* **275,** 17407-17411.
2. Dunbar, A. Y., Kamada, Y., Jenkins, G. J., Lowe, E. R., Billecke, S. S., Osawa, Y. (2004) Ubiquitination and degradation of neuronal nitric-oxide synthase in vitro: dimer stabilization protects the enzyme from proteolysis *Mol Pharmacol* **66,** 964-969.
3. Noguchi, S., Jianmongkol, S., Bender, A. T., Kamada, Y., Demady, D. R., Osawa, Y. (2000) Guanabenz-mediated inactivation and enhanced proteolytic. *J Biol Chem* **275,** 2376-2380.
4. Hershko, A., Ciechanover, A. (1998) The ubiquitin system *Annu. Rev. Biochem.* **67,** 425-479.
5. Laney, D. J., Hochstrasser, M. (1999) Substrate targeting in the ubiquitin system *Cell* **97,** 427-430.
6. Pickart, C. M. (2001) Mechanisms underlying ubiquitination *Annu. Rev. Biochem.* **70,** 503-533.
7. Boutet, S. C., Disatnik, M-. H., Chan, L. S., Lori, K., Rando, T. A. (2007) Regulation of Pax3 by proteasomal degradation of monoubiquitinated protein in skeletal muscle progenitors *Cell* **130,** 349-362.
8. Kamada, Y., Jenkins, G. J., Lau, M, Dunbar, A. Y., Lowe, E. R., and Osawa, Y. (2005) Tetrahydrobiopterin depletion and ubiquitylation of neuronal nitric oxide synthase *Mol Brain Res* **142:** 19-27.
9. Bender, A. T., Silverstein, A. M., Demady, D. R., Kanelakis, K. C., Noguchi, S., Pratt, W. B., Osawa, Y. (1999) Neuronal nitric oxide synthase is regulated by the hsp90-based chaperone system in vivo *J. Biol. Chem.* **274,** 1472-1478.
10. Roman, L. J., Sheta, E. A., Martasek, P., Gross, S. S., Liu, Q., Masters, B. S. (1995) High-level expression of functional rat neuronal nitric oxide synthase in Escherichia coli *Proc. Natl. Acad. Sci. U.S.A.* **92,** 8428-8432.
11. Rozhkova, E. A., Fujimoto, N., Sagamai, I., Daff, S. N., and Shimizu, T. (2002) Interactions between the isolated oxygenase and reductase domains of neuronal nitric-oxide synthase: assessing the role of calmodulin *J Biol Chem* **277:** 16888-16894.
12. Hershko, A., Heller, H., Elias, S., Ciechanover, A. (1983) Components of ubiquitin-protein ligase system. Resolution, affinity purification, and role in protein breakdown *J Biol Chem* **258,** 8206-8214.
13. Peng, J., Schwartz, D., Elias, J. E., Thoreen, C. C., Cheng, D., Marsischky, G., Roelofs, J., Finley, D., and Gygi, S. P. (2003) A proteomics approach to understanding protein ubiquitination *Nature Biotech* **21(8):** 921-926.
14. Dunbar, A. Y., Jenkins, G. J., Jianmongkol, S., Nakatsuka, M., Lowe, E. Z., Lau, M., and Osawa, Y. (2006) Tetrahydrobiopterin protects against guanabenz-mediated inhibition of neuronal nitric-oxide synthase invitro and in vivo *Drug Met Dis* **34(9):** 1448-1456.
15. Salerno, J. C., Harris, D. E., Irizarry, K., Patel, B., Morales, A. J., Smith, S. M., Martasek, P., Roman, L. J., Masters, B. S., Jones, C. L., et al. (1997) An

16. Hicke, L. (2001) Protein regulation by monoubiquitin *Nat Rev Mol Cell Biol* **2,** 195-201.
17. Thrower, J. S., Hoffman, L., Rechsteiner, M., and Pickart, C. M. (2000) Recognition of the polyubiquitin proteolytic signal *EMBO J* **19,** 94-102.
18. Janse, D. M., Crosas, B., Finley, D., and Church, G. M. (2004) Localization to the proteasome is sufficient for degradation *J Biol Chem* **279,** 21415-21420.
19. Coffino, P. (2001) Antizyme, a mediator of ubiquitin-independent proteasomal degradation *Biochimie* **83,** 319-323.
20. Peng, H. -M., Morishima, Y., Jenkins, G. J., Dunbar, A. Y., Lau, M., Patterson, C., Pratt, W. B., Osawa, Y. (2004) Ubiquitylation of neuronal nitric-oxide synthase by CHIP, a chaperone-dependent E3 ligase *J. Biol. Chem.* **279,** 52970-52977.
21. Johnson, P. R., Swanson, R., Rakhilina, L., Hochstrasser, M. (1998) Degradation signal masking by heterodimerization of MATalpha2 and MATa1 blocks their mutual destruction by the ubiquitin-proteasome pathway *Cell* **94,** 217-227.
22. Pickart, C. M., Fushman, D. (2004) Polyubiquitin chains: polymeric protein signals *Current Opinion in Chemical Biology* **8,** 610-616.
23. Hershko, A., Heller, H. (1985) *Biochem Biophys Res Commun* **128,** 1079.
Jentoft, N., Dearborn, D. G. (1979) *J Biol Chem* **254,** 4359.

Chapter V

Conclusions

The initial findings of Furchgott and Zawadzki (1) led to an explosion in research on the many critical physiological processes that are regulated by the highly diffusible radical, NO. Since NO plays an important role in a wide variety of physiological processes, any changes in the amount of NO produced by NOS can result in pathology. These changes include the overproduction, as well as the lack of NO. Since the molecule is so short lived, steady state levels of NO are due entirely to the synthesis of the molecule by NOS. Thus, regulation of the protein level of NOS is a critical determinant of signaling by NO. Given the wide range, and importance of NO function, the ability to control NO levels in specific regions through the manipulation of the individual NOS isoforms could be a powerful therapeutic tool. Understanding how cells regulate NOS protein levels would be very helpful in designing strategies to inhibit or stimulate NO production. This thesis focused on understanding the regulation of the nNOS isoform with respect to degradation of the enzyme.

The initial studies that provided the foundation for this thesis project showed that nNOS was ubiquitinated and proteasomally degraded (2, 3). It was also shown that some metabolism-based inhibitors of nNOS enhance the proteasomal degradation of the enzyme, suggesting a selective labilization of nNOS for recognition by the ubiquitin-proteasome system (2, 4). Some reversible inhibitors can actually stabilize the protein, showing that the labilization is not merely due to the loss of nNOS function (2, 4). How

proteins become recognized and degraded by the ubiquitin proteasome system is a fundamental question in understanding cellular quality control mechanisms. Certain modifications or structural features must occur on damaged and altered proteins to differentiate them from their needed functional counterparts. These differences must be recognized by some cellular factors that can decide the fate of the modified protein. In the case of some liver cytochrome P450 enzymes, cross-linking of the heme to the protein is a signal for ubiquitination and proteasomal degradation (11-13). Consistent with this, the heme-deficient form of nNOS (apo-nNOS) is selectively ubiquitinated and degraded with respect to the heme-containing, dimeric, holo-nNOS (3). The initial conclusion may be that the loss or damage of heme is the critical event that is recognized, but subsequent work showed that destabilization of the dimeric structure of nNOS, not heme loss per se, was sufficient for selective ubiquitination and proteasomal degradation *in vitro* (6).

To better understand the molecular trigger for nNOS ubiquitination and proteasomal degradation, we examined how guanabenz, a clinically used antihypertensive agent and known suicide inactivator of nNOS, labilizes nNOS for enhanced ubiquitination and proteasomal degradation. In Chapter II of this thesis, we discovered that guanabenz causes a destabilization of the dimeric structure of nNOS. This destabilization was due to the guanabenz-mediated oxidation of tetrahydrobiopterin (BH_4) by nNOS-derived superoxide. BH_4 binds near the heme active site of nNOS, and is known to stabilize the active, dimeric form of the enzyme. BH_4 was able to protect nNOS from the guanabenz-mediated inhibition *in vitro*. Similarly, treatment of rats with BH_4 completely protected from the guanabenz-mediated loss of NOS protein and activity.

BH_4 is an important factor in a variety of pathological conditions involving NOS enzymes, from impaired vascular function (7) to inhibited immune response (8). The specific effects of BH_4 depletion on nNOS have not been well characterized, although both an increased vulnerability to hypoxia and nNOS dysfunction in neurons has been observed (9). The work done in Chapter III investigated whether the loss of BH_4 was sufficient to elicit the enhanced turnover of nNOS. We inhibited the enzyme catalyzing the rate limiting step of BH_4 synthesis, GTP cyclohydrolase I, with 2, 4-diamino-6-hydroxypyrimidine in HEK293 cells, and found that a 75% drop in BH_4 levels resulted in a 2-fold increase in nNOS-ubiquitin conjugates. Consistent with this finding, BH_4 was able to protect nNOS from ubiquitination and degradation in an *in vitro* degradation mixture containing rabbit reticulocyte lysate proteins. Our data show that BH_4 deficiency can cause nNOS dysfunction and increase its ubiquitination and proteasomal degradation. The lower levels of nNOS would cause a depletion of NO in the body, explaining the pathological conditions previously described. These results also show that a mechanism that may replenish or enhance cellular pools of BH_4 could be a viable therapeutic target. Furthermore, it does appear that perturbations of the heme active site resulting in the destabilization of the active, dimeric form of the enzyme are somehow recognized by cellular factors that selectively target nNOS for ubiquitination and degradation. This hypothesis is further supported by the finding that stabilization of the nNOS dimer by the binding of reversible inhibitors to the heme active site protects the protein from proteasomal degradation (6).

In Chapter IV of this thesis we provided the first identification of a site of interaction with the cellular factors that recognize labilized nNOS for selective

ubiquitination and degradation. Specifically, we determined the site of ubiquitination, which directly identifies the region on nNOS that an E3 ubiquitin ligase interacts with to conjugate ubiquitin to a target lysine residue. We discovered that nNOS ubiquitination could occur in the calmodulin binding region (residues 720-756), as described below. Direct blocking of the region by the binding of calmodulin greatly reduced the ubiquitination of nNOS. The mutation of the seven lysines in the calmodulin binding region of the 7R nNOS mutant (residues 725, 732, 733, 739, 743, 751 and 754) to arginines, which cannot conjugate to ubiquitin, greatly reduced the level of ubiquitin conjugates formed, and stabilized the protein from proteasomal degradation *in vitro*. The restoration of just one of the lysines in the region, whether in the C-terminal end (residue 733), middle (residue 739) or N-terminal end (residue 754), was able to fully restore the ability of the protein to be ubiquitinated and degraded back to the levels seen for the wild type protein. The ability of the wild type protein to be ubiquitinated in the calmodulin region was also supported using peptide mapping by MS/MS analysis of trypsinized ubiquitinated nNOS. This method was previously shown to identify multiple ubiquitination sites of proteins from *S. cerevisiae* using a signature diglycine remnant of ubiquitin attached to a lysine residue that is resistant to trypsin proteolysis (10). Lysine 754 in the calmodulin binding region was identified as a potential site of ubiquitin conjugation using this technique, supporting the notion that the findings from our mutagenesis studies are applicable to the wild type protein. The site of ubiquitination would have to be a region that is easily accessible for interactions with an E3 ligase, since not only are there protein-protein interactions involved, but the E3 ligase must be able to conjugate ubiquitin to nNOS, forming a covalent linkage between a target lysine and

ubiquitin. The calmodulin binding region is located between the oxygenase and reductase domains of nNOS. It is established that limited trypsinolysis results in a selective cleavage at lysine residue 727, located in the calmodulin binding region (14). The ability of the calmodulin binding domain to be selectively cleaved by trypsin, combined with the fact that it is a linker region between two bulky domains that must interact for nNOS to be active, is consistent with the notion that the calmodulin binding region is an easily accessible and flexible region of nNOS that can interact with cellular factors, such as an E3 ubiquitin ligase.

Additionally, we found that mono-ubiquitination can serve as a signal for the proteasomal degradation of nNOS *in vitro*, consistent with the finding that the main ubiquitin conjugate of nNOS detected from cells and of nNOS ubiquitinated *in vitro* appears to be the mono-ubiquitinated form (3). Combining the information currently available with the data presented in this thesis, it is feasible that perturbations in the heme active site of nNOS destabilize the protein enough that hydrophobic regions that were hidden in the active dimeric structure are now exposed. These hydrophobic regions can be recognized by cellular factors, such as Hsp70, that can recruit an ubiquitin E3 ligase. The ligase can then bind to the flexible and easily accessible calmodulin binding region, transferring ubiquitin to the region. This mono-ubiquitinated nNOS can then be proteasomally degraded, destroying the dysfunctional nNOS enzyme.

These studies provide some insight on how nNOS becomes selectively targeted for ubiquitination, and what regions of the enzyme must be accessible for recognition by cellular quality control machinery. The approaches described here can be applied to continue the elucidation of the mechanisms of cellular triage decisions for nNOS and

other tightly regulated proteins. In particular, the 7R mutant could serve as a powerful tool for the continued identification of the components of the cellular quality control and ubiquitination systems that recognize dysfunctional nNOS to facilitate its degradation by forming more stable protein complexes that are not rapidly degraded. Many factors such as drug treatment, xenobiotics or cellular conditions can produce dysfunctional proteins. Understanding the process by which these dysfunctional proteins become targeted for ubiquitination will aid in predicting potential drug toxicities and in the development of specific inhibitors.

References

1. Furchgott, R. F., Zawadzki, J. V. (1980) The obligatory role of endothelial cells in the relaxation of arterial smooth muscle by acetylcholine *Nature* **288,** 373-376
2. Noguchi, S., Jianmongkol, S., Bender, A. T., Kamada, Y., Demady, D. R., Osawa, Y. (2000) Guanabenz-mediated inactivation and enhanced proteolytic degradation of neuronal nitric-oxide synthase *J. Biol. Chem.* **275,** 2376-2380
3. Bender, A. T., Demady, D. R., Osawa, Y. (2000) Ubiquitination of neuronal nitric oxide synthase in vitro and in vivo *J. Biol. Chem.* **275,** 17401-17411
4. Nakatsuka, M., Nakatsuka, K., Osawa, Y. (1998) Metabolism-based inactivation of penile nitric oxide synthase activity by guanabenz *Drug Metab. Dispos.* **26,** 497-501
5. Vasquez-Vivar, J., Whitsett, J., Martasek, P., Hogg, N., Kalyanaraman, B. (2001) Reaction of tetrahydrobiopterin with superoxide: EPR-kinetic analysis and characterization of the pteridine radical *Free Radical Biol Med* **31,** 975-985
6. Dunbar, A. Y., Kamada, Y., Jenkins, G. J., Lowe, E. R., Billecke, S. S., Osawa, Y. (2004) Ubiquitination and degradation of neuronal nitric-oxide synthase in vitro: dimer stabilization protects the enzyme from proteolysis *Mol Pharmacol* **66,** 964-969
7. Werner, E. R., Gorren, A. C., Heller, G., Werner-Felmayer, G., Mayer, B. (2003) Tetrahydrobiopterin and nitric oxide: mechanistic and pharmacological aspects *Exp Biol Med.* **228,** 1291-1302
8. Gross, S. S., Levi, R. (1992) Tetrahydrobiopterin syntesis. An absolute requirement for cytokine-induced nitric oxide generation by vascular smooth muscle *J Biol Chem* **267,** 25722-25729
9. Delgado-Esteban, M., Almeida, A., Medina, J. M. (2002) Tetrahydrobiopterin deficiency increases neuronal vulnerability to hypoxia *J Neurochem* **82,** 1148-1159
10. Peng, J., Schwartz, D., Elias, J. E., Thoreen, C. C., Cheng, D., Marsischky, G., Roelofs, J., Finley, D., Gygi, S. P. (2003) A proteomics approach to understanding protein ubiquitination *Nature Biotech* **21(8),** 921-926
11. Tierney, D. J., Haas, A. L., Koop, D. R. (1992) *Arch Biochem Biophys* **293**, 9-16
12. Correia, M.A., Davoll, S.H., Wrighton, S.A., Thomas, P.E. (1992) *Arch Biochem Biophys* **297**, 228-238
13. Korsmeyer, K. K., Davoll, S., Figueiredo-Pereira, M. E., Correia, M. A., (1999) *Arch Biochem Biophys* **365**, 31-44
14. Salerno, J. C., Harris, D. E., Irizarry, K., Patel, B., Morales, A. J., Smith, S. M., Martasek, P., Roman, L. J., Masters, B. S., Jones, C. L., et al. (1997) An autoinhibitory control element defines calcium-regulated isoforms of nitric oxide synthase *J Biol Chem* **272**, 29769-29777